12-2016

Environmental Signaling through the Target of Rapamycin Complex 1 (TORC1) and the Regulation of Epigenetic Mechanisms

Jason J. Workman
University of Tennessee Health Science Center

Environmental Signaling through the Target of Rapamycin Complex 1 (TORC1) and the Regulation of Epigenetic Mechanisms

ORCID
http://orcid.org/0000-0002-9071-5207

DOI
10.21007/etd.cghs.2016.0415

Environmental Signaling through the Target of Rapamycin Complex 1 (TORC1) and the Regulation of Epigenetic Mechanisms

A Dissertation
Presented for
The Graduate Studies Council
The University of Tennessee
Health Science Center

In Partial Fulfillment
Of the Requirements for the Degree of
Doctor of Philosophy
From The University of Tennessee

By
Jason J. Workman
December 2016

DEDICATION

This work is dedicated to my loving wife, for continually reminding me what I'm capable of, and for giving me something to look forward to at the end of the day.

ACKNOWLEDGEMENTS

We would like to acknowledge the people who made this work, and my matriculation through The University of Tennessee Health Science Center, possible.

First, I want to thank my fantastic Dissertation Committee, Dr. Larry Pfeffer, Dr. Sunny Wu, Dr. Mondira Kundu and Dr. Janet Partridge, for their thoughtful reading of this dissertation and guidance throughout the process. Next, my track director Dr. Tiffany Seagroves and program director Dr. Ren Ostrom, for helping me to stay on top of all the courses and paperwork necessary to complete the process. Additionally, I have to mention the great group of people in the Graduate Health Sciences and Pathology offices, particularly Ms. Barbara Frederick, Ms. Felicia Washington, Ms. Elizabeth Webb, and CGHS dean Dr. Don Thomason.

We also would like to recognize Dr. Dan Klionsky (University of Michigan) for providing us with the Tap42 temperature sensitive plasmids, and Dr. Mary Miller (Rhodes College) for assisting with tetrad dissections.

Lastly, I want to thank my colleagues in the Laribee Laboratory. Dr. Hongfeng Chen for providing me with great ideas and feedback throughout the process (and for teaching me a little Chinese), and my mentor Dr. Nick Laribee, who has my sincere gratitude for taking me in as his first student trainee and providing an environment that allowed me to explore my potential and become the scientist that I am today. My work in the Laribee Laboratory was supported by funding from the American Heart Association and the National Institute of Health.

ABSTRACT

The gene expression profile of a eukaryotic cell is responsive to a variety of extracellular stimuli, including nutrient availability, which allows cells to toggle between anabolism and catabolism based on the favorability of their environment. Much of this information is relayed through signaling complexes, such as the target of rapamycin complex 1 (TORC1), to downstream chromatin modifying enzymes. These enzymes impact the gene regulatory process through altered histone post-translation modifications, changes in chromatin structure, and docking of chromatin regulatory complexes. Yet, despite preliminary studies suggesting that TORC1 affects epigenetic mechanisms, including histone H3 lysine 56 acetylation (H3K56ac), almost nothing is known about how the complex functions in this regard. In this report, we demonstrate that inhibition of TORC1 results in a site-specific reduction in acetylation on N-terminal residues of both histone H3 and H4. This effect is dependent on sirtuin histone deacetylases (HDACs), as inactivation of these enzymes, specifically Hst4, rescues the acetylation defect. We also find that this sirtuin-mediated deacetylation response requires a functional protein phosphatase 6 complex (PP6). PP6 is under direct negative regulation of TORC1, and relief of this inhibition initiates a rapid cytoplasmic to nuclear redistribution of Hst4 which correlates temporally with our observed loss of histone acetylation. The nuclear accumulation of Hst4 precedes an increase in Hst4 protein levels that occurs due to a reduction in Hst4 turnover. Notably, deletion of a subset of sirtuins (*hst3Δ* or *hst4Δ*) rescued the sensitivity of a non-essential TORC1 mutant (*tco89Δ*) to an array of TORC1 inhibitors. This result suggests the link between TORC1 and acetylation may play an essential role in cell cycle regulation and the DNA damage response. We further evaluated whether these TORC1-mediated acetylation marks contribute to the chromatin association of high mobility group proteins (HMGs). And while TORC1-dependent displacement of the HMGs coincides with vacuolar acidification, hyperactivation of TORC1, and significant cell death, it appears to occur independently of TORC1's regulation of Hst4. We conclude by investigating mitochondrial function in a *tco89Δ* mutant and mapping the functional domains of Tco89 necessary to sustain TORC1 activity and respond to extracellular stress.

TABLE OF CONTENTS

LIST OF TABLES

LIST OF FIGURES

LIST OF ABBREVIATIONS

AsO_3	Arsenic trioxide
CFDA	5(6)-carboxyfluorescein diacetate
ChIP	Chromatin immunoprecipitation
ChIP-seq	Chromatin immunoprecipitation sequencing
CR	Caloric restriction
DHE	Dihydroethidium
FITC	Fluorescein isothiocyanate
FKBP	FK506-binding protein
GAP	GTPase-activating protein
GEF	Guanine exchange factor
HATs	Histone acetyltransferases
HDACs	Histone deacetylases
HMG	High-mobility group protein
HMG (A/B/N)	High-mobility group protein A/B/N family member
HMGB1	High-mobility group box 1 protein
IB	Immunoblot
MCRS1	Microspherule protein 1
MES	2-(N-morpholino) ethanesulfonic acid
MMS	Methyl methanesulfonate
MSX	L-methionine sulfoximine
mTor	Mechanistic target of rapamycin (in reference to the kinase)
mTORC1	Mechanistic target of rapamycin complex 1

NAD+/NADH	Nicotinamide adenine dinucleotide
NCR	Nitrogen catabolite repression (response)
PGC-1α	Peroxisome proliferator-activated receptor-gamma coactivator-1 α
PHO pathway	Phosphate-responsive signaling pathway
PI	Propidium iodide
PI3K	Phosphoinositide 3-kinase
Pkh1/2	Pkb-activating kinase homolog 1/2
PP2A	Protein phosphatase 2A complex
PP4	Protein phosphatase 4 complex
PP6	Protein phosphatase 6 complex
PPG1	Protein phosphatase involved in glycogen accumulation
PPP6C	Protein phosphatase 6, catalytic subunit (mammalian)
PPP6R1/2/3	Protein phosphatase 6, regulatory subunits 1/2/3 (mammalian)
PTEN	Phosphatase and tensin homolog
Rab1A	Ras-related protein 1A
rDNA	Ribosomal DNA
RNA-seq	RNA sequencing
RNAPI/II/III	RNA polymerase I/II/III
ROS	Reactive oxygen species
RP	Ribosomal protein (genes)
rRNA	Ribosomal RNA
RSC	Remodels structure of chromatin complex
S6K1	S6-kinase 1

SAGA	Spt-Ada-Gcn5-acetyl-transferase
SASP	Senescence-associated secretory phenotype
SCF	Skp, Cullin, F-box containing complex
SD	Standard deviation
SEACIT	SEAC subcomplex inhibiting TORC1 signaling
SIRT1-7	Silent mating type information regulation 2 homolog 1/2/3/4/5/6/7
SOD1	Superoxide dismutase 1
SWI/SNF	Switch/Sucrose non-fermentable
TCFI	Total cellular fluorescence intensity
TNFI	Total nuclear fluorescence intensity
TIF-IA	Transcription initiation factor 1A
Tor1/2	Target of rapamycin 1 or 2 (in reference to the kinases)
TORC1/2	Target of rapamycin complex 1/2
TSC	Tuberous sclerosis complex
v-ATPase	Vacuolar H+-ATPase
WCEs	Whole cell extracts
YEATS	Yaf9, ENL, AF9, Taf14, Sas5 (in reference to the domain)
Ypk3	Yeast protein kinase 3

CHAPTER 1. INTRODUCTION

Histone Proteins and Chromatin Organization

The histone family of DNA packaging proteins is comprised of four isoforms: H2A, H2B, H3 and H4. Each histone consists of a globular core and a pair of N- and C-terminal tails. All of the core histones exist as heterodimers of H2A/H2B or H3/H4, and assembly of four of these heterodimers (two of each) results in formation of an octameric structure collectively known as the nucleosome [1, 2]. Approximately 146 base pairs of DNA are wound around each nucleosome, resulting in the "beads on a string" structure, noted initially in early electron microscopy analyses of intact chromatin [3]. From there, interactions between the nucleosomes themselves produce a more compacted form of chromatin known as the 30 nm fiber. Additional higher order folding and packaging condenses the 30 nm fiber even further to ultimately form chromosomes (**Figure 1-1**).

The Epigenome

The epigenome consists of a heritable set of highly complex histone post-translation modifications, including acetylation, methylation, phosphorylation and ubiquitination, which essentially establish a secondary layer of genetic information that is stored above the chromatin. These epigenetic moieties occur predominantly on the N-terminal tails of the histones (**Figure 1-2**), where they function to coordinate a multitude of chromatin-based processes; most notably, enabling changes to an organism's phenotype through adjustments in gene expression rather than alterations to the genotype. Methylation of lysines and arginines on the histone tails has a very context specific effect on transcription, which is most often coordinated through mediating the association of methyl-binding proteins (i.e. Tudor domains, MBT domains, PHD domains, chromodomains, and WD proteins) [4-11]. On the other hand, acetylation status of these residues impacts the availability of the histone's positively charged amino groups to bind to the negatively charged DNA backbone. Specifically, increased acetylation results in a more open and transcriptionally accessible chromatin state, while reduction in these marks promotes a more heterochromatic and transcriptionally occlusive environment (**Figure 1-3**). Intriguingly, histone acetylation at the ribosomal protein (RP) genes and the ribosomal DNA (rDNA) has been shown to be responsive to signaling through nutrient sensing complexes [12, 13]. This suggests that epigenetic mechanisms could coordinate changes in gene expression in response to environmental nutrient availability. Despite a recent swell of scientific and mainstream interest, there are some who still believe the importance of the histone code and transgenerational epigenetic inheritance has been overstated [14-19].

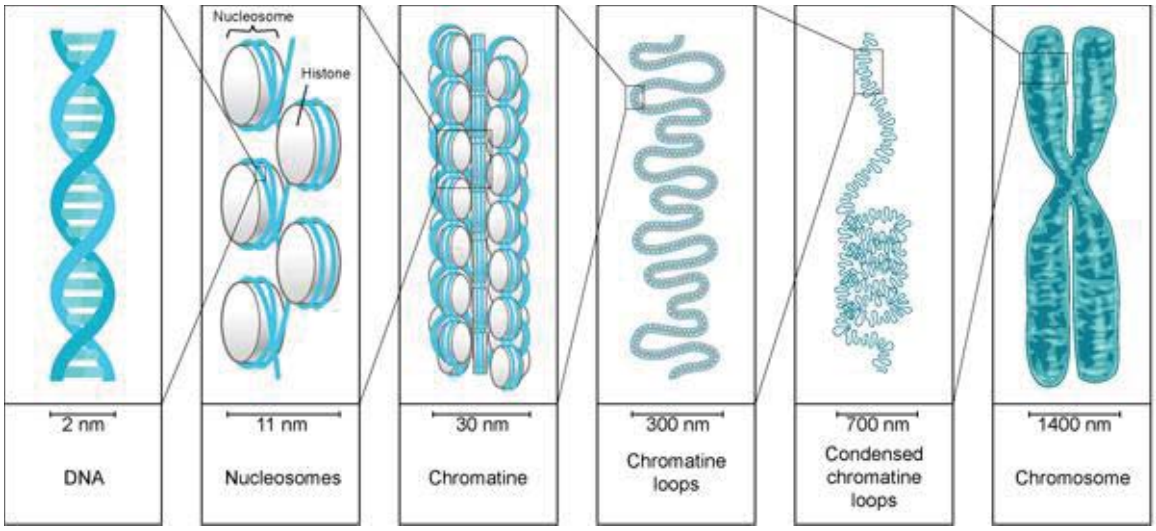

Figure 1-1. Cartoon representation of chromatin packaging.
DNA is spooled around the nucleosomes to form a loosely condensed, 11 nm fiber, sometimes referred to as the "beads on a string" configuration. Nucleosomal interactions drive additional levels of chromatin packaging, ultimately leading to the formation of chromosomal DNA. See text for more details. Reprinted with permission *[20]. DNA Packaging - Shmoop Biology. 2008 [cited 2016 May 11]; Available from: http://www.shmoop.com/dna/dna-packaging.html.*

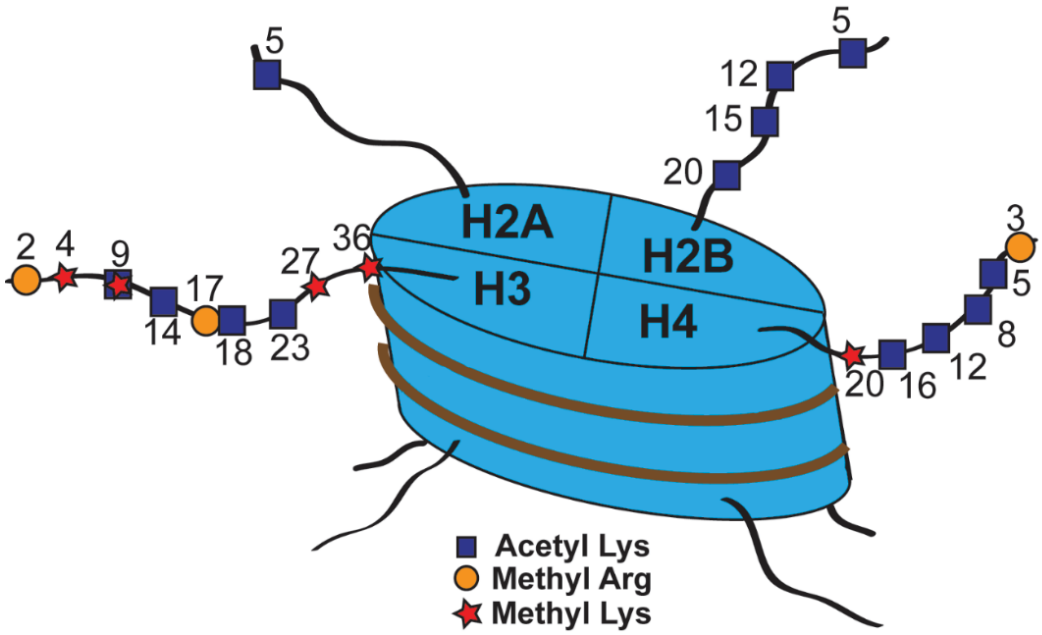

Figure 1-2. Schematic of the nucleosome.
The nucleosome is a histone octamer complex which consists of two heterodimers of both H2A/H2B and H3/H4. The most topical post-translation modifications on the N-terminal tails of each histone are denoted.

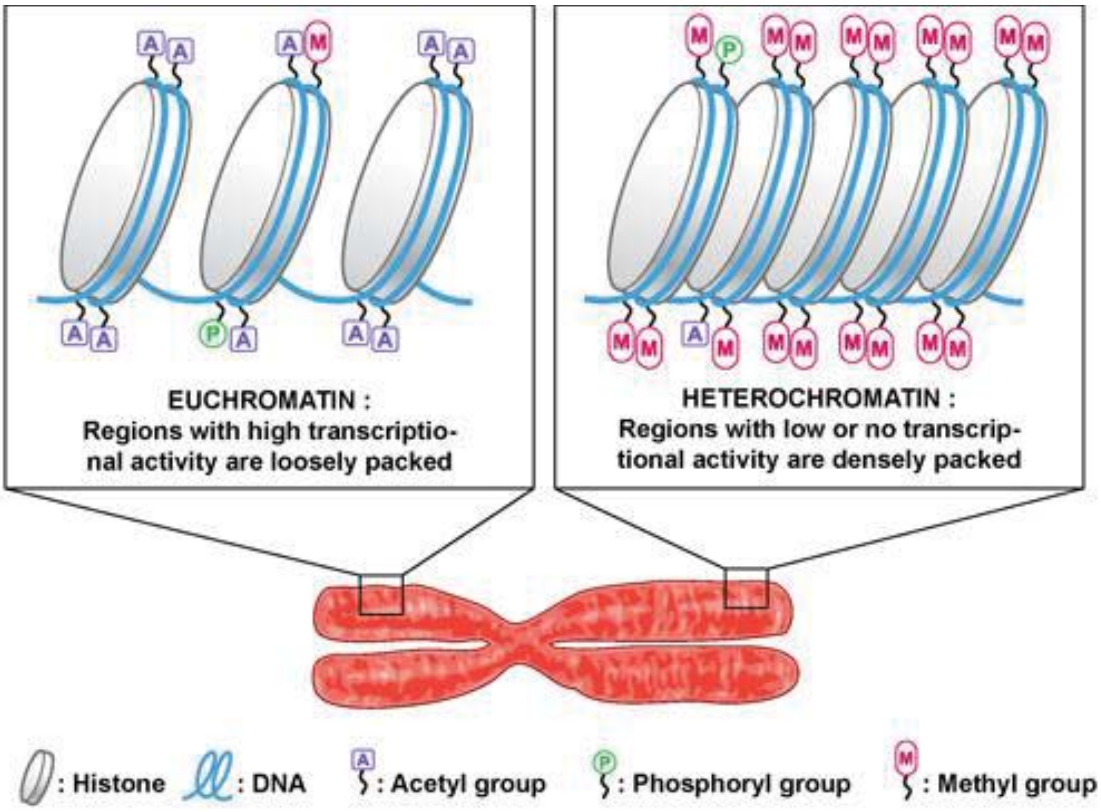

Figure 1-3. Transcriptional availability of DNA is mediated by the epigenetic modifications of histones.
Cartoon representation of the dynamic effects acetylation and methylation can have on chromatin packaging, and subsequently, the accessibility of particular regions of DNA for efficient gene transcription. Reprinted with permission *[20]. DNA Packaging - Shmoop Biology. 2008 [cited 2016 May 11]; Available from: http://www.shmoop.com/dna/dna-packaging.html.*

Advantages of the *S. cerevisiae* Model System for Epigenetic Studies

The study of chromatin, particularly at single nucleosome resolution, proves very challenging in most models or cell lines due to the multicopy nature of the core histone genes. As an example, human cells have 15 copies of the H3 gene, encoding canonical H3 and two additional H3 sequence variants [21, 22]. This high level of redundancy makes probing the specific chromatin contributions of individual histone amino acid residues incredibly difficult. However, due to the evolutionary conservation of the core histones, and because the budding yeast genome encodes only two copies of canonical H3 and H4, *S. cerevisiae* has become an essential model organism for conducting cutting-edge, mechanism-based experiments that are highly translatable. Indeed, our current knowledge of functional genomics, histone dynamics and epigenetic modifications was built on work conducted in budding yeast [23].

Coordination of Nutrient Availability, Anabolism and Cellular Aging

It is critical for all eukaryotic organisms to be able to rapidly adjust their growth and proliferative profiles to account for changing extracellular conditions or intracellular deficits. This principle is most critical as it relates to active cell division, as an inability to coordinate mitosis with nutrient and energy states may prevent sufficient biomass accumulation and have adverse downstream consequences on cell viability [24-27]. In response to these pressures, cells have developed highly conserved nutrient sensing complexes, such as the target of rapamycin complex 1 (TORC1), which couples extracellular nutrient signals with the appropriate intracellular response [28]. Aberrant flux through these sensing pathways contributes to a number of age-related diseases, including diabetes, cancer and cardiovascular disease [29].

Identification of the Target of Rapamycin Genes

The discovery of target of rapamycin (Tor), a protein kinase responsible for mediating cell growth and proliferation in coordination with growth factors and environmental nutrient status, can be traced back to the isolation of rapamycin, a macrolide produced by the Easter Island soil bacterium *Streptomyces hygroscopicus* [30]. Though once a promising antifungal compound, rapamycin's adverse effects on host T-cell proliferation has led to its present day use as an immunosuppressant and anti-cancer agent (as reviewed by Benjamin)[31]. The rapamycin-dependent effects on T-cell proliferation require the FK506-binding protein (FKBP), a binding partner now known to bridge the association of rapamycin and the FKBP-rapamycin binding domain of Tor [32-34].

The proliferation defect first identified in rapamycin treated T-cells is also observed in the budding yeast *Saccharomyces cerevisiae*, and in both instances, deficiencies are attributable to an early G1 cell-cycle arrest [35]. Genome sequencing of spontaneously rapamycin resistant yeast mutants identified the two genes responsible for

mediating the rapamycin phenotype, and they were aptly named target of rapamycin 1 and 2 (TOR1 and TOR2) [35]. These genes encode a unique pair of PI3-like serine/threonine kinases. Subsequently, an orthologous kinase was discovered in higher order organisms, termed mechanistic TOR (mTor), and since then, Tor kinases have been reported to be conserved across all eukaryotes [36-38]. Characterization of Tor kinase substrates has proven difficult due to the lack of a true consensus sequence, though a few are known and will be discussed below. For clarity and simplicity, nomenclature for the yeast Tor pathway will be used from herein unless otherwise noted.

The TORC1 Complex

The Tor kinases are incorporated into one of two signaling complexes: target of rapamycin complex 1 or 2 (TORC1/2) [39-41]. In metazoans, these complexes are known as mechanistic TORC1/2 (mTORC1/2). There are considerable structural and functional differences between TORC1 and TORC2, the most relevant being that TORC1 is sensitive to environmental stimuli and rapamycin-dependent inhibition while TORC2 is not. Because the overarching interest of our lab is in environmentally regulated epigenetic processes, TORC1 will be our focus for the remainder of this work.

TORC1 consists of the Tor1/2 kinase, Lst8, Kog1, and Tco89 [42]. Lst8 and the Tor2 kinase can be found in both TORC1 and TORC2, but Tor1, Kog1 and Tco89 appear to be TORC1-specific [43]. Accordingly, temperature sensitive mutants of Kog1 (essential), or *tco89Δ* mutants (non-essential), sensitize cells to direct TORC1 inhibition [43, 44]. Electron microscopy studies have characterized the association between the C-terminal WD40 domain of Kog1 and the N-terminal HEAT repeats of the Tor kinases [45]. Kog1 and its mammalian ortholog, Raptor, contribute to TORC1 function by facilitating a series of interactions, including between the kinase and its substrates [46, 47], and between TORC1 and the vacuole (discussed in detail below) [48, 49]. Further, when nutrients are limiting, the Rho1 GTPase associates with Kog1, resulting in inhibition of TORC1 [50]. Recently, it was reported that TORC1-bound Kog1 is more stable than free Kog1, suggesting association with the complex may also serve to stabilize Kog1 [51].

By comparison, little is known about Tco89. It is currently believed to be a yeast-specific component of TORC1, and homologs have been identified in *S. pombe* and *C. albicans* [52, 53]. The existence of a mammalian Tco89 seems likely however, given the considerable conservation of the TORC1 axis. *tco89Δ* cells have abnormal cellular physiology and budding patterns, as well as dramatically increased sensitivity to stress; including heat, caffeine, MMS, rapamycin and salt [52, 54-60]. *tco89Δ* mutants phenotypically resemble vacuole mutants (*ego1Δ, ego3Δ, gtr1Δ* and *gtr2Δ*), as these strains are all acutely sensitive to rapamycin and unable to reengage the cell cycle following TORC1 stress [43, 61] (discussed in detail later). In support of the above, Tco89 has been reported to mediate physical interactions between TORC1 and the vacuole [49]. Tco89 has also been shown to directly associate with Vac8, an armadillo repeat protein which affects vacuolar functions and caffeine resistance [62], and fructose-

1,6-bisphosphate to mediate its vacuolar turnover [63]. Still, the majority of studies that mention *tco89Δ* do so in the context of suppressor screens [64, 65]. Most of these screens also identify *tor1Δ*, suggesting that Tco89's most prominent function involves maintaining TORC1 activity. Interestingly, our group has shown that TORC1-dependent histone acetylation is responsive to *tco89Δ* but not *tor1Δ* [66]. A mammalian ortholog of Tco89 could be an attractive therapeutic target given the dramatic and permanent cell cycle arrest that occurs in its absence when sub-inhibitory doses of rapamycin are administered [43, 49].

Downstream Effectors of TORC1

When nutrient status and environmental conditions are favorable, TORC1 actively promotes growth programs and simultaneously suppresses stress responses through coordination of a downstream kinase (Sch9) and a series of Tap42-associated phosphatases (**Figure 1-4**). Conversely, diminished TORC1 signaling during times of starvation or rapamycin treatment causes cells to enter a quiescent state where anabolic flux is suppressed. Fascinatingly, long-term TORC1 inhibition, and subsequent suppression of anabolism, has been shown to extend lifespan across a number of model systems [67-74]. These rapid and dramatic changes in intracellular processes require a coordinated shift in gene expression, which TORC1 has been shown to regulate at the level of mRNA transcription (via transcription factor localization [75]) and translation (at the initiation step of elongation [76-78]). But how TORC1 regulates gene expression, particularly as it relates to chromatin structure, remains a poorly defined function of the pathway.

Recently, it was demonstrated that TORC1 also signals through the Ypk3 kinase to promote phosphorylation of the ribosomal proteins Rps6a/b, though the mechanism remains unclear [79]. Phosphorylation of S6 serves as a readout for TORC1 activity in eukaryotic cells [80], and it will be used as such in the studies presented herein. For now though, we will focus on the Sch9 kinase and the Tap42 phosphatases as they are the best-characterized effector molecules downstream of yeast TORC1 (**Figure 1-4**).

Sch9 kinase

Sch9 is an AGC protein kinase whose activity is directly promoted by TORC1-dependent phosphorylation [80]. The degree of control TORC1 exerts on Sch9 is evident in the fact that *sch9Δ* cells phenocopy the effects of caloric restriction (CR), including extended lifespan, and behave very similarly to a *tor1Δ* [71, 72, 80, 81]. It is important to note that there is also evidence that Sch9 and TORC1 may function synergistically, rather than redundantly, in sensing environmental stressors [82]. This concept is supported by the fact that phosphorylation of the Sch9 activation loop may occur independently of TORC1 via the Pkh1/2 kinases, possibly tying Sch9 into sphingolipid homeostasis as well as to classical TORC1 stimuli [83-85]. In the case described above, an additional

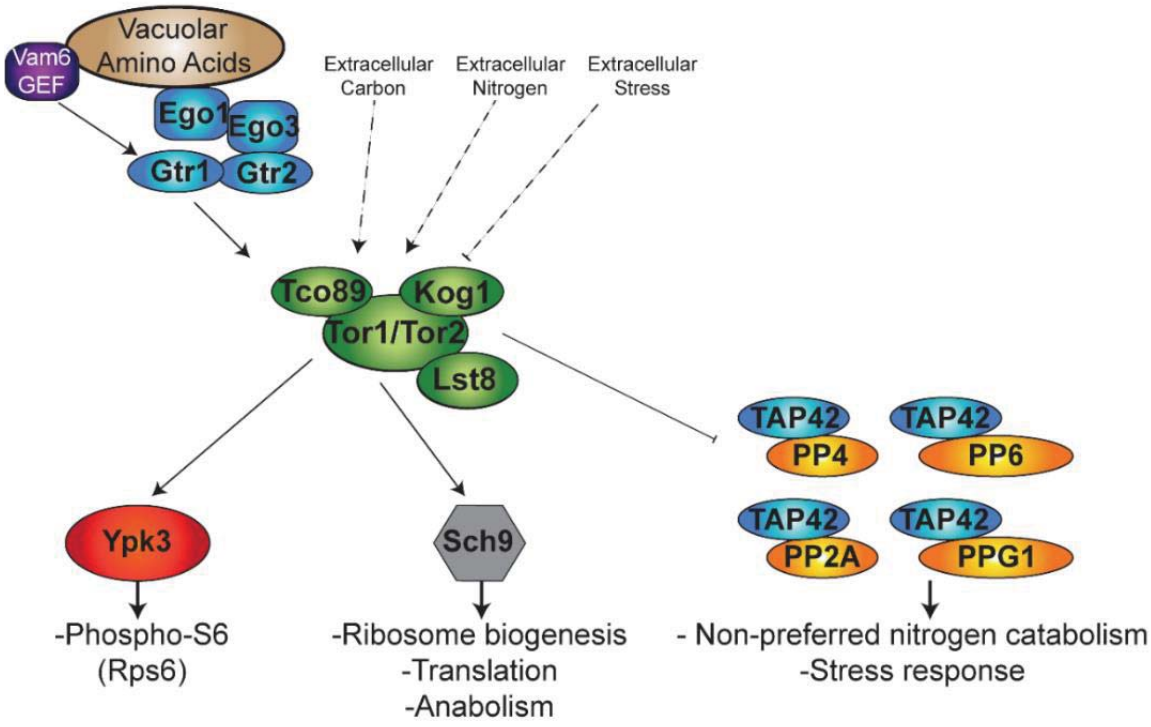

Figure 1-4. Downstream effectors of the TORC1 signaling pathway and their functions in *S. cerevisiae*.
TORC1 effectors include yeast protein kinase 3 (Ypk3), the Sch9 kinase, and the Tap42-associated phosphatases. Cellular processes mediated by each are presented as well. See text for more details.

TORC1-dependent phosphorylation mark on the hydrophobic motif of Sch9 is able to fine-tune the Pkh1/2-initiated activity.

The basic function of Sch9 is to promote proper cell cycle progression, transcription initiation, and translation, while simultaneously suppressing induction of autophagy [80, 86-88]. Under favorable environmental conditions, Sch9 phosphorylates and inhibits the transcriptional repressors Maf1, Dot6, Tod6 and Stb3, ensuring transcription of genes necessary for ribosomal biogenesis [60, 86, 89]. Sch9 activity also feeds into the suppression of autophagy, seemingly in concert with RAS/PKA, via regulation of the Atg1-Atg13-Atg17 kinase complex [88]. Additionally, to promote cell cycle progression, Sch9 targets the ubiquitin conjugating enzyme, Cdc34 [90]. An interesting study from Weisman et al. also ties Sch9 into cell cycle control through a unique vacuolar inheritance mechanism. They demonstrate that if this inheritance fails, the cell cycle arrests at G1 in an Sch9-dependent fashion [91]. Conversely, inhibition of Sch9 during times leads to Gcn2-mediated phosphorylation of the translation factor eIF2a, which inhibits its function and blocks protein synthesis [82]. It was also suggested recently that Sch9 regulation of Maf1 may contribute to CR-induced lifespan extension [92].

The PP6 phosphatase complex and Tap42

The Tap42-associated phosphatases are a family of functionally distinct, modular protein phosphatase complexes, which include PP2A, PP4, PP6 and PPG1 [93-96]. These complexes are best known as regulators of non-preferred nitrogen catabolism and the stress response. For brevity, and because PP6 will be the major focus of our work, it will be the only complex discussed in-depth.

The PP6 phosphatase complex exists as a heterodimer consisting of the ceramide-responsive catalytic subunit, Sit4, and one of four Sit4-associated regulatory proteins (Sap4, Sap155, Sap185, or Sap190) [97]. Sit4 regulates expression of the cyclin genes and is required for the execution of cell cycle START (G_1), bud formation, initiation of DNA synthesis, and spindle pole body duplication [98, 99]. Overexpression of the Saps in a temperature sensitive Sit4 mutant can partially reverse the observed growth defects, while a complete ablation of the Saps in an otherwise wild-type cell induces a *sit4Δ*-like slow growth phenotype and G1 delay [97]. Association of the catalytic and regulatory subunits appears to be cell-cycle dependent and indispensable for Sit4 activity *in vivo*. And while some speculate that the Saps regulate PP6 substrate specificity, their exact function is currently unknown. There is evidence which suggests that each Sap has a unique and distinct contribution to PP6 function, but there is also data that demonstrates at least moderate functional redundancy exists as well [97, 100, 101]. Interestingly, overexpression of metazoan PP6 regulatory subunits (PP6R2 and PP6R3) in the absence of the Saps restores growth and reverses rapamycin sensitivity, suggesting rather significant evolutionary conservation of this modular phosphatase complex [102].

Sit4 is highly influential in the cellular response to altered nutrient states, particularly to changes in amino acid availability. During starvation, the Gln3, Gat1, and Nil1 transcription factors are dephosphorylated by Sit4, which triggers dissociation from their cytoplasmic anchors and entry into the nucleus [103]. There, these factors drive high level expression of genes encoding permeases and enzymes needed to transport and utilize poor nitrogen sources. At the same time, the Sit4 phosphatase is also known to target the Npr1 kinase, leading to its activation and the subsequent stabilization of the general amino acid permease Gap1 [104]. These effects are known collectively as the Nitrogen Catabolite Repression (NCR) response.

Tap42's association with its family of phosphatases has a somewhat muddled history. It was initially identified in yeast as a 42kDa protein that specifically associates with the PP2A and PP6 protein phosphatase complexes [105]. Tap42 is now known to associate with all of the other PP2A-like phosphatase complexes, including the aforementioned PPG1 and PP4 [96]. Somewhat surprisingly, there is far less Tap42 in the cell than there are phosphatases, as only about 5-10% of cellular PP2A-like phosphatases are bound to Tap42 [105]. Such stoichiometry could suggest that these phosphatases possess Tap42-independent functions or possibly additional substrates that have yet to be identified. Chen et al. utilized a yeast two-hybrid screen to identify a mammalian protein they dubbed α4, which is also capable of binding the N-terminal portion of these phosphatase complexes [106]. The authors report significant sequence conservation between α4 and Tap42, suggesting the proteins may be homologs.

In the late 1990's, evidence began accumulating that Tap42 and α4 act as negative regulators of the PP2A-like phosphatases. First, Nanahoshi's group reported that PP2A-dependent dephosphorylation of eIF-4E binding protein was inhibited by the presence of Tap42 and α4 [107]. Subsequently, Beck and Hall suggested that Tap42 and Sit4 form a complex following Tap42 phosphorylation by TOR, and postulated that this was the inactive form of the phosphatase [75]. They found that when phosphatases were dissociated from Tap42, this was accompanied by a dephosphorylation of many downstream targets, concluding that phosphatase release led to its activation. This idea was supported by Jiang and Broach, who later demonstrated that Tap42 association to Sit4 is indeed rapamycin responsive and dependent on TORC1 phosphorylation of Tap42 [108]. Gene expression profiling identified dynamic expression level changes that mirror the release and disassembly of the Tap42-Sit4 complex [109]. Similarly, the inactivation of Tap42 was shown to severely attenuate the rapamycin-induced expression of genes under control of the Sit4-regulated Gln3 transcription factor [110].

More recently, however, many of the initial claims made about Tap42's function as a negative regulator, as well as its identity as a homolog to α4, have been questioned. In 2006, it was reported that rather than Tap42 functioning as a negative regulator, it may actually be a positive effector of the phosphatases [111]. The timing of this paradigm-shifting experiment proved to be key as it utilized shorter, more closely spaced time points than the Hall study [75]. The authors demonstrated by fractionation that Tap42-phosphatase complexes exist primarily on membrane structures through association with TORC1. They also showed that the TORC1-associated population of Tap42 is almost

exclusively phosphorylated, while the cytoplasmic pool is not. Importantly, they reported that the TORC1-Tap42-Sit4 association is environmentally sensitive, as rapamycin treatment or nutrient starvation releases the Tap42-phosphatase complex into the cytosol. The cytosolic complex then dissociates further, leaving Tap42 and the free phosphatase. Finally, the authors demonstrated that Tap42 dephosphorylation and complex dissociation occurs long after phosphatase activation. ***These results ultimately illustrated that the cytoplasmic Tap42-PP6 phosphatase complex is indeed the active form, and that the dissociation of Tap42 from Sit4 is not the trigger for phosphatase activity as was previously believed.*** Interestingly, the interaction between Tap42 and PP6 is independent of whether the Saps are present [105].

This conclusion has subsequently been supported by other groups that have demonstrated that phosphatase activity, and particularly Sit4 function, depends on the presence of Tap42 [96]. In fact, loss of Tap42 prevents Sit4-dependent stress-response genes from being activated [110]. It has also been reported that overexpression of Tap42 along with these phosphatases leads to a growth inhibition phenotype that is more substantial than is seen with the phosphatases alone [105]. Altogether, these results show that Tap42 is indispensable for PP6 phosphatase activity, and we speculate that like α4 [112], Tap42 may be functioning as a chaperone to protect the integrity of the phosphatase complexes.

To summarize, when conditions are favorable for growth, phosphatases are sequestered at the vacuole due to TORC1 phosphorylation of both Tip41, a cytoplasmic binding partner of Tap42, and Tap42 itself (**Figure 1-5A**). During the initial stages of nutrient stress (**Figure 1-5B**), the Rho1 GTPase competitively inhibits the Tap42-Kog1 association at the vacuole, which releases and activates the Tap42-PP6 phosphatase complex [50]. Sit4-dependent dephosphorylation of the stress responsive transcription factors results in their localization to the nucleus, and a corresponding shift in the gene expression patterns of the cell. Later in the starvation response (**Figure 1-5C**), the TORC1-dependent phosphorylation marks on Tip41 and Tap42 are removed, although the responsible phosphatase remains unclear (some postulate it may actually by a self-regulatory function of Sit4). At this point, Tip41 competes for the binding of Tap42 and promotes Tap42-Sit4-Sap complex disassembly [113]. This inactivating event usually occurs approximately 30 minutes after initial introduction of the stress, though it is unclear whether Sit4 remains associated with the Sap following release from Tap42 (denoted by question mark in **Figure 1-5C**). Eventually, when the environment permits, an inactive holocomplex of Tap42-Sit4-Sap is reformed at the vacuolar surface through associations with active TORC1. As was mentioned above, only a small amount of the Sit4 in a cell is bound to Tap42, and this is almost exclusively the TOR-responsive fraction. What the remainder of Sit4 is doing in the cell, and how phosphatase molecules are “selected” by Tap42, remains to be seen.

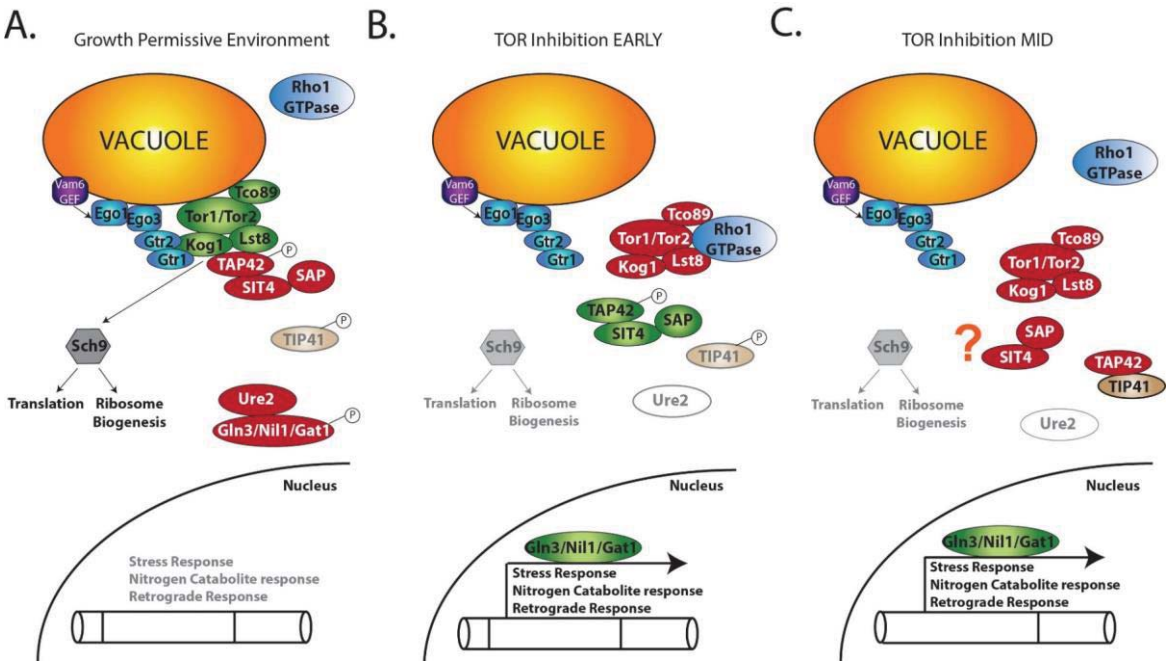

Figure 1-5. The activation of Tap42-associated phosphatases in response to TORC1 inhibition.

Cartoon schematic describing the sequence of events culminating in Tap42-associated phosphatase activation as a cell transitions from a nutrient complete environment (A) to an amino acid deficient one (B and C). Active signaling molecules are indicated in green while inactive complexes are shown in red. The question mark in (C) denotes a point which requires future study. See text for more information.

Amino Acid Signaling through TORC1

In order to sense environmental quality, one of the upstream nutrients TORC1 is particularly sensitive to is nitrogen, typically in the form of free amino acids. The quality of a nitrogen source is defined by its ability to promote glutamine accumulation. These catabolites must fuel the equilibrium reactions which maintain cellular levels of α-ketoglutarate, ammonia, glutamine and glutamate. The mechanism through which TORC1 responds to fluctuations in nitrogen donor quality and amino acid availability is only now being delineated, and yet there is already a striking level of similarity between yeast and mammals, as described below.

Yeast

In yeast, the major amino acid sensing node is the EGO complex, consisting of the structural subunit Ego1, the newly discovered Ego2, a homodimer of Ego3, and the Rag GTPases Gtr1 and Gtr2 [61, 114, 115]. The active conformation of the Rag GTPases includes GTP-bound Gtr1 and GDP-bound Gtr2. When amino acids are not limiting, the guanine nucleotide exchange factor (GEF) activity of Vam6 is activated, which subsequently inhibits the Gtr1-targeted GTPase activating protein (GAP) function of the SEACIT complex [49, 116]. Concurrently, activity of the recently discovered Gtr2 GAP, Lst4-Lst7, is promoted and when combined with the effects of SEACIT inhibition, results in the active Gtr1(GTP)-Gtr2(GDP) configuration [117]. This stabilizes the association between EGO and the TORC1 subunits Kog1 and Tco89, leading to activation of the TORC1 complex [49, 61, 114, 118].

Mammals

The lysosome is the critical amino acid sensing organelle in mammals, and functionally, it is quite similar to the yeast vacuole. The Ragulator complex resides on the lysosomal surface and is analogous to the EGO complex found in yeast. Ragulator consists of a scaffolding subunit p18 (LAMTOR1, analogous to Ego1), a heterodimer of p14 and MP1 (LAMTOR2 and LAMTOR3, analogous to Ego3), and a heterodimer of C7orf59 and HBXIP (LAMTOR4 and LAMTOR5, suggested analogy to EGO2) [119-123]. Additionally, Ragulator is associated with a heterologous pair of Rag GTPases, RagA/B and RagC/D. Regulation of these GTPases occurs in response to nucleotide loading, very similar to how Gtr1 and Gtr2 function in yeast. Specifically, when amino acids levels are sufficient, Ragulator's intrinsic RagA/B GEF activity is stimulated by the v-ATPase, the RagA/B GAP activity of GATOR1 is diminished, and the RagC/D GAP activity of FLCN-FNIP1/2 is activated [123-126]. These events coordinate the active nucleotide configuration of the Rag GTPases, with GTP-bound RagA/B and GDP-bound RagC/D [127]. In their active conformation, the Rag GTPases function to bridge mTORC1 and the lysosome [128]. At the lysosomal surface, mTORC1 is activated via interactions with the Rheb1 GTPase [129]. A recent study from Fawal et al. suggests that in addition to amino acid dependent spatial regulation of mTORC1, there may be a

mechanism in place which also links amino acid availability and the cellular distribution of Rheb1 [130]. The group identified microspherule protein 1 (MCRS1) as a critical mediator of Rheb lysosomal localization and nucleotide loading status in an amino acid-dependent fashion. Until recently, it was unclear how cells relayed amino acid levels in the lysosomal lumen to the Ragulator complex and mTORC1. A number of groups now report that the transmembrane solute carrier SLC38A9 is able to monitor amino acid accumulation in the lysosomal lumen and interact with the Ragulator complex in an amino acid-dependent fashion [131-133]. In total, activation of mTORC1 requires significant spatial and temporal coordination, as the Rags are responsible for promoting mTORC1's localization to the lysosome, MCRS1 is responsible for bringing active Rheb to the lysosome, and Rheb is responsible for activation of mTORC1 [128].

The oncoprotein Rab1A was also recently identified as an amino acid responsive activator of mTORC1, but interestingly, it does so independently of the Rag GTPases [134]. Rab1A is overexpressed in colorectal cancer and this correlates with tumor invasiveness and an overall poor prognosis. High levels of Rab1A means cells are far more sensitive to amino acid starvation. In fact, they require high levels to continue growing and are said to be nitrogen "addicted". Altogether, this suggests that deregulation of amino acid signaling through mTORC1 can contribute to cellular dysfunction and organismal disease.

TORC1's Nuclear Functions

Given the array of environmental stimuli that influence TORC1 activity, and the role TORC1 plays in regulating the cell cycle, gene expression and anabolism, the complex is uniquely qualified to serve as a link between nuclear processes and nutrient availability. Yet to date, most of what is known about TORC1 is in reference to its cytoplasmic functions. This is due in large part to a number of publications in both yeast and mammalian cell culture models that suggest the majority of TORC1 resides in the cytoplasm, and more specifically, at the vacuole/lysosomal compartments [119, 124, 128, 135]. And while this view represents the historical understanding of TORC1, it fails to account for an emerging body of literature which has identified a role for nuclear-localized Tor kinase, and even components of TORC1, in transcriptional regulation [136-139]. There is still a considerable amount of research to be done in order to fully understand the nuclear functions of Tor kinases. However, the fact that TORC1 can be found in the nucleus, and even at specific gene promoters, means that the complex may directly bridge environmental status to cell cycle regulation, gene transcription, and/or the epigenome.

Effects on ribosomal DNA transcription

Traditionally, there have been two levels at which TORC1 can affect transcription, particularly as it relates to ribosome biogenesis. The first involves regulation of RNA polymerase I (RNAPI) promoter binding through phosphorylation of

Rrn3 (TIF-IA in mammals); an integral transcription factor which localizes to the rDNA to recruit RNAPI. At the rDNA, RNAPI is responsible for production of the 35S pre-ribosomal RNA (rRNA), which is ultimately co-transcriptionally processed into the 25S, 18S, and 5.8S rRNAs. These rRNAs are critical components of the ribosome machinery. Inhibition of TORC1 results in a rapid redistribution of RNAPI from the nucleus to the nucleoplasm, as well as enhanced Rpd3 binding to the rDNA [140, 141]. Subsequent Rpd3-dependent histone H4 lysine 5 and 12 deacetylation promotes condensin complex association, which compacts and stabilizes chromatin leading to decreased nucleolar volume [140, 142]. There is controversy in the field as to whether the RNAPI redistribution is a consequence of Rpd3-dependent transcriptional repression (via deacetylation), or is independent of Rpd3 [140, 143]. TORC1 has also been identified as a regulator of RNAPII-dependent RP gene expression, and RNAPIII-dependent 5S rRNA and tRNA production. It does so via Sch9-dependent phosphorylation of RP transcription factors such as Rtg1/3, Gln3, Tod6 and Dot6, or the RNAPIII negative regulator Maf1 [75, 86, 144-149]. These phosphorylation events mediate both the activity and localization of these factors as was mentioned in the previous sections.

TORC1, sirtuins, and the epigenetic modification of histones

Besides the direct mediation of polymerase function and transcription factor localization, there seems to be a poorly characterized third layer of TORC1-dependent effects on gene expression that involves regulation of chromatin structure through histone post-translational modifications [12, 66, 150-152]. Work from our lab shows that direct inhibition of yeast TORC1, either through subunit deletion or rapamycin treatment, results in globally diminished histone H3 lysine K56 acetylation (H3K56ac); a mark tied to DNA repair, maintenance of rDNA copy number, and overall genomic stability [66, 153, 154]. We also demonstrate that TORC1-regulated H3K56ac influences RNAPI binding to the 35S rDNA, as well as binding of the key Pol I transcriptional regulators Hmo1 and the SSU processome [66]. Although the exact mechanism linking TORC1 to this acetyl mark is currently unknown, our previous data suggests that regulation of the sirtuin histone deacetylases may be involved. Specifically, deletion of *HST3* or *HST4* is sufficient to restore H3K56ac in a TORC1 mutant [66].

The sirtuins are a conserved, NAD^+-dependent family of histone deacetylases that in yeast includes Hst1, Hst2, Hst3, Hst4 and Sir2 (summarized in **Table 1-1**). They are sometimes referred to as class III histone deacetylases. Interestingly, despite their varied functions, all seven human sirtuins (SIRT1-7) most closely resemble yeast Sir2 according to standard BLAST alignment [155]. The relationship between sirtuins and TORC1 is particularly interesting as both have been heavily discussed as regulators of aging [70, 81, 156]**.** As mentioned previously, inhibition of TORC1 with rapamycin or CR extends lifespan and, fascinatingly, activation of sirtuin function with resveratrol mimics these effects [70, 157-159]. As a whole, the sirtuins' best characterized role in the cell is transcriptional silencing, particularly at the silent mating type loci, telomeres and rDNA. To date, there are only a few characterized substrates for the yeast sirtuins, including the non-histone protein Ifh1 (deacetylated by Hst1 and Sir2), and the histone residues

Table 1-1. Summary of sirtuin histone deacetylase localization and substrate specificity in yeast.

HDAC	Subcellular Localization	Genomic Localization	Histone Substrates	Non-Histone Substrates
Hst1	Primarily Nuclear [160]	Telomeric repeats, tRNA genes, Pol-II transcribed genes [161]	H3K4Ac [162]	Ifh1 [163]
Hst2	Primarily Cytoplasmic (shuttled out of nucleus [160, 164, 165])	Telomeric repeats, rDNA, Silent mating type loci, Stationary phase granules [165-167]	H4K16Ac [168]	
Hst3	Primarily Nuclear [160]	Telomeric repeats, rDNA, Silent chromatin, Sites of DNA repair [153, 169-173]	H3K56Ac [154, 174, 175]	
Hst4	Primarily Nuclear (shuttles to mitochondria [160, 176])	Telomeric repeats, rDNA, Silent chromatin, Sites of DNA repair [153, 169-173]	H3K56Ac [154, 174, 175]	
Sir2	Primarily Nuclear [160]	Telomeric repeats, rDNA, Silent mating type loci [13, 161, 172, 173]	H3K4Ac [162] H3K9Ac [177], H4K16Ac [177, 178]	Ifh1 [163]

H3K4ac (deacetylated by Hst1 and Sir2), H3K9ac (deacetylated by Sir2), H3K56ac (deacetylated by Hst3 and Hst4), and H4K16ac (deacetylated by Hst2 and Sir2) [154, 162, 163, 168, 170, 174, 175, 177, 178]. The sirtuins are primarily found in the nucleus, with two exceptions; Hst2 is actively shuttled from the nucleus to the cytoplasm in a Crm1-dependent fashion due to the presence of a nuclear export signal [164], while Hst4 is known to move from the cytoplasm to the mitochondria in response to biotin starvation [176]. A similar shuttling phenomena is also seen with the mammalian sirtuins, SIRT1 and SIRT2 (see **Table 1-2**).

Hst3 and Hst4 are unique in that they appear to be regulated in a cell-cycle dependent fashion. The protein levels of Hst3 fluctuate throughout the cell-cycle in response to Mec1- or Cdk1-dependent phosphorylation, which promotes SCF^{Cdc4}-dependent polyubiquitination and degradation via the proteasome [179, 180]. A high-throughput screen designed to identify phosphoproteins that bind the SCF^{Cdc4} ubiquitin ligase determined that Hst4 may be regulated in a similar fashion [181]. Importantly, the phosphatase that opposes these SCF^{Cdc4} binding phosphomarks is still unknown.

Of all the sirtuins, the best characterized is Sir2. Its role in cellular aging and CR-mediated lifespan extension has been investigated over the last decade, with many groups linking deletion of *SIR2* to rDNA instability and yeast senescence [13, 69, 182, 183]. Specifically, inhibition of yeast TORC1 promotes rDNA association of Sir2, possibly in concert with the RENT complex, ultimately resulting in a hypoacetylated and deactivated rDNA chromatin architecture [13]. Sir2-dependent rDNA deacetylation enhances stability, suppresses extra-ribosomal circle formation, and significantly extends yeast replicative lifespan [13].

There are also noted interactions between mTORC1 and sirtuins in mammals. For example, SIRT4 gene expression is tied directly into glutamine metabolism via mTORC1 [184]. When amino acids are limiting, mTORC1 promotes proteasomal destruction of CREB2, a transcriptional regulator of SIRT4, which ultimately results in a decrease in SIRT4 levels. In this way, mTORC1 can modulate activation of the glutamine dehydrogenase promoter, a critical regulatory step in the production of key TCA cycle metabolites. There are a number of cancers that display aberrant SIRT4 expression, suggesting that dysfunctional mTORC1 activity may promote transformation through altered cell metabolism at the level of chromatin regulation. A second mammalian sirtuin, SIRT1, has been identified as a negative regulator of mTORC1 via interactions with the upstream TSC complex [185]. Interestingly, SIRT1 overexpression can complement loss of Sir2 at the level of rDNA stabilization, and SIRT6 (like Hst3 and Hst4) deacetylates H3K56ac, suggesting there is evolutionary conservation of function of these enzymes [177, 186].

A number of fascinating genetic interactions between TORC1 and histone H3 suggest signaling through the TORC1 pathway, or TORC1-mediated epigenetic modifications, may directly influence other chromatin-based processes. Our laboratory screened individual mutants of the majority of residues on the H3 and H4 tails and found only one, H3K37, whose maintenance is indispensable in response to decreased TORC1

Table 1-2. Summary of sirtuin histone deacetylase localization and specificity in mammals.

HDAC	Subcellular Localization	Histone Substrates	Non-Histone Substrates
SIRT1	Actively shuttles between nucleus and cytoplasm, primarily nuclear [187, 188]	H3K9Ac [177], H4K16Ac [177, 189, 190], H3K9me2 [191] (indirect)	LC3 [192, 193], Atg5/7/8 [194], p300 [195], MOF [196], Tip60 [197, 198], p53 [199-201], FOXO factors [202, 203], NFκB [204], c-Myc [205], HIF-1α [206-208], PGC-1α [209], LKB1 [210], Ku70 [211], PARP1 [212, 213]
SIRT2	Actively shuttles between nucleus and cytoplasm, primarily cytoplasmic except during G2-M [187, 214, 215]	H4K16Ac [168]	p53 [216], FOXO3a [217, 218]
SIRT3	Mitochondrial, small nuclear fraction at stress response genes [187, 219-221]	H4K16Ac [222] (indirect)	AceCS2 [223, 224], ALDH2 [225], SdhA [226, 227], Ku70 [228]
SIRT4	Mitochondrial [187, 221, 229]		GDH [230]
SIRT5	Mitochondrial [187, 221]		CPS1 [231, 232]
SIRT6	Nuclear [187, 233]	H3K9Ac [234-236], H3K18Ac [237], H3K56Ac [236]	CtIP [238]
SIRT7	Nucleolar [187, 239]	H3K18Ac [240]	

activity [152]. These dramatic phenotypes are independent of glucose-dependent Ras/PKA signaling, suggesting the linkage between TORC1 and H3K37 is specific. Interestingly, because TORC1 is also sensitive to glucose, this may indicate that H3K37 is more strongly coupled to the amino acid sensing arm of TORC1. Mutation of this lysine to an alanine (H3K37A) results in a dramatic redistribution of high mobility group proteins (HMGs), including Nhp10, from chromatin to the cytoplasm accompanied by accelerated chronological aging. This is particularly fascinating considering that Nhp10 is a member of the INO80 chromatin remodeler, and TORC1 has already been shown to affect transcription through altered recruitment of histone chaperones and chromatin modifying complexes [241, 242]. A number of other remodelers are also anchored to chromatin through their HMG-containing subunit, a family of structural proteins that will be discussed further below.

High-Mobility Group Proteins: "The Architectural Transcription Factors"

HMGs are highly charged, extremely abundant, and the second most common protein found on chromatin besides the histones. There are three families of HMGs in mammals: HMGA, HMGB and HMGN. All three compete with H1 for binding to the linker DNA, and weakening of this H1 association results in decreased chromatin compaction [243-245]. Because yeast do not have obvious HMGA and HMGN factors, the HMGB class will be our main focus. HMGB family members bind the minor groove of B-form DNA with relatively low sequence specificity to introduce sharp bends or kinks into the strand. They are particularly enriched at the nucleosomes flanking transcriptional start sites, but can also be found at four way DNA junctions and significantly under twisted DNA [246]. The effect HMGBs have on gene expression (stimulatory or inhibitory) is often context dependent. Some data suggest the HMGBs simply distort DNA to promote incorporation of the transcriptional machinery, while others argue that in addition to bending DNA, HMGBs may also bridge associations of basal transcription factors (ex. TBP) with the transcriptional machinery [247-250].

The best-characterized mammalian HMGB member is the prototypical HMGB1. It has been identified as the most mobile of all nuclear proteins, as it can traverse the entire nuclear compartment in just over a second [251]. Interestingly, during cellular apoptosis, HMGB1 movement in the nucleus ceases and it remains anchored to chromatin, though the mechanism regulating this process is unknown [251]. This effect is believed to promote severely under-acetylated heterochromatic DNA. *In vitro* nucleosome binding studies, conducted with an array of HMGB1 truncation mutants, identified a specific C-terminal acidic sequence of HMGB1 that is necessary to promote transcription [252]. Crosslinking experiments show that the acidic region functions to enable HMGB1 to associate with the nucleosome via the histone tails, and specifically H3. Kawase et al. followed up on this work, utilizing mass spectrometry to perform a characterization of the association between HMGB1 and the nucleosome [253]. They reported that the acidic C-terminal tail of HMGB1 makes direct contact with H3K36 and H3K37 on H3, suggesting these sites play a vital role in securing HMGB1 to chromatin. HMGB1 is released from chromatin during necrosis to promote the innate immune

response by binding the Toll-like and RAGE receptors on immune cells [251, 254]. Association of HMGB1 with its RAGE receptor in tumor cell mitochondria is essential for optimal mitochondrial function, enhanced ATP production, and the dysfunctional bioenergetics observed in tumor microenvironments [255]. The nuclear to cytoplasmic translocation, and subsequent extracellular secretion, of HMGB proteins in senescent cells also promotes the senescence-associated secretory phenotype (SASP), which increases cancer risk in aging tissues [256]. Considering all of the evidence described above, deregulation of HMGB chromatin binding in mammals, particularly as cells age, has the potential to be transformative.

Yeast HMGBs fall into two general categories based on the number and structure of their HMG domains: a single sequence-specific HMG box, or two relatively sequence-independent HMG boxes. There are seven known HMGBs in yeast, Hmo1, Nhp6a/b, Nhp10, Ixr1 [257-259], Rox1 [258, 260-262] and Abf2 [263-266]. We will elaborate on the function of the HMGs that are particularly relevant to this work; Hmo1, Nhp6a/b and Nhp10.

Hmo1 is probably the best-characterized member of the yeast HMGB family. Hmo1 is exclusively nuclear and organized into three domains, including a classical HMG box required for DNA binding and bending ("HMG Box B"), a non-traditional HMG box whose function is controversial ("HMG Box A"), and a lysine-rich C-terminal nucleolar targeting sequence that also contributes to DNA binding and bending [267, 268]. The HMG boxes can interact with one and other, and HMG box A is also able to associate with Hmo1's C-terminal tail. Hmo1 chromatin binding promotes compaction, the introduction of DNA loops or bends, and SWI/SNF- and ISWIa-dependent chromatin remodeling [267, 269, 270]. Hmo1 is involved heavily in ribosome biogenesis, an anabolic process significantly regulated by TORC1 (discussed previously). It is highly enriched in the nucleolus (nucleolar/nucleoplasmic interface) on active rDNA, and also localizes to the promoter of the RP genes [66, 271-274]. An elegant complementation study by Albert et al. identified Hmo1 as an rDNA binding component of yeast Pol I [275]. The authors also demonstrated that Hmo1 has a robust genetic interaction with Rpa49, suggesting involvement in Pol I initiation.

Nhp6a and Nhp6b are functionally redundant HMG family members, although Nhp6a is expressed at much higher levels in the cell. They are homologous to mammalian HMGB1/2, and play a significant role in chromatin remodeling [276, 277]. Nhp6a contributes to the recruitment of the FACT histone chaperone complex, which promotes a chromatin state permissive for transcription, replication, and repair [278-281]. Nhp6a also enhances the nucleosome sliding ability of the SWI/SNF ATP-dependent chromatin-remodeling complex [269]. *In vivo* studies with Nhp6a find that even in the absence of its acidic domain, chromatin context is still a key determinant of genome-wide binding [279, 282]. Given these interactions with well-characterized mediators of chromatin structure, aberrant Nhp6a/b localization or abundance is certain to impact gene expression patterns and overall cellular function. And finally, similar to the mammalian HMGB1 [251, 254], the nuclear to cytoplasmic translocation of Nhp6A is a hallmark of necrosis suggested to occur as a consequence of chronological aging [283].

Nhp10 is somewhat unique as it is the only HMGB known to associate with the INO80 ATP-dependent chromatin remodeling complex [284]. Nhp10 functions in INO80 to bridge the remodeler's interaction with phosphoH2A.Z at double strand breaks, and also to protect DNA ends from exonucleatic cleavage at the break site [284-287]. Sekiguchi et al. find that in strains where INO80's catalytic subunit has been mutated, loss of EGO function is synthetically lethal, implicating INO80 in TORC1-dependent chromatin regulation [288]. As described above, Nhp10 chromatin binding also appears to be linked with TORC1 activity via the H3K37 residue, though the exact nature of this relationship is currently unclear [152].

Tor Dysfunction and Age-Related Pathologies

Aging is a very complex process which remains poorly understood at the molecular, cellular, and organismal level. Studies over the past several decades have identified significant overlap between lifestyle, environmental factors, and epigenetics in determining the long-term health and viability of an organism. Fascinatingly, TORC1 may lie at the center of all three of these. It is clear that as an organism ages, a number of pathologies become more prevalent, including cardiovascular disease, cancer, diabetes and dementia. These diseases are all believed to be driven at some level by mTORC1 hyperfunction, which is itself a result of aging [289]. But it remains unclear as to why overactive mTORC1 has such a profound effect on cellular physiology and longevity.

The apparent association of TORC1, sirtuins and chromatin dynamics is intriguing as they have all been heavily cited as regulators of aging. Yet to our knowledge, there is very minimal mechanistic understanding to link all three. Inhibition of TORC1 with rapamycin or CR extends lifespan [68, 70-74, 290], activation of sirtuin function through treatment with resveratrol mimics these effects [67, 157-159, 291], and deletion of sirtuins dramatically reduces lifespan [170, 292]. This fact is incredibly important because we will present data showing that TORC1 inhibition promotes sirtuin function and histone deacetylation through a novel subcellular accumulation and stabilization mechanism. Such a relationship could also explain why there is controversy regarding which target (mTor vs. sirtuins) would be best to pursue in slowing or reversing cellular aging (as reviewed by Sinclair) [290].

The majority of tissues in the body consist of a large population of post-mitotic, fully-differentiated cells, and a smaller stem cell niche tasked with replenishing and maintaining the population over time. Classical aging phenotypes are most often attributed to cellular chronological aging, which is marked by an overall decline in cell health and function, culminating in physiological defects on the organismal scale. Recent evidence in skeletal muscle and the brain suggests that the longevity and viability of both the long-lived post-mitotic populations, as well as their stem cell niches, depends on sustained maintenance of chromatin as cells mature/age. Jurk et al. demonstrate that upon proliferative cessation, mature neurons enter a senescent-like state marked by heterochromatinization, elevated ROS production, persistent DNA damage, and other

traditional indicators of the senescence-associated secretory phenotype [293]. These effects become more prominent and deleterious with age but can be partially reversed by CR. And although the authors do not address the nature of this effect, it does suggest the possibility that nutrient responsive TORC1 function may contribute to the development of age-related senescence. We are particular fascinated with the chromatin effects observed in these cells, because it is now known that chromatin states in non-mitotic neurons are not nearly as static as they once seemed [294-297]. Gong et al. show that in aging mouse brains, there is a notable shift in the epigenetic landscape, including the acetylation and methylation of H3/H4, and many of these same modifications are responsive to CR or rapamycin treatment [298]. Liu et al. report that maintenance of quiescence in skeletal muscle stem cells correlates to a unique epigenetic signature which degrades with age [299]. Corruption of these signatures, specifically a genome-wide overrepresentation of H3K27me3, results in heterochromatin accumulation which the authors speculate contributes to an observed loss of stem cell function with age.

The above demonstrates how chromatin deregulation contributes to loss of function in vital cell populations, which ultimately results in organismal aging. It is the goal of this dissertation to characterize the mechanism by which TORC1 activity affects these processes, and to evaluate their potential contribution to organismal viability and longevity. In other words, to functionally understand the intersection between an organism's environment, lifestyle, and epigenome as it relates to health and longevity. The project presented below is guided by the following Specific Aims:

> **(1)** *Define the contribution of TORC1 signaling to the regulation of histone acetylation modifications and elucidate the mechanisms involved.*
>
> **(2)** *Determine the impact that TORC1-regulated histone acetylation has on cellular functions.*
>
> **(3)** *Define the role of the poorly-understood TORC1 subunit Tco89 in TORC1 signaling and epigenetic regulation.*

Addressing these Specific Aims will provide significant insight into TORC1-dependent coordination of epigenetic mechanisms under normal biological conditions, while also identifying how TORC1 dysfunction and epigenetic corruption may contribute to disease mechanisms on an organismal scale.

CHAPTER 2. MATERIALS AND METHODOLOGY

Yeast Strains, Plasmids, and Culture Conditions

All of the yeast strains and plasmids used in this work are described in **Tables A-1** and **A-2** (in **Appendix A**), respectively. Strains constructed in our lab, including gene deletions and epitope tags, were made using PCR-generated targeting cassettes as previously described [300]. Unless otherwise stated, cells were grown in YPD (1% yeast extract, 2% peptone, and 2% dextrose) at 30° C with shaking. For experiments conducted in synthetic complete media, dropout mix was incorporated and supplemented with the appropriate amino acids to compensate for the auxotrophy of the strains. All media components were purchased from US Biologicals or Research Products International (RPI). Phos-tag was purchased from Wako Chem. Rapamycin, nicotinamide, sodium butyrate, trichostatin A, L-methionine sulfoximine (MSX), 2-(N-morpholino) ethanesulfonic acid (MES), and caffeine were purchased from either Fisher Scientific or Sigma-Aldrich. Galactose was purchased from MP Biomedical. The concentrations of these reagents are noted in the text.

Cloning primers for Tco89 fragmentation and Tco89/Sit4 complementation studies were designed as discussed in the text and as previously described [300]. The open reading frames of *TCO89* and *SIT4* were cloned as C-terminal mono-FLAG fusions into the BamHI/XbaI (Tco89FL and fragments) or BamHI/EcoRI (Sit4FL) restriction sites of the pRS416ADH plasmid, which contains an *ADH1* promoter and *CYC1* terminator [301]. PSI/PRED prediction software was used to avoid disruption of any potential secondary amino acid structure (discussed in Chapter 5) [302]. See **Table A-2** for more information.

Antibodies and Stains

Antibodies used in this work were obtained from the following; α-RPS6 (Abcam), α-phosphoS6 (Cell Signaling), α-FLAG (Stratagene), goat α-rabbit HRP conjugated secondary (Jackson), α-Myc 4A6 (Millipore), α-HA and α-Myc A14 (Santa Cruz), G6PDH (Sigma), α-FLAG (Thermo), goat α-rabbit FITC-conjugated secondary (Rockland). Histone antibodies were all obtained from Active Motif. IgA- and IgG-conjugated beads for immunoprecipitation were from Santa Cruz. For live cell work, 5(6)-Carboxyfluorescein diacetate (CFDA) vacuolar stain was obtained from Invitrogen, dihydroethidium (DHE) from Fisher, and Hoechst nuclear stain from Life Technologies. For fixed cells, the Vectashield mounting media containing DAPI was purchased from Vector Labs. The apoptosis and necrosis staining experiments were conducted using an AnnexinV-FITC apoptosis kit from Clontech, and YO-PRO-1, propidium iodide (PI) and SYTOX from Life Technologies.

Western Blotting and Statistical Analysis

Cells were grown to log phase (OD_{600} ≈0.8) in the indicated media as described above prior to treatment with drug (rapamycin or MSX) or galactose (2% final concentration), unless noted. Typically, cultures were set up to double 3 to 4 times before reaching this OD, ensuring that the majority of cells were replicatively young and metabolically active. Cells were then transferred to 50 mL falcon tubes using sterile technique, pelleted in a tabletop centrifuge, and frozen at -80°C. Pellets were resuspended in pre-chilled cracking buffer (10 mM Tris pH 8.0, 150 mM NaCl, 0.1% Nonidet P-40, 10% glycerol, 1 mM DTT) with additional phosphatase, histone deacetylase, and protease inhibitors. Glass beads were added to each tube, and the cells were lysed using a cold-room bead beater (3x 30 sec pulse with 3 min on ice in-between). Supernate was clarified at 4°C and stored at -80°C. Extract concentrations were determined using a traditional Bradford assay, and 35 µg samples were resolved by SDS-PAGE and transferred to PVDF membrane. In the case of samples subjected to SDS-PAGE with Phos-tag additive (50 µM), the included manufacturer's instructions were followed. Membranes were probed overnight at 4°C with primary Ab. The blots were washed in TBST (10% TBS, 0.1% tween) for at least an hour with buffer replacement every 15 minutes. The blots were then incubated in secondary Ab for between 2 and 4 hours before developing using autoradiography. Films were scanned and analyzed by ImageJ where denoted. For determining significance, we used a two-tailed, unequal variance, pairwise Student's t-test. *p<0.05, **p<0.01, ***p<0.001.

Spotting Assays

Cells were grown overnight at 30°C with shaking to saturation. OD_{600} readings were taken and equivalent numbers of cells were aliquoted into column A of a sterile 96-well culture plate (see formulas below). The volumes in column A were made up to 200 µL with sterile water.

$$\mu L\ cells = \frac{200}{OD_{600}\ of\ stationary\ culture} \qquad \mu L\ H_2O = 200 - \mu L\ cells$$

Five-fold serial dilutions were then performed in which 40 µL of column A were transferred into 160 µL of water in column B and so forth. Cells were spotted to plate media and incubated as noted. Images were taken daily for 5-7 days using a UVP Digital Imaging System.

RT-qPCR

cDNA was synthesized from DNase I treated cellular RNA using random hexamer primers and the ImProm II reverse transcriptase system from Promega. Gene specific qPCR was conducted and normalized to the *SPT15* housekeeping gene as previously described [303]. Primers are available upon request.

Indirect Immunofluorescence Confocal Microscopy

For studies regarding sirtuin localization, the following technique was utilized. First, cells were grown to log phase and treated as indicated. The cells were then fixed with 37% formaldehyde, pelleted at 800xg for 4 minutes, and washed twice with 4 mL of 0.1 M potassium phosphate buffer (K_2HPO_4, pH=6.5) and once with 4 mL P solution (1.2 M sorbitol, 0.1 M K_2HPO_4, pH=6.5). Pellets were then gently resuspended in 1 mL P solution and incubated at room temperature with 15 µL zymolase (15 mg/mL in P solution) and 5 µL β-mercaptoethanol for 25 minutes. Cell wall digestion (spheroplasting) was confirmed using a phase contrast microscope. After spheroplasting, cells were gently pelleted and resuspended in 150 µL of P solution. The resulting suspension was aliquoted to a poly-lysine coated slide and cells were allowed to settle for 20 minutes prior to blocking (8% bovine serum albumin/PBS/0.5% Tween 20). Slides were then placed in a humidified chamber and incubated in primary antibody overnight at 4°C. Following primary incubation, slides were washed four times with blocking solution, prior to the addition of fluorophore-conjugated secondary antibody (60 minutes at room temperature). From here on slides were protected from light. After the secondary incubation, slides were washed four times with blocking solution and twice with PBS. Finally, a drop of DAPI-containing Vectashield mounting media was placed on the slides and coverslips were positioned and sealed. Samples were imaged with the 63x oil Olympus objective on a Zeiss LSM 700 confocal microscope.

Direct Immunofluorescence Confocal Microscopy

For studies measuring HMG localization, cells were grown to log phase in duplicate 10 mL cultures and treated as indicated. Treatments often occurred over 60 minutes, so immediately following addition of drug, the process to image the untreated cells began. Untreated cells were spun down, washed with sterile water, transferred to a microfuge tube and pelleted. The cells were then resuspended in 100 µL sterile water with 2 µL Hoechst and incubated with agitation away from light for 15 minutes. Finally, the untreated cells were spun down, resuspended in 10 µL sterile water with 0.5 µL Hoechst and cover slipped as quickly as possible to avoid effects the altered nutrient state may have on the results. Slides were imaged with the 63x oil Olympus objective on a Zeiss LSM 700 confocal microscope. Following the one hour incubation of the treated cells, the above steps were repeated.

Image Analysis in Zen 2 Blue

In order to quantitate the subcellular localization of the tagged proteins, images taken on the Zeiss LSM 700 were analyzed in the Zen Lite Version 2.0.0 software program (blue edition) as previously described [304]. Briefly, using the Spline Contour tool, a border was drawn around the outer edge of each cell. Then, a second border was drawn around the nucleus. Upon closure of each border, information was provided, including the area within the border, and the mean intensity of each channel inside that

space. The mean intensity value for the green channel within the nucleus was multiplied by the area within the nuclear border to obtain our total nuclear fluorescence intensity (TNFI).

$$TNFI = nuclear\ mean\ intensity\ value * nuclear\ area\ (nm^2)$$

This calculation was repeated for the values from the outer cell border, providing us a value we refer to as the total cellular fluorescence intensity (TCFI).

$$TCFI = cellular\ mean\ intensity\ value * cellular\ area\ (nm^2)$$

From there, we simply divided the total nuclear intensity by the total cellular intensity and multiplied by 100 to get the percentage of our protein of interest that resides in the nucleus.

$$\%\ nuclear = \frac{TNFI}{TCFI} * 100$$

Analysis fields were chosen at random, with approximately 20-40 cells quantified per condition, per independent biological replicate (4-6 replicates). Cells with a cellular mean intensity value under 50 units were excluded from calculations as we believe this is the threshold of adequate immunostaining.

Sirtuin Turnover/Half-Life Analysis

Cells were grown to log phase in 200 mL YPD flasks. At T_0, 50 mL aliquots were sterilely sampled from each sample, pelleted, and frozen. Cycloheximide (CHX) was then added to each flask at a concentration of 100 µg/mL. 50 mL aliquots were retained as described above at the time points indicated. Whole cell extracts (WCEs) were prepped and analyzed by α-Myc immunoblot. Films were scanned, quantified with ImageJ, and sirtuin signals were normalized to total protein via G6PDH.

Apoptosis, Necrosis, DHE and CFDA Assays

For analysis of apoptosis and necrosis, log phase cells were pelleted, washed twice with sterile PBS, and incubated for 20-30 minutes in the respective dyes: PI (50 µg/mL) and YO-PRO-1 (10 µM). Cells were then transferred to flow cytometry tubes, processed on a BD LSRII flow cytometer, and analyzed using FLOWJO V10. DHE (30 µM) and CFDA (100 µM) staining experiments were identical to the above except for the use of the different stains, and the retention of cells for additional confocal analysis.

Scoring for Tco89 Fragment Phenotypes

WT and *tco89Δ* cells were transformed with control vector or Tco89 N-terminal truncation fragments as indicated, grown to saturation, and spotted as detailed previously (see "Spotting Assays" section of this chapter). Growth on the spotting plates was scored as described by Rizzardi et al. [305]. Briefly, mutants were scored on a scale of -3 to 3, with a score of 1 representing an approximate 5-fold difference in growth and a value of 3 being a 125-fold difference. Strains exhibiting growth defects compared to wild-type cells received a negative value, while those with enhanced growth were given a positive value. A value of 0 indicates growth essentially equivalent to the control. Scores from at least five independent transformations were averaged, and a heat map was constructed in Microsoft Excel.

CHAPTER 3. TORC1 FUNCTION MAINTAINS HISTONE ACETYLATION BY OPPOSING THE SIT4-DEPENDENT NUCLEAR ACCUMULATION OF SIRTUINS[1]

TORC1 Mediates Site-Specific Histone H3 and H4 Acetylation in Response to Environmental Stress, Particularly Glutamine Starvation

Our previous work identified a connection between TORC1 and the control of global H3K56ac [66]. We wanted to determine whether this effect was unique to H3K56ac, or if TORC1 also regulated other acetylation states on the histone H3/H4 tails. To do so, wild-type and *tco89Δ* cells were grown to log phase and wild-type cells were either mock or rapamycin treated (300 nM) for 60 minutes. The concentration and length of rapamycin treatments selected were confirmed to diminish TORC1 activity by phosphoS6 blot (**Figure B-1** in **Appendix B**). WCEs prepared from these samples were screened for alterations to distinct histone acetylation states by immunoblotting (IB) with the indicated antibodies **(Figure 3-1A)**. Films were scanned and analyzed by ImageJ, and relative histone acetylation was calculated by normalizing to total H3 with the mock treated samples set to 1 (graphed in **Figure 3-1B**). As shown in **Figure 3-1A**, TORC1 inhibition resulted in a dramatic site-specific reduction of acetylation at H3K18 (H3K18ac), H3K23 (H3K23ac), and H4K12 (H4K12ac), while other acetylation states were unaffected. These changes cannot be attributed solely to downregulation of transcription-coupled marks as we find that H3K4me3, a histone modification that demarcates actively transcribed genes, was unaffected. Loss of these histone modifications is unlikely to be explained by indirect consequences of TORC1 inhibition, since the acetylation reduction was observed as early as 20 minutes post-rapamycin treatment (**Figure 3-1C**). Furthermore, we demonstrated that exogenous Tco89 expression in the *tco89Δ* rescued acetylation, thus confirming that reduction of histone acetylation was due solely to the loss of this TORC1 subunit (**Figure 3-1D**).

Nitrogen metabolism, described in Chapter 1, is an established activator of TORC1 via the vacuolar-localized EGO and v-ATPase complexes. Prior evidence suggested carbon metabolism may regulate many of the histone acetylation states identified in **Figure 3-1A** [306]. Therefore, we next compared the impact of these nutrient signals on our sites of interest to determine whether the mechanisms which link carbon and nitrogen to the epigenome are overlapping, via TORC1, or are distinct. We first utilized the glutamine synthetase inhibitor MSX to block glutamine biosynthesis and impair nitrogen metabolism (**Figure 3-2A**). Treatment with 2 mM MSX mimicked the decrease in H3K18ac that occurs in response to direct TORC1 inhibition (**Figure 3-2B,** upper panel and graph). We confirmed MSX treatment reduced TORC1 activity by α-phosphoS6 IB (**Figure 3-2B,** lower panel). However, changing the quality of the carbon source from glucose to non-fermentable carbon (glycerol) failed to affect acetylation in

[1] Modified with permission from Genetics Society of America. Workman, J.J., H. Chen, and R.N. Laribee, *Saccharomyces cerevisiae TORC1 Controls Histone Acetylation by Signaling Through the Sit4/PP6 Phosphatase To Regulate Sirtuin Deacetylase Nuclear Accumulation.* Genetics, 2016.

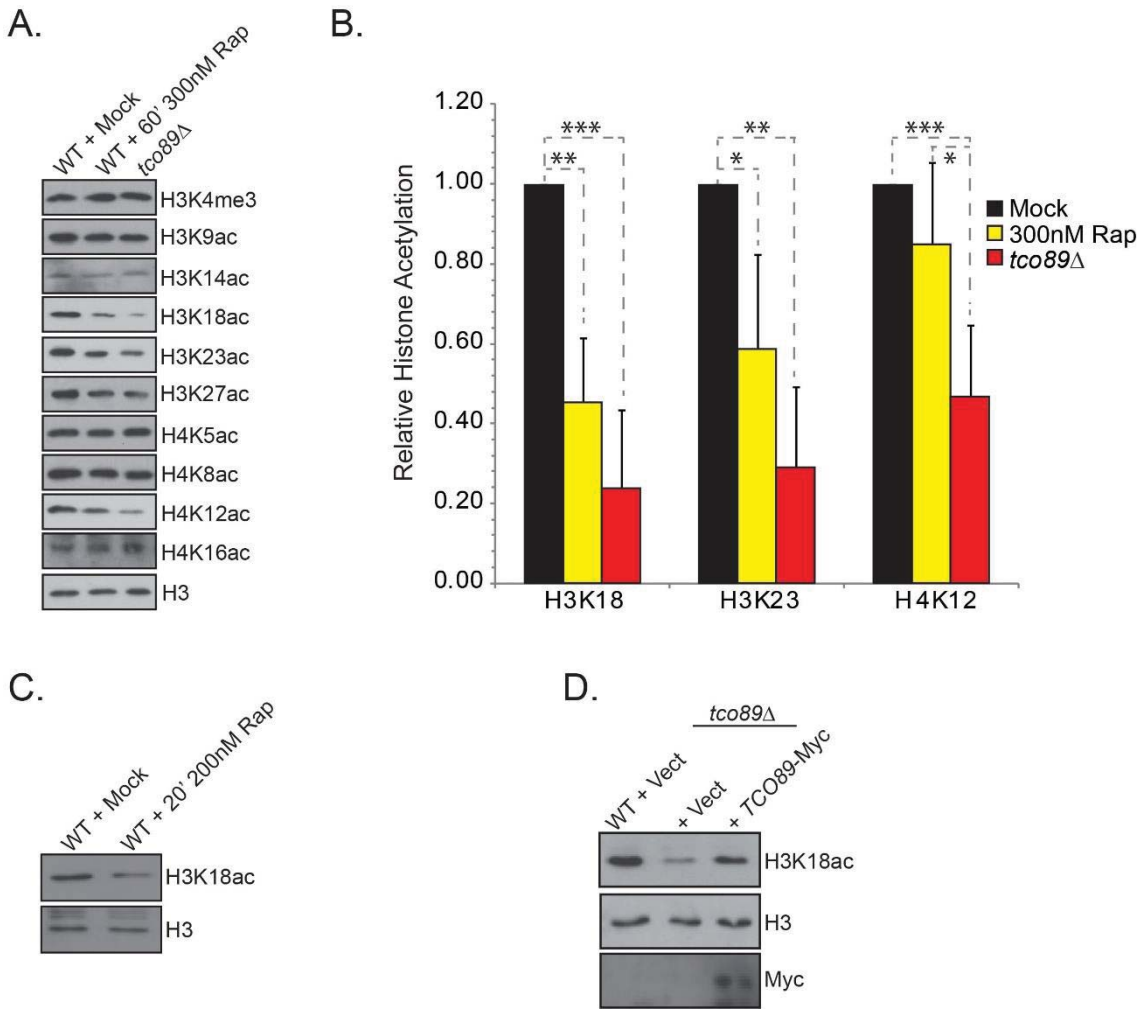

Figure 3-1. TORC1 signaling coordinates site-specific lysine acetylation on a subset of histone H3 and H4 N-terminal residues.
A. Wild-type (WT) and *tco89Δ* cells were grown to log phase and subjected to mock or 300 nM rapamycin treatment for 60 minutes. Cells were harvested and whole-cell extracts (WCEs) were analyzed by immunoblot (IB) with the indicated antibodies. **B.** ImageJ quantification of the results from (A). Data are representative of four or more biological replicates. Means and standard deviations (SDs) are provided, and significance was determined by pairwise Student's t-test. *-$p<0.05$; **-$p<0.01$; ***-$p<0.001$. **C.** As in (A), except WT cells were treated with 200 nM rapamycin for 20 minutes. **D.** WT and *tco89Δ* cells were transformed with control vector (CV) or *Tco89-9xMyc* expression vectors and WCEs were analyzed as in (A).

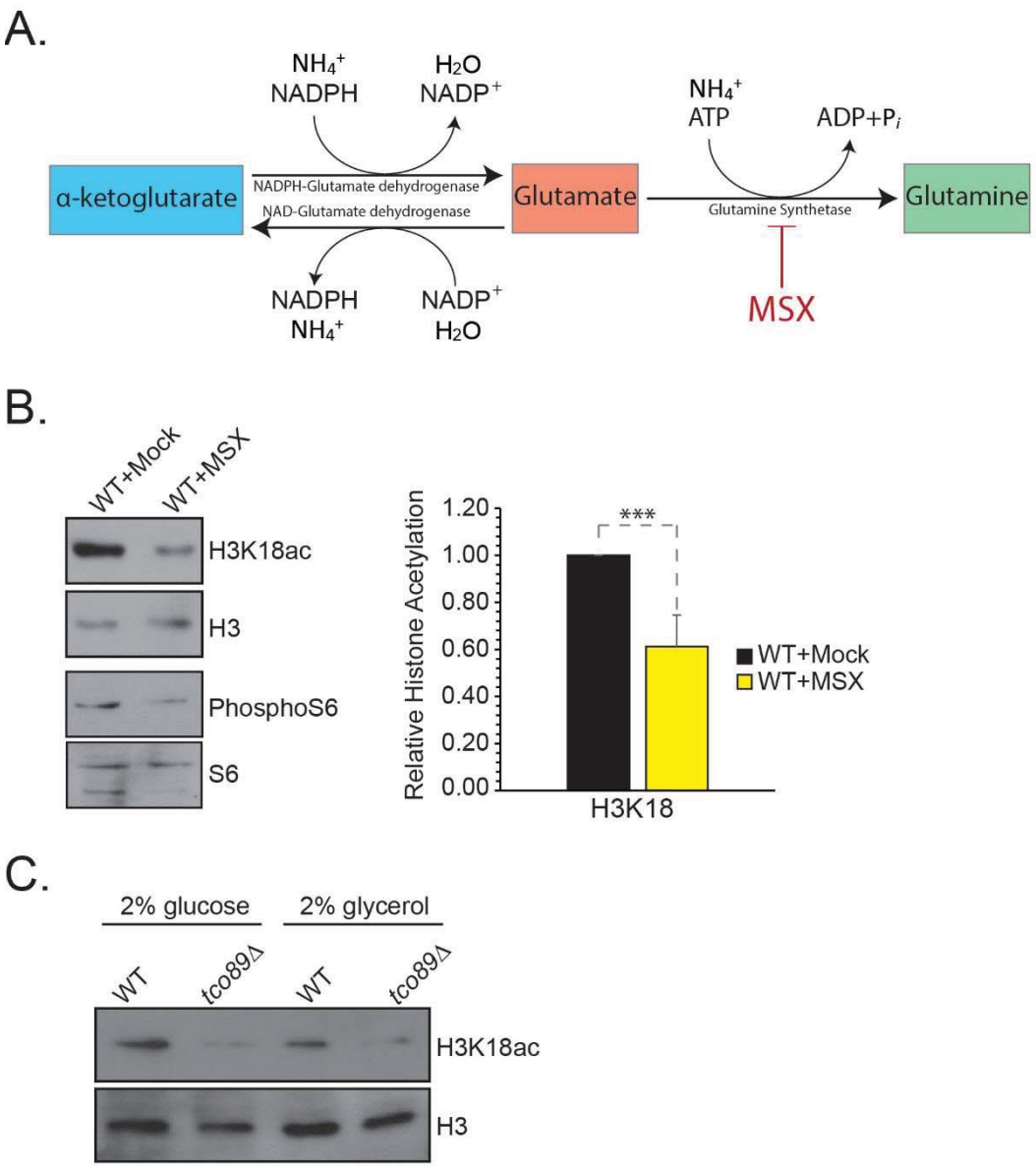

Figure 3-2. TORC1-dependent histone acetylation is responsive to nitrogen, but not carbon, limitation.

A. Schematic showing the step in the glutamine biosynthetic pathway inhibited by MSX [307, 308]. **B.** WT cells were cultured to log phase and then mock treated or treated with 2 mM MSX for 20 minutes. Cells were harvested and extracts were analyzed by immunoblot with the indicated antibodies. ImageJ quantification was conducted, and a graphical representation of the mean and SD obtained over 9 independent experiments is provided. Significance was determined by pairwise Student's t-test. ***-$p<0.001$. **C.** WT and *tco89Δ* cells were grown to log phase in YP 2% glucose or YP 2% glycerol. Extracts were prepared as above and blotted with the indicated antibodies.

either the wild-type or the *tco89Δ* mutant (**Figure 3-2C**). Given that cells grow more slowly in non-fermentable carbon, these findings also ruled out the possibility that the acetylation differences in *tco89Δ* are attributable to the reduced growth rate of this mutant. All together, these findings suggest a mechanism in which TORC1 activation, in response to nitrogen metabolism, functions to regulate this subset of histone acetyl sites.

TORC1 Signals through the Tap42-Sit4 PP6 Phosphatase Complex to Regulate Site-Specific Histone Acetylation Globally

After defining the TORC1-regulated histone acetylation states on histones H3 and H4, we next wanted to identify which TORC1 downstream effector was responsible for mediating these changes. Initially, we examined whether the TORC1-activated Sch9 kinase contributed to the control of these histone modifications using a series of previously described Sch9 expression vectors [80]. These included vectors expressing wild-type Sch9 ($Sch9^{WT}$), a mutant form of Sch9 in which the TORC1 phosphotarget sites have been changed to alanines to prevent activation ($Sch9^{5A}$), and another mutant Sch9 with those same sites mutated to acidic residues to mimic constitutive TORC1-dependent Sch9 phosphorylation ($Sch9^{2D3E}$). We first demonstrated that wild-type and mutant Sch9 were expressed at relatively similar levels, thus ruling out the possibility that these mutations altered protein stability (**Figure B-2A)**. From there, a series of control experiments were conducted, beginning with confirmation that in an *sch9Δ* mutant, introduction of the $Sch9^{2D3E}$ plasmid enabled growth on non-preferred carbon sources and rapamycin (**Figure B-2B**). We also determined that the mutant plasmid promotes Maf1 phosphorylation (a direct substrate of Sch9) regardless of upstream TORC1 activity (**Figure B-2C**) [87]. These findings confirmed that the $Sch9^{2D3E}$ mutant did behave independently of TORC1 as expected. Introduction of the $Sch9^{2D3E}$ mutant into *tco89Δ* failed to rescue acetylation (**Figure 3-3A)**. Furthermore, histone acetylation was not reduced in *sch9Δ* (**Figure 3-3B**). We conclude that the Sch9 kinase does not function downstream of TORC1 to regulate histone acetylation.

We next investigated whether the other well-characterized downstream TORC1 effector, Tap42, contributes to the regulation of histone acetylation. *TAP42* is an essential gene, so we utilized *tap42Δ* cells possessing a plasmid-based temperature-sensitive (*ts*) Tap42 allele [309]. In **Figure 3-4A**, we confirmed these three *ts* strains are indeed acutely sensitive to heat stress. We chose to specifically analyze the *tap42Δ+tap42-106ts* mutant as it had the least dramatic temperature sensitivity, which we predicted would limit non-specific acetylation changes due to impaired viability. Wild-type and *tap42-106ts* mutant cells were grown to log phase at the permissive (25°C) temperature and then shifted to a non-permissive condition (30°C) for 1 hour. WCEs were prepared and histone acetylation was analyzed by IB. Strikingly, in cells whose TORC1 function was intact, simply inactivating Tap42 led to dramatically reduced H3K18ac (**Figures 3-4B** and **C**). Even at the permissive temperature, there was a specific reduction in TORC1-regulated H3K18ac but no effect on H3K9ac, which we know is not responsive to TORC1 (**Figure 3-1A**). These results demonstrate that TORC1 likely signals through a Tap42-associated phosphatase to regulate site-specific histone acetylation.

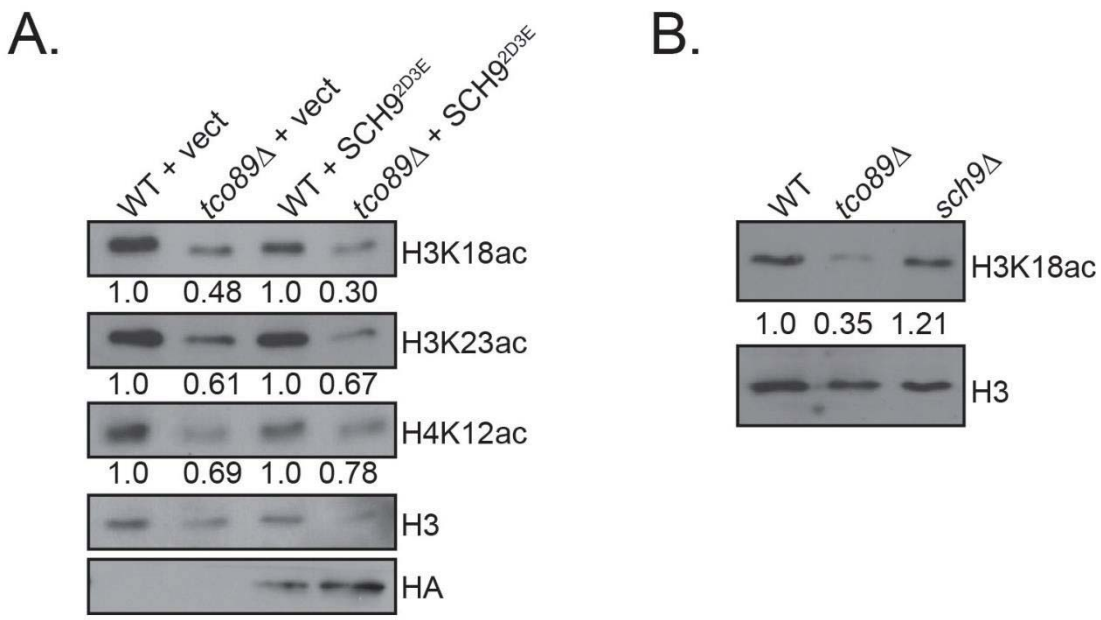

Figure 3-3. Regulation of histone acetylation downstream of TORC1 occurs independently of the Sch9 kinase.
A. Wild-type (WT) and *tco89Δ* cells were transformed with control vector (CV) or $Sch9^{2D3E}$-expression vector and grown to log phase in selective media before preparation of WCEs. Extracts were analyzed by immunoblot with indicated antibodies. **B.** WT, *tco89Δ* and *sch9Δ* cells were grown in YPD and WCEs were prepared. Analysis by immunoblot was conducted as indicated. Western blots and histone acetylation averages provided are representative of at least three independent experiments, normalized to H3, with corresponding WT samples set to 1.

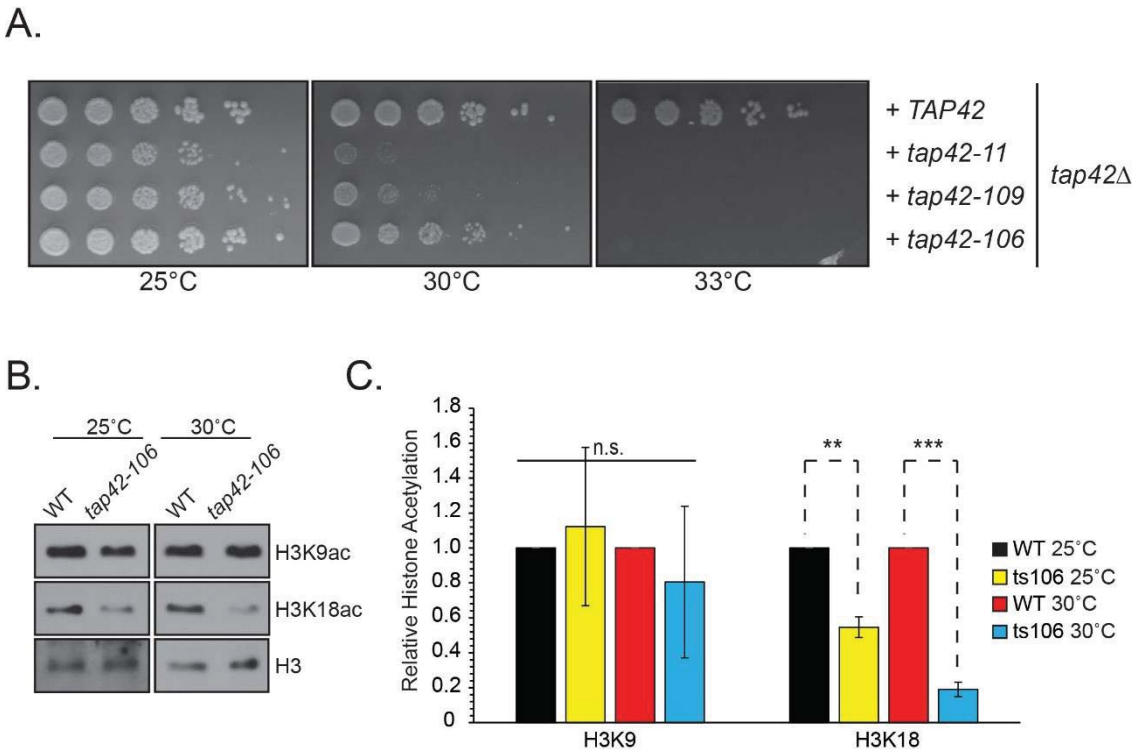

Figure 3-4. TORC1-responsive histone acetylation is regulated in a Tap42-dependent fashion.

A. *tap42Δ* cells containing endogenously expressed wild-type Tap42, or various temperature sensitive mutants (*tap42-11, -109, -106*) [309], were grown to saturation, five-fold serially diluted, and spotted onto YPD. Plates were cultured at permissive (25°C), semi-permissive (30°C), and non-permissive (33°C) temperatures and images were taken on day 2. **B.** Cells from (A) were grown to log phase in liquid culture at 25°C before being shifted to 30°C for 1 hour. WCEs were prepared and analyzed by immunoblot. **C.** Quantification of results presented in (B). Data is representative of three biological replicates. Means and SDs are provided, and significance was determined by pairwise Student's t-test. **-$p<0.01$; ***-$p<0.001$.

The Tap42-associated phosphatases are organized into modular complexes. Typically, they are structured such that Tap42 associates with a catalytic subunit, and one or more regulatory subunits. To identify which of the phosphatases is required for TORC1-regulated acetylation, we screened catalytic mutants of individual Tap42-associated phosphatase complexes (PPG1/*ppg1Δ*, PP4/*pph3Δ*, and PP6/*sit4Δ*) for the loss of rapamycin-induced deacetylation. Since PP2A possesses redundant catalytic subunits (Pph21 and Pph22), we instead used a *tpd3Δ* mutant, which eliminates the PP2A regulatory subunit and impairs PP2A function [310]. Notably, only deletion of *SIT4*, the catalytic subunit of the PP6 phosphatase complex, prevented the rapamycin-induced loss of H3K18ac (**Figure 3-5A**). We saw an identical effect on H3K56ac in *sit4Δ* cells before and after rapamycin, strengthening our hypothesis that TORC1 is mediating H3K18ac, H3K23ac, H3K56ac and H4K12ac through a conserved mechanism. Importantly, we show in **Figure 3-5B** that transformation of the *sit4Δ* mutant with a Sit4 expression vector was sufficient to restore the rapamycin sensitivity of H3K18ac. Finally, the *tco89Δ* acetylation defect was completely rescued in a *sit4Δ tco89Δ* combinatorial mutant (**Figure 3-5C**), further demonstrating that TORC1 inhibition promotes loss of histone acetylation through the activation of the Sit4 phosphatase.

The PP6 complex is a heterotrimer consisting of Tap42, Sit4, and one of four Sit4-associated regulatory proteins (Saps). To probe whether a particular Sap was responsible for Sit4-dependent acetylation repression, we conducted a similar experiment as described in **Figure 3-5A**, except individual Sap deletions were screened. Loss of either the Sap4 (*sap4Δ*) or Sap185 (*sap185Δ*) subunits led to significant rescue of acetylation in rapamycin-treated samples (**Figure 3-6**). However neither mutant alone was sufficient to promote the rapamycin resistance observed in a *sit4Δ* (**Figure 3-5A**). This suggests that while Sap4 and Sap185 are most likely linked to Sit4-dependent regulation of acetylation, there appears to be a degree of functional redundancy between the Saps in this regard.

Sit4's best-known function in the cell is to regulate the NCR response by modulating the phosphorylation, and subsequent localization, of the transcription factors Gln3 and Gat1 [75, 113, 145]. When cells are starved for amino acids, Gln3 dissociates from the cytoplasmic anchor Ure2 and moves to the nucleus in a Sit4-dependent fashion. Nuclear Gln3 then activates transcription of genes required for the utilization of non-preferred nitrogen sources. Because TORC1 suppression promotes Gln3 nuclear localization through Sit4 activation, we probed whether induction of the NCR was required for the effect on histone acetylation.

While loss of Sit4 led to an increase in basal H3K18ac as expected, we found surprisingly that deletion of the NCR transcription factors, Gln3 or Gat1, did not result in a similar increase in acetylation (**Figure 3-7**). In support of the above, loss of the cytoplasmic anchor Ure2 did not phenocopy the *tco89Δ* hypoacetylation response (**Figure 3-7**). Taken together, these data suggest that the PP6 protein phosphatase complex is responsible for connecting TORC1 to the regulation of histone acetylation and that Sit4's contribution exists outside of the NCR response.

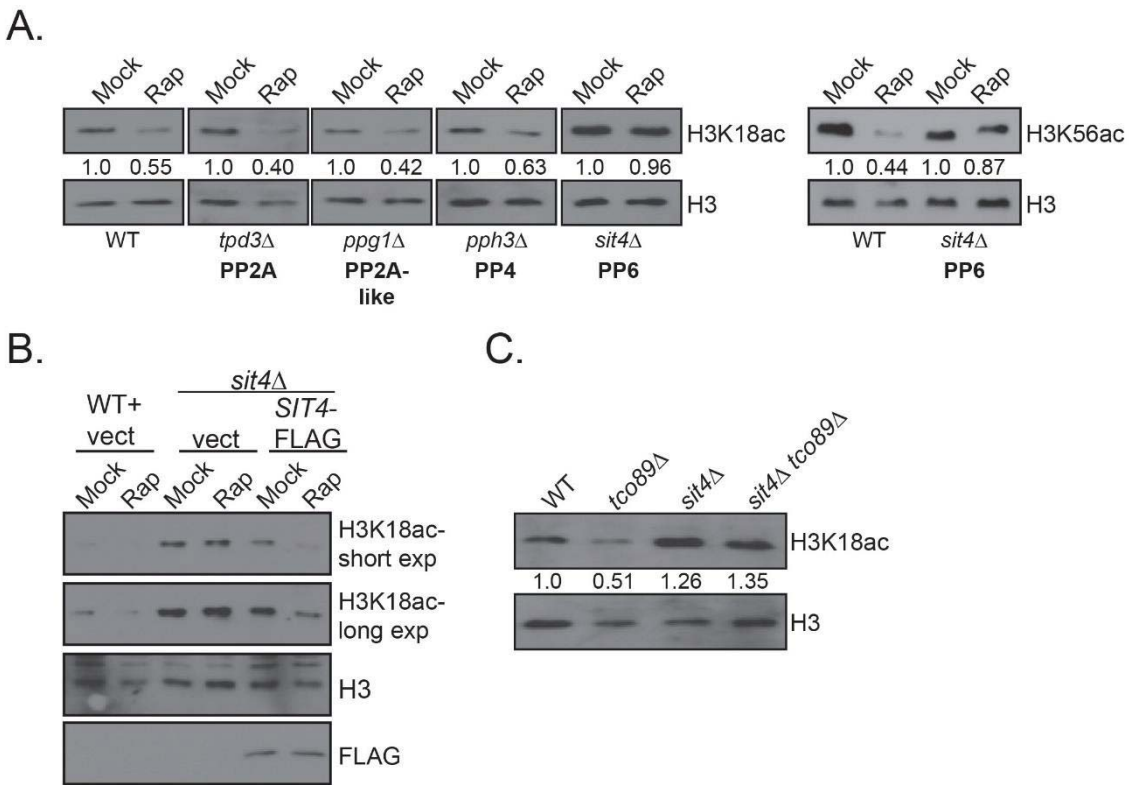

Figure 3-5. Sit4-catalyzed PP6 complex activity is required for TORC1-responsive histone acetylation.

A. Wild-type (WT), *tpd3Δ, ppg1Δ, pph3Δ* and *sit4Δ* cells were grown in YPD to log phase before treatment with 300 nM rapamycin for 60 minutes. WCEs were prepared and analyzed by immunoblot and ImageJ. **B.** WT cells transformed with control vector (CV) and *sit4Δ* cells transformed with CV or full-length pSit4-FLAG, were grown to log phase in selective media and treated with rapamycin as in (A). Extracts were prepped and probed by immunoblot. **C.** WT, *tco89Δ, sit4Δ* and *tco89Δ sit4Δ* were grown to log phase, extracts were prepared and blotted as described above. Data are representative of at least 3 independent replicates, with average histone acetylation values relative to H3 (mock set to 1) provided.

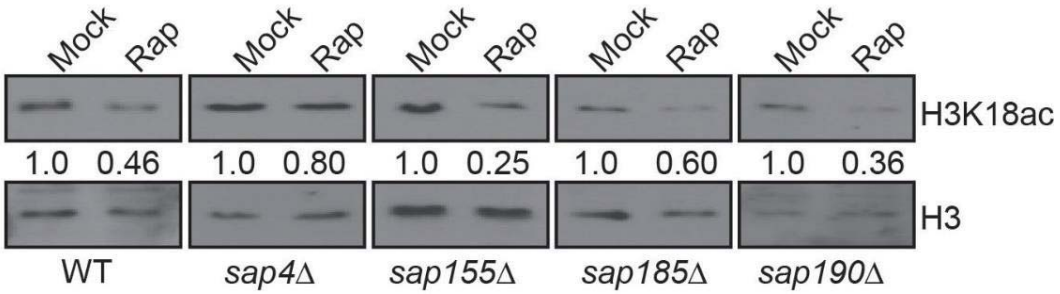

Figure 3-6. Regulatory subunits of the PP6 phosphatase complex display overlapping function in relation to TORC1-responsive histone acetylation.
As in **Figure 3-5A**, except mutants are various Sit4-associated protein (SAP) deletions, including *sap4Δ, sap155Δ, sap185Δ* and *sap190Δ.* Blots are representative of at least 3 independent replicates and average histone acetylation values relative to H3 (mock set to 1) are provided.

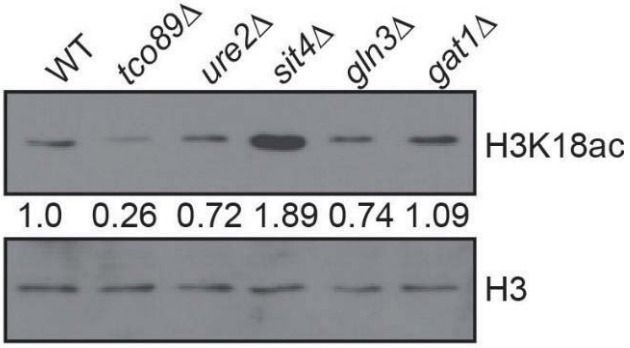

Figure 3-7. Sit4-dependent, nitrogen-responsive chromatin modifications are separable from the canonical nitrogen catabolite response (NCR) pathway.
Mutants of the Sit4-mediated NCR stress response, including *ure2Δ, gln3Δ* and *gat1Δ,* were grown to log phase alongside WT, *tco89Δ* and *sit4Δ,* and analyzed by immunoblot as indicated. Blots are representative of 3 independent replicates and average histone acetylation values relative to H3 (WT set to 1) are provided.

TORC1-Responsive Histone Acetylation Is Specifically Regulated by the Sirtuin Histone Deacetylases

In our previous analysis of TORC1-dependent regulation of H3K56ac, we reported that loss of either of the sirtuins, Hst3 or Hst4, in a *tco89Δ* background restored acetylation to wild-type levels. This prompted us to investigate whether these newly identified TORC1-dependent acetylation states were similarly regulated. Initially, we cultured wild-type and *tco89Δ* cells to log phase and mock treated or treated with nicotinamide, a naturally occurring pan-sirtuin inhibitor. Treatment with nicotinamide led to an increase in basal H3K18ac in wild-type cells, and also rescued the acetylation defect observed in *tco89Δ* (**Figure 3-8A**). Strikingly, *tco89Δ* cells treated with FK866, a compound which inhibits sirtuins by blocking NAD^+ biosynthesis [311], displayed robust restoration of histone acetylation (**Figure 3-8B,** left panel). The effect of FK866 on acetylation in wild-type cells was negligible. A pathway exists in yeast by which active TORC1 represses transcription of *PNC1*, a gene which encodes a nicotinamidase that scavenges nicotinamide and shunts it into the NAD^+ biosynthetic cycle [67]. This means that TORC1 suppression results in both a reduction in the level of sirtuin inhibitor (nicotinamide), as well as an increase in sirtuin co-factor availability (NAD^+). We next asked whether increased *PNC1* expression could explain our observed link between TORC1 and sirtuin-dependent histone deacetylation. Surprisingly, combining *pnc1Δ* with *tco89Δ* failed to rescue TORC1-dependent acetylation (**Figure 3-8B,** right panel).

To probe whether class I or II histone deacetylases were also contributing to the regulation of TORC1-dependent acetylation states, we initially utilized the pharmacological inhibitors sodium butyrate and trichostatin A. However, for unknown reasons, these compounds failed to provide effective HDAC inhibition (data not shown). To circumvent this issue, we combined *tco89Δ* with a gene deletion of the major class I (Rpd3) or class II (Hda1) histone deacetylases to ask whether loss of these HDACs would diminish TORC1-dependent deacetylation. While the *rpd3Δ* and *hda1Δ* single mutants displayed elevated acetylation across our residues of interest, combining these with a *tco89Δ* still led to a significant reduction in acetylation (**Figure 3-9**, compare 2^{nd} and 4^{th} lanes). These results further support the hypothesis that TORC1-dependent histone acetylation specifically involves suppression of the sirtuins. To gain a more complete understanding as to the contributions of each sirtuin, we created another set of combinatorial mutants that paired *tco89Δ* with individual sirtuin deletions. These strains were used to repeat the experiment in **Figure 3-9**. Strikingly, we found dramatic differences in the ability of these sirtuin deletions to rescue site-specific acetylation in *tco89Δ* (**Figure 3-10A** and **B**). For example, H3K18 is deacetylated primarily by Hst2, Hst3 and Hst4, while H3K23 is solely targeted by Hst4. In all, our findings support the idea that active TORC1 promotes acetylation of the H3/H4 N-termini via repression of the Sit4/Sap4 PP6 phosphatase and the sirtuin deacetylases, and that this novel mechanism does not involve changes in Pnc1 levels or NAD^+ biosynthesis.

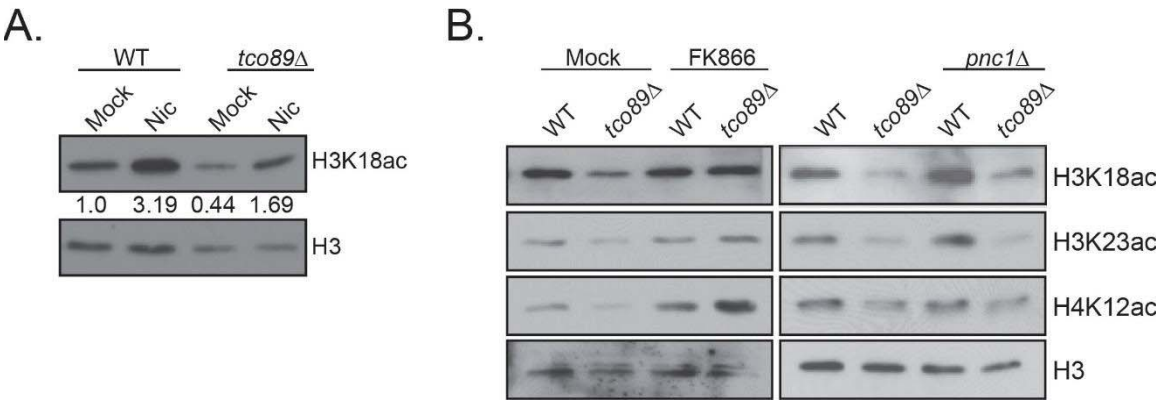

Figure 3-8. TORC1-PP6 catalyzed histone H3/H4 deacetylation is promoted by the NAD$^+$-dependent sirtuin family of histone deacetylases.
A. Wild-type (WT) and *tco89Δ* cells were grown to log-phase before mock or 25 mM nicotinamide (sirtuin inhibitor) treatment for 60 minutes. WCEs were prepared and immunoblotted as indicated. Blots are representative of 3 independent replicates and average histone acetylation values relative to H3 (WT mock set to 1) are provided. **B.** In left panel, as in (A) except cells were treated with 500 nM FK866. In right panel, WT, *tco89Δ, pnc1Δ* and *tco89Δ pnc1Δ* were grown and analyzed by immunoblot as indicated.

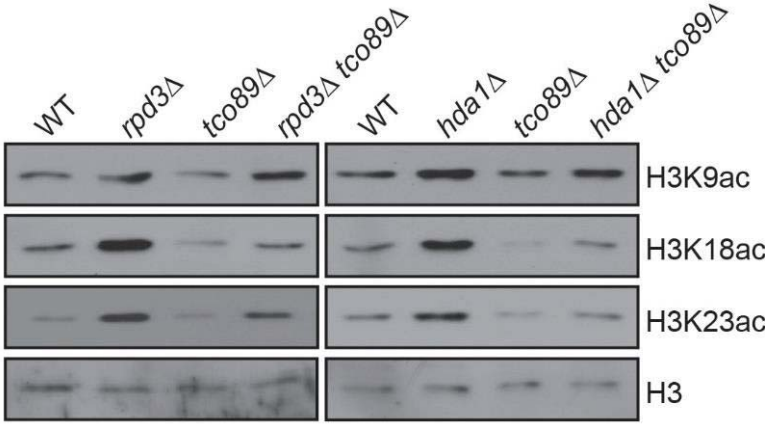

Figure 3-9. Class I and II histone deacetylases are not involved in the observed TORC1-PP6 hypoacetylation response.
WT, *rpd3Δ, tco89Δ, tco89Δ rpd3Δ, hda1Δ* and *tco89Δ hda1Δ* were grown to log-phase. Extracts were prepped and analyzed by immunoblot. Blots are representative of 4 independent replicates.

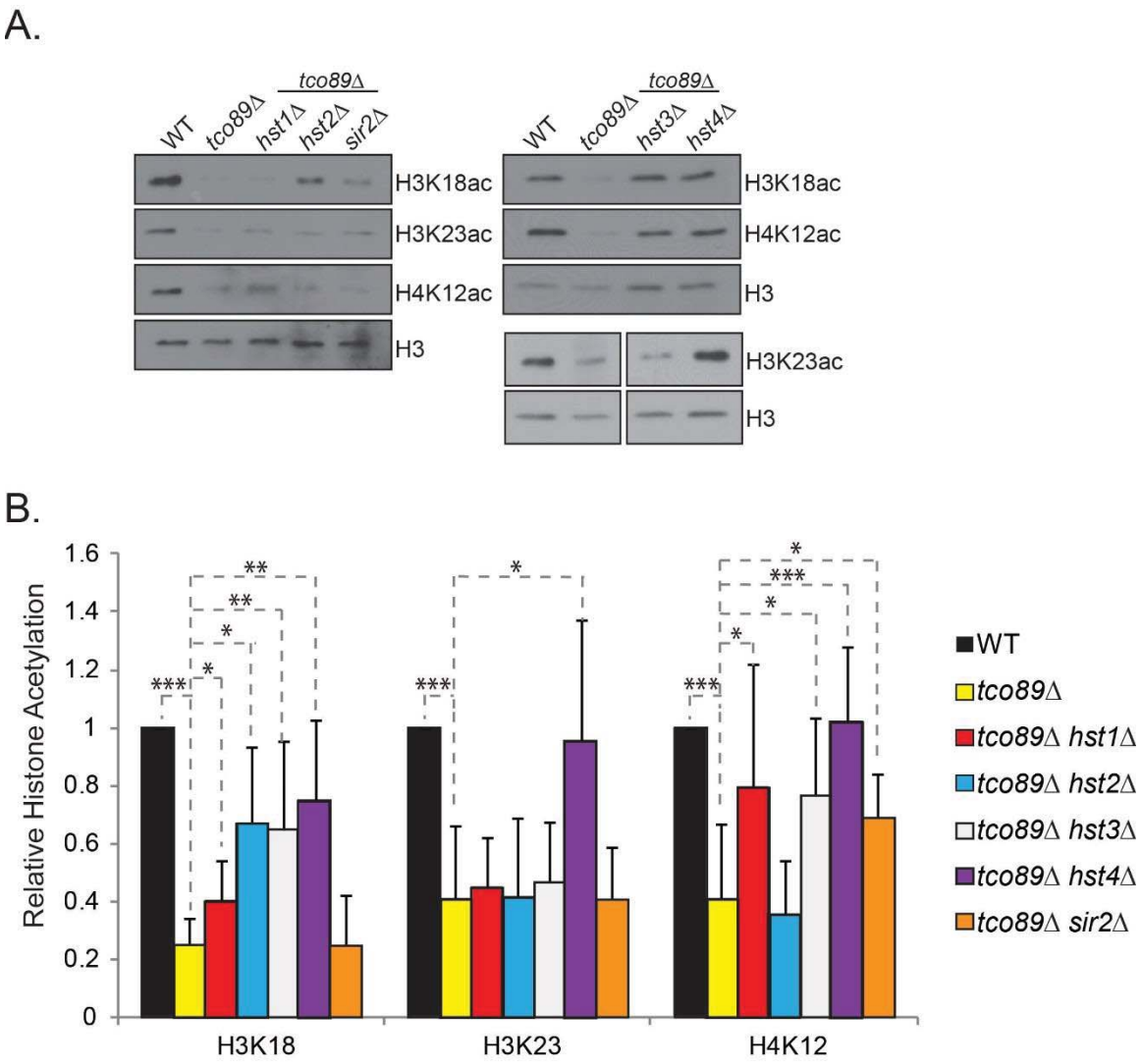

Figure 3-10. TORC1-responsive histone acetylation is modulated by a subset of sirtuin histone deacetylases in a site-specific fashion.
A. Combinatorial *tco89Δ sirtuin* gene deletion mutants were grown and analyzed by immunoblot as indicated. **B.** ImageJ quantification of data shown in (A). Data are representative of at least four biological replicates. Means and SDs are provided, and significance was determined by pairwise Student's T-test. *-$p<0.05$; **-$p<0.01$; ***-$p<0.001$.

Sit4 Activation Downstream of TORC1 Inhibition Promotes Hst4 Stabilization

Mammalian mTORC1 activity was previously shown to regulate glutamine metabolism and TCA cycle replenishment by transcriptional suppression of *SIRT4* [184]. We speculated that TORC1 inhibition in yeast might function similarly by promoting deacetylation through an increase in sirtuin expression. To address this, we epitope-tagged the sirtuin genomic loci with a 9xMyc epitope in both WT and *tco89Δ* cells. Cells were grown, WCEs prepared, and expression was analyzed by immunoblot. We observed dramatic increases in Hst4 and Sir2 protein expression in the *tco89Δ* mutants relative to wild-type cells (**Figure 3-11A**). Given that we previously identified Hst4 as the only sirtuin able to control all of the TORC1-dependent acetylation modifications (**Figure 3-10**), we selected it for further examination across a variety of TORC1 inhibitory conditions. Short-term rapamycin and MSX treatment had no effect on Hst4 levels in wild-type cells; however, both *tco89Δ* and 60-minute exposure to rapamycin led to elevated Hst4 expression compared to the mock-treated wild-type cells (**Figure 3-11B**). Considering that 20-minute TORC1 inhibition was sufficient to reduce histone acetylation (**Figures 3-1C, 3-2B**), we were surprised to find that Hst4 levels did not significantly increase until later in the treatment period.

To assess the contribution of Sit4 to these dynamic changes in Hst4 protein levels, we engineered *sit4Δ* and *tco89Δ sit4Δ* into the Hst4-9xMyc background and again examined Hst4 expression. Excitingly, we found that deletion of *SIT4* in the wild-type Hst4-tagged strain significantly reduced Hst4 levels, and the combinatorial mutant, *tco89Δ sit4Δ,* brought the elevated Hst4 levels observed in the *tco89Δ* single mutant back to approximately wild-type levels (**Figure 3-11C,** upper panel). We saw a much more muted response when the experiment was repeated with a series of *sap4Δ* mutants, a result consistent with the idea that there is functional redundancy among the Saps (**Figure 3-11C,** lower panel**)**. Given TORC1's known role in regulating transcription, we used qPCR and confirmed that the increase in Hst4 protein levels was not due to elevated HST4 mRNA expression (**Figure 3-12**). Therefore, these data suggest that the Sit4-dependent effect on Hst4 expression is either translational or post-translational in nature.

Hst3 exhibits rapid proteasomal turnover, in a cell-cycle dependent fashion, in response to Cdk1 phosphorylation and subsequent SCF^{Cdc4} ubiquitination [179, 180]. The phosphatase that opposes Cdk1-dependent Hst3 turnover is currently unknown. Hst4 was also identified as a potential SCF^{Cdc4} substrate, but its proteolytic turnover has not been studied in nearly as much detail. We next asked whether the Sit4-dependent increase in Hst4 protein levels could be explained by a reduction in Hst4 turnover. To assess this possibility, we utilized our wild-type and *tco89Δ* strains expressing Hst4-9xMyc, and we examined the kinetics of Hst4 turnover in each. Cells were grown to log phase and then treated with cycloheximide (CHX), an inhibitor of protein synthesis. Excitingly, we found that relative to wild-type cells, the *tco89Δ* promoted a significant increase in Hst4 stability (**Figure 3-13A**). We demonstrate this stabilization is Sit4-dependent, as the *tco89Δ sit4Δ* Hst4-9xMyc strain displays a turnover rate very similar to that of the wild-type. We conducted the same experiment with WT and *tco89Δ* strains possessing an Hst3-9xMyc epitope for comparison, and surprisingly, found that in addition to the

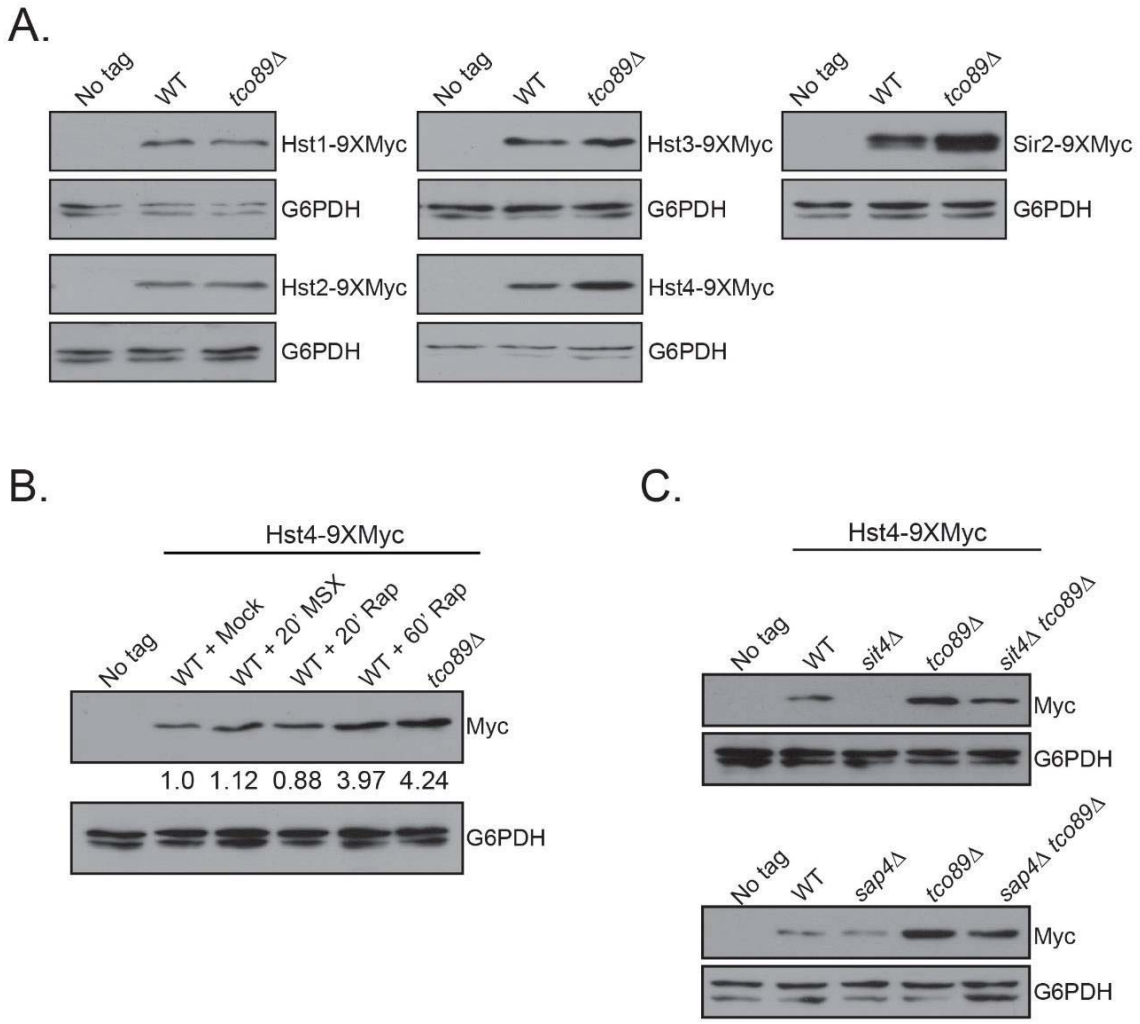

Figure 3-11. Reduced TORC1 signaling activates PP6 to increase Hst4 protein levels.

A. No tag, and WT or *tco89Δ* cells expressing indicated epitope-tagged sirtuins, were grown to log phase and analyzed by IB with Myc or G6PDH antibodies. **B.** No tag, WT Hst4-9xMyc, and *tco89Δ* Hst4-9xMyc cells were grown to log phase before treatment with MSX or rapamycin as indicated. WCEs were blotted for Myc and G6PDH and analyzed by ImageJ. Quantification of Hst4 levels relative to G6PDH are provided with the WT mock set to 1. **C.** No tag, WT Hst4-9xMyc, *sit4Δ* Hst4-9xMyc, *sap4Δ* Hst4-9xMyc, *tco89Δ* Hst4-9xMyc, *tco89Δ sit4Δ* Hst4-9xMyc, and *tco89Δ sap4Δ* Hst4-9xMyc cells were grown to log phase and analyzed as in (B). Blots and expression values are representative of at least 3 independent biological replicates.

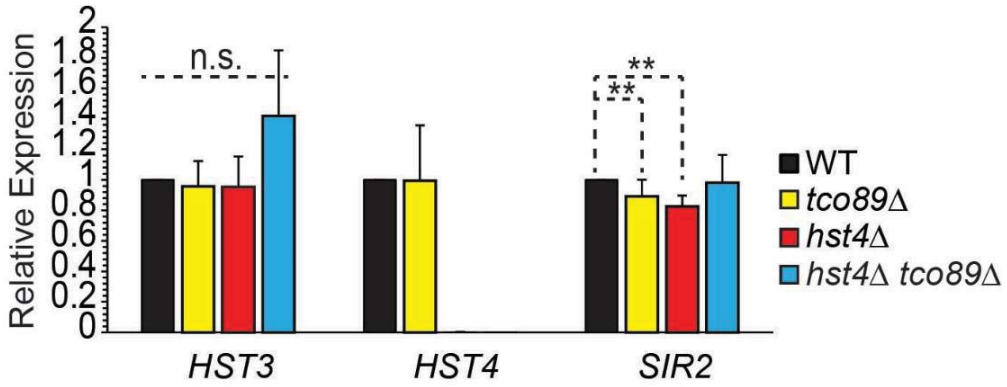

Figure 3-12. PP6-dependent changes in Hst4 protein levels are not due to increased *HST4* mRNA expression.
Hst3, Hst4 and Sir2 mRNA expression in wild-type, *tco89Δ*, *hst4Δ*, and *tco89Δ hst4Δ* cells. Means and SDs are presented and the data is representative of five independent experiments. Significance was determined by pairwise Student's T-test. **-$p<0.01$; ***-$p<0.001$.

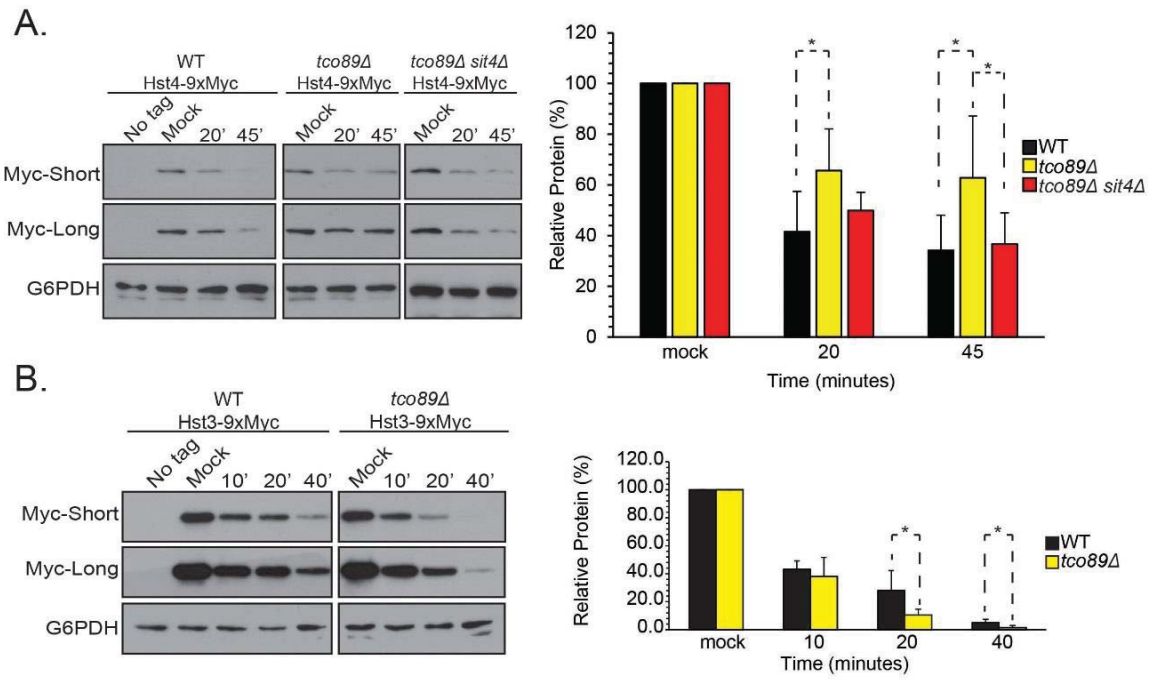

Figure 3-13. PP6 activation downstream of TORC1 inhibition initiates a reciprocal shift in Hst3/Hst4 stability.

A. No tag, WT Hst4-9xMyc, *tco89Δ* Hst4-9xMyc and *tco89Δ sit4Δ* Hst4-9xMyc cells were grown to log phase and treated with 50 µg/mL cyclohexamide (CHX). Samples were taken just before CHX addition and then at subsequent intervals. Two exposures of the α-Myc blot are provided for clarity, and data quantification is shown on the right. Values are the mean and SD of four independent biological replicates, and significance was determined by pairwise Student's t-test. *-$p<0.05$. **B.** As in (A) except Hst3 stability is measured. Time points differ as indicated.

increase in Hst4 stability in the *tco89Δ* mutant, there is also a reciprocal decrease in Hst3 stability (**Figure 3-13B**). It is currently unclear whether this decrease is in direct response to the enhanced level of Hst4, or it is because Hst3 is a biologically relevant substrate of Sit4.

We next asked whether the Sit4-dependent change in Hst4 stability could be traced to direct opposition of sirtuin phosphorylation. To probe this possibility, we immunoprecipitated Myc-tagged Hst3 or Hst4 from WT and *tco89Δ* extracts and resolved them on Phos-tag containing SDS-PAGE gels. Phos-tag is a reagent that binds phosphorylated residues and reduces their electrophoretic mobility, allowing for more distinct resolution of phosphorylated compared to non-phosphorylated forms of a given protein. We observed a marked reduction in the slower migrating forms (phosphorylated) of both Hst3 and Hst4 in wild-type extracts treated with lambda phosphatase; however, no discernible difference was detected in the phosphorylation pattern of either sirtuin when wild-type and *tco89Δ* extracts were compared (**Figure 3-14A**). As a control, we repeated the experiment shown in **Figure 3-14A** using the downstream TORC1 phosphotarget Sch9 (**Figure 3-14B**). We found a dramatic downward shift in Sch9 mobility in both the lambda phosphatase treated sample, as well as the rapamycin treated sample, confirming that the Phos-tag reagent behaves as expected. In all, these findings identify a novel mechanism in which TORC1 inhibition promotes Sit4 activation and site-specific histone deacetylation via stabilization of Hst4. These effects appear to occur independently of a direct role for TORC1 in Hst4 phosphorylation status.

Hst4 Nuclear Accumulation Occurs Rapidly as a Consequence of TORC1 Inhibition and Sit4 Activation, and Precedes the Increase in Hst4 Stability

It was previously reported that metazoan SIRT1 and SIRT2, as well as yeast Hst2 and Hst4, actively shuttle between subcellular compartments in response to starvation, cellular stress or cell-cycle progression (summarized in **Tables 1-1** and **1-2**) [168, 176, 188, 222, 312]. As outlined in Chapter 1, the best-known function of Sit4 activation downstream of TORC1 inhibition involves regulation of transcription factor localization to coordinate the NCR response. We therefore considered whether Sit4/PP6 activity might stabilize Hst4 by altering its subcellular distribution. Utilizing the wild-type and *tco89Δ* sirtuin 9xMyc-tagged strains described above, indirect immunofluorescence (**Figures 3-15** and **B-3**) and quantitative analysis (**Figure 3-16A**) was performed as detailed in Chapter 2. Of the five sirtuins, Hst4 exhibited the most significant alteration in cellular localization, as diffuse staining throughout wild-type cells was considerably more nuclear focused in *tco89Δ* (**Figures 3-15, 3-16A, B-3D**).

To determine whether the increase in Hst4 protein levels occurred before or after the nuclear accumulation of Hst4, we repeated the experiment described in **Figure 3-16A**, this time including an additional wild-type sample treated with 200 nM rapamycin for 20 minutes. Importantly, we saw that the 20-minute rapamycin treatment, which previously had very little effect on protein levels (**Figure 3-11B**), was sufficient to promote maximal nuclear accumulation of Hst4 (**Figures 3-16B** and **B-3D**). This

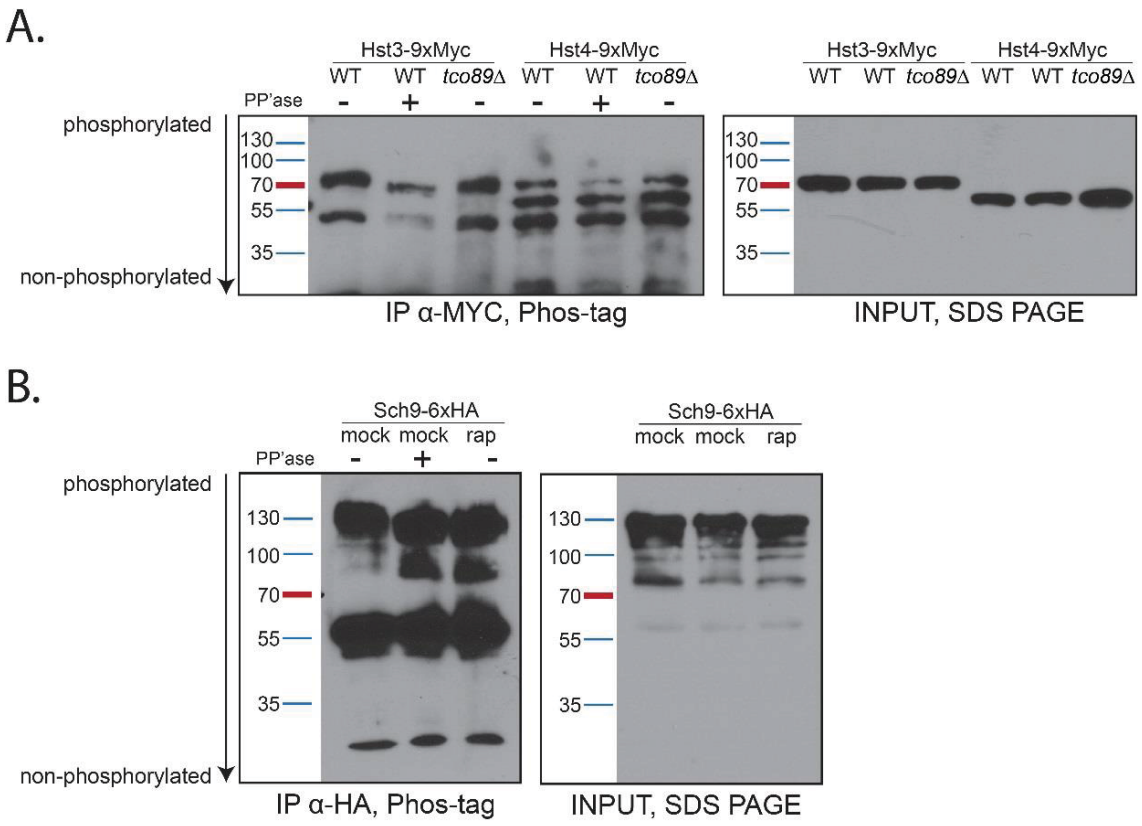

Figure 3-14. Hst3 and Hst4 phosphorylation state is independent of TORC1 function.

A. Wild-type (WT) Hst3-9xMyc, *tco89Δ* Hst3-9xMyc, WT Hst4-9xMyc and *tco89Δ* Hst4-9xMyc were grown to log phase and extracts were prepared. Hst3 and Hst4 were immunoprecipitated from 1 mg of extract, and the sirtuin bound IgG-conjugated beads then were treated with lambda phosphatase for 1 hour at 30°C as indicated. IP samples were resolved on 10% SDS PAGE gels containing Phos-tag (50 μM) and evaluated by α-Myc IB. Input gels were run in parallel where 35 μg extract was resolved on 10% SDS PAGE gel without Phos-tag present. **B.** As in (A), except Sch9-6xHA strains were utilized.

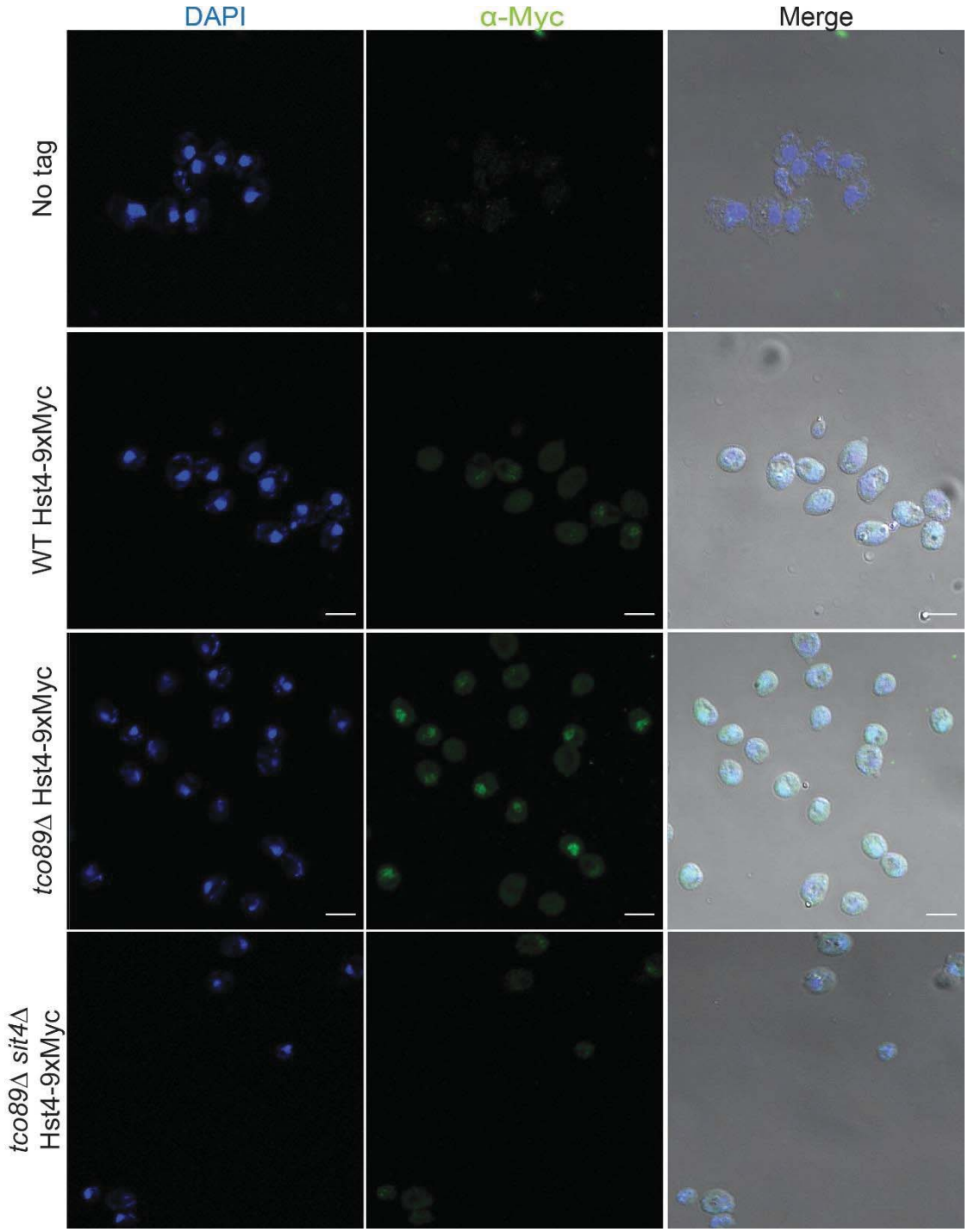

Figure 3-15. TORC1 suppression drives Hst4 nuclear accumulation in a Sit4-dependent fashion.
Wild-type, *tco89Δ,* and *tco89Δ sit4Δ* strains containing either no tag or a 9XMyc epitope on Hst4 were grown to log-phase, fixed, permeabilized, and imaged using indirect immunofluorescence as described in Chapter 2. Images are representative of at least five biological replicates. DAPI staining denotes the nucleus and the α-Myc (FITC) tracks the localization of Hst4.

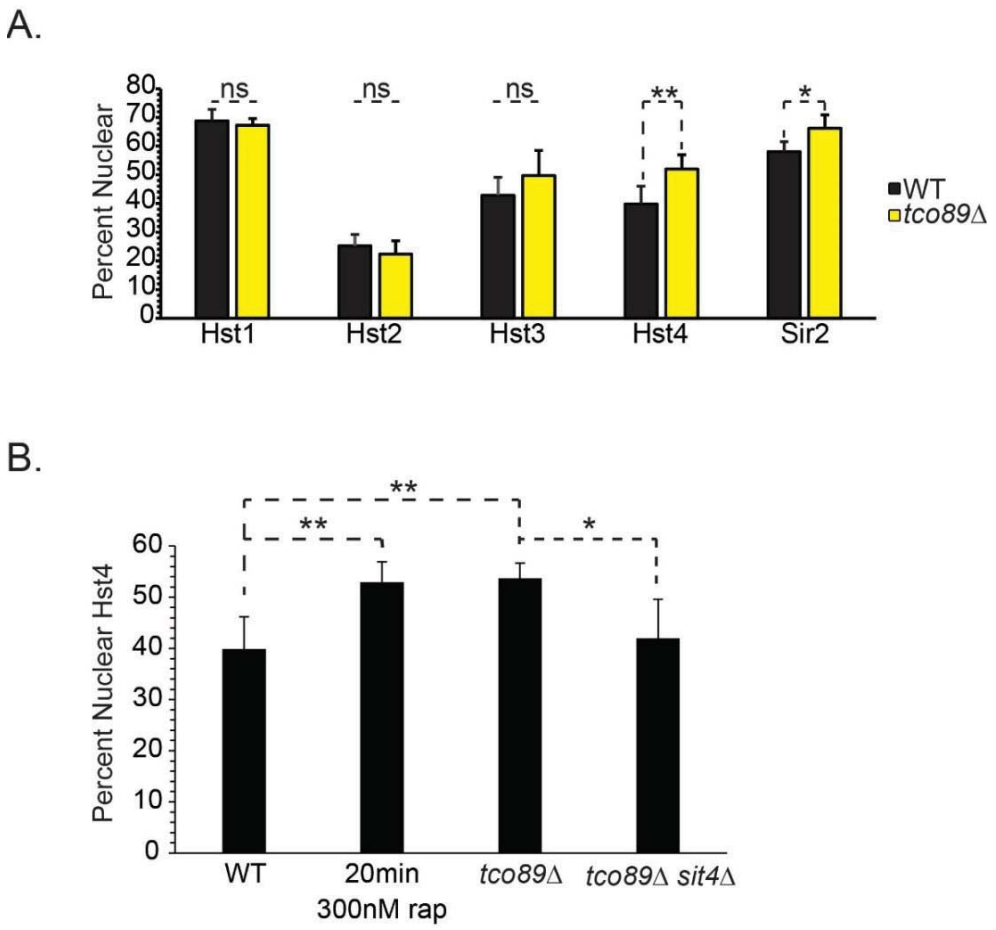

Figure 3-16. Hst4 nuclear accumulation occurs rapidly as a consequence of TORC1 inhibition and precedes the increase in Hst4 protein stability.
A. Nuclear ratios of the sirtuins were determined from a series of images, as described in Chapter 2, and graphed. Means and SDs presented are representative of five or more biological replicates. Each replicate contained 20-40 randomly selected cells. **B.** Wild-type Hst4-9xMyc cells were grown to log phase and mock or rapamycin treated (300 nM rap, 20 min) before analysis as described in (A). *tco89Δ* Hst4-9xMyc and *tco89Δ sit4Δ* Hst4-9xMyc strains were included for comparison. Significance was determined by pairwise Student's t-test. *-$p<0.05$; **-$p<0.01$.

correlated well with the timing of the acetylation response (**Figure 3-1C**). Finally, in a *tco89Δ sit4Δ* Hst4-9xMyc strain, which displays a wild-type level of Hst4 expression and turnover (**Figures 3-11C** and **3-13A**), the cellular distribution of Hst4 was corrected **(Figures 3-15** and **3-16B**). Therefore, Sit4 activation is required to promote Hst4 nuclear localization and rapid histone deacetylation (within 20 minutes), and the subsequent stabilization of this nuclear HDAC (60 minutes post-TORC1 inhibition) likely sustains the hypoacetylation phenotype until TORC1 activity is restored.

TORC1-Dependent Histone Acetylation Does Not Impact RP Gene Transcription, But Does Contribute to a Subset of TORC1-Regulated Biological Functions

TORC1 had been previously identified as a regulator of acetylation at the rDNA and the RP genes, and our lab recently characterized a critical role for TORC1-mediated H3K56ac in RNA polymerase I-dependent rDNA transcription [12, 13, 66, 140, 142]. Given this, and TORC1's well-established link to anabolism, we next asked whether these TORC1-regulated acetylation states contributed to the transcriptional regulation of ribosome biogenesis. In the initial characterization of Tco89, it was reported that *tco89Δ* mutants had no effect on ribosomal protein gene expression [43]. However, we chose to revisit these claims as the authors did not present the data or identify the genes they had assayed. Utilizing cDNA from **Figure 3-12**, we examined how decreased acetylation (WT to *tco89Δ*), and subsequent restoration (*tco89Δ* to *tco89Δ hst4Δ*), impacted expression of a subset of RP genes encoding both small and large ribosomal subunits. We found that in the *tco89Δ* mutant, where TORC1 function is decreased (**Figure B-1**) and we observe a global site-specific reduction in acetylation (**Figure 3-1A**), there is not a significant effect on RP mRNA levels (**Figure 3-17**). The *hst4Δ* had a similarly negligible effect, while *tco89Δ hst4Δ* resulted in a moderate yet significant reduction in *RPL23B* expression (**Figure 3-17**).

tco89Δ mutants have been reported to enter an irreversible, growth-arrested state following TORC1 inhibition [49]. A number of characterized physiological states and compounds can promote this permanent growth-arrest, including nutrient starvation, rapamycin, the DNA damaging agent hydroxyurea, and the metalloid arsenic trioxide [57, 313]. And while the ultimate cellular response is often similar, the mechanisms underlying these effects can be very diverse [314]. We next determined if restoration of TORC1-regulated acetylation could rescue the sensitivity of *tco89Δ* mutants to these TORC1 inhibitors. Excitingly, we found that pairing an *hst3Δ* or *hst4Δ* with *tco89Δ* reversed its sensitivity to low dose rapamycin (5 nM), as well as to hydroxyurea and arsenic trioxide (**Figure 3-18**). These spotting data were surprisingly distinct from what was observed with the *tco89Δ sit4Δ* across the same spectrum of conditions. Although *tco89Δ sit4Δ* was sufficient to restore wild-type growth on hydroxyurea and arsenic, it failed to enable growth on rapamycin (**Figure 3-18**).

A previous study suggested that Hst4 may be the functional ortholog of the metazoan mitochondrial SIRT3 [176]. This study demonstrated that Hst4 localization to the mitochondria fluctuates in response to vitamin availability (biotin), and that this effect

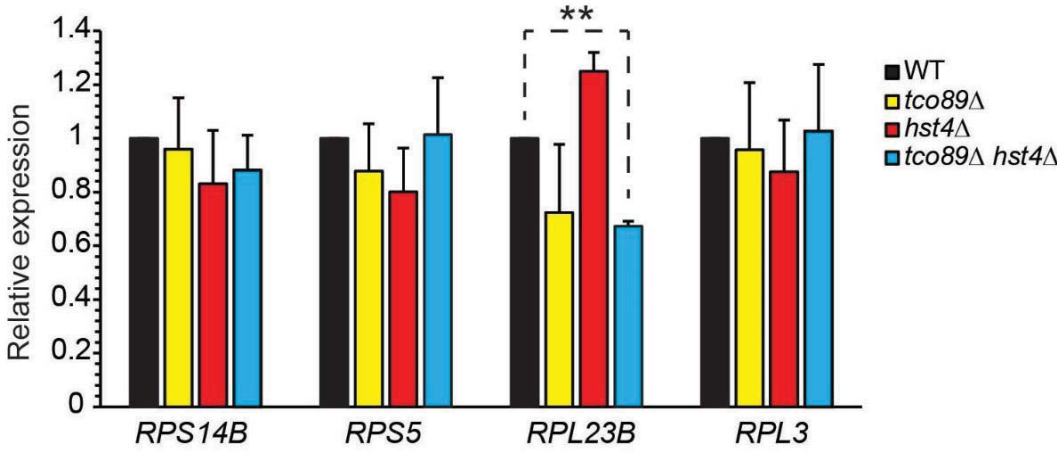

Figure 3-17. Global loss of TORC1-responsive acetylation marks does not correlate with a change in expression of a subset of ribosomal protein genes.
WT, *tco89Δ, hst4Δ and tco89Δ hst4Δ* cells were grown to log phase, cDNA was synthesized from total RNA, and qPCR was performed with the primer sets indicated. Data are the average and SD of four independent experiments and significance was determined by pairwise Student's t-test. **-$p<0.01$.

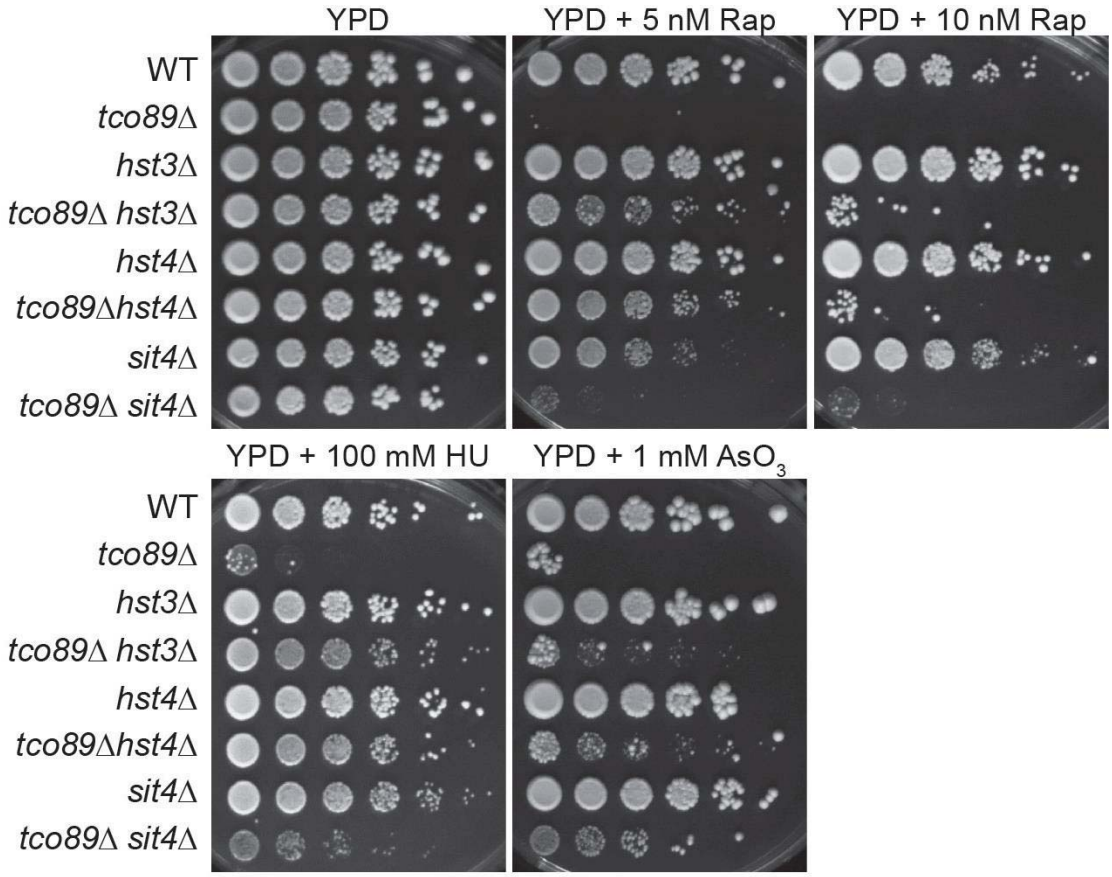

Figure 3-18. TORC1-PP6 regulated histone acetylation is functionally significant for a subset of TORC1-dependent processes.
WT, *tco89Δ, hst3Δ, tco89Δ hst3Δ, hst4Δ, tco89Δ hst4Δ, sit4Δ* and *tco89Δ sit4Δ* were cultured to saturation overnight. Cells were five-fold serially diluted and spotted onto the indicated plate media. Images were obtained after four days at 30°C.

correlates with changes in mitochondrial protein acetylation, cellular respiration, and reactive oxygen production. Given the similarities between the biotin signaling mechanism, and the one we described above, we asked whether the nitrogen responsive TORC1-PP6-sirtuin cascade may also impact mitochondrial function. To explore this concept, wild-type, *tco89Δ, hst4Δ* and *tco89Δ hst4Δ* cells were either mock treated or treated with a low concentration (5 nM) of rapamycin for 2 hours. Cells were then stained with DHE to detect reactive oxygen species (ROS). TORC1 inhibition, via rapamycin treatment or *tco89Δ,* had relatively little effect on ROS production relative to wild-type mock-treated cells (**Figure 3-19**). In agreement with the biotin study [176], deletion of *HST4* did indeed trigger a decrease in basal ROS levels in both the wild-type and the *tco89Δ* backgrounds (**Figure 3-19**). Considering TORC1 inhibition did not have an effect on ROS production, it would seem that the link between Hst4 and ROS occurs independently of our newly-characterized PP6-dependent mechanism. Still, this is an interesting development and provides insight into another biologically relevant function for this sirtuin.

In all, our data illustrate the existence of a novel TORC1-PP6-sirtuin signaling cascade that coordinates the epigenetic modification of histones with changes in environmental nitrogen availability. Further, we demonstrate that the downstream activation of sirtuins, in response to TORC1 inhibition, plays a critical role in an array of cellular operations, including cell cycle re-initiation following stress and DNA repair.

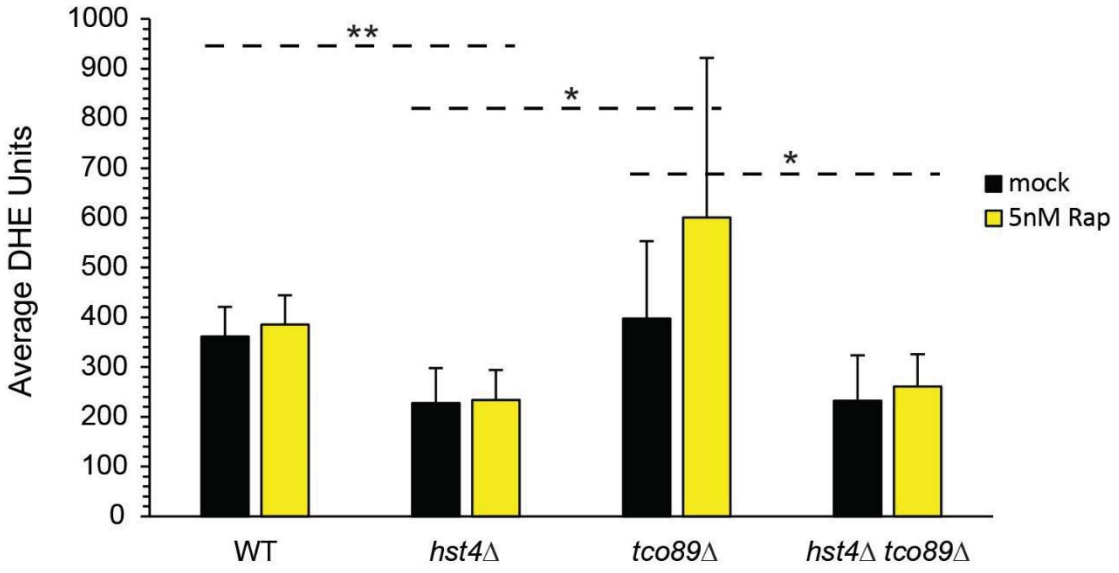

Figure 3-19. Hst4 contributes to cellular ROS levels independently of TORC1. WT, *hst4Δ, tco89Δ* and *tco89Δ hst4Δ* cells were cultured to log phase and mock or rap treated (5 nM) for 2 hours. Cells were then washed and stained with DHE for 20 minutes prior to analysis by flow cytometry. Data presented are the average and standard deviations of five independent experiments. Significance was determined by pairwise Student's t-test. *-$p<0.05$; **-$p<0.01$.

CHAPTER 4. HMG DISPLACEMENT OCCURS INDEPENDENTLY OF TORC1-MEDIATED HISTONE ACETYLATION TO PROMOTE A NOVEL, STRESS-RESPONSIVE CELL DEATH

H3K37A Mutation Correlates with HMGB Nuclear Delocalization and Is Sufficient to Change Rapamycin from a Cytostatic to a Cytotoxic Agent

Our lab previously identified a significant and unique genetic link between TORC1 signaling and one particular histone tail residue, H3K37 [152]. Using a library of histone mutants in which each residue has been individually mutated to alanine [315], we screened for altered sensitivity to the TORC1 inhibitor rapamycin. H3K37A turned out to be the only mutant in the library that, when treated with low doses of rapamycin, exhibited a dramatic loss of viability ([152] and **Figure 4-1A**). This rapamycin sensitivity proved to be independent of histone post-translational modification however, as replacing the native lysine with an amino acid that mimics acetylation (glutamine), or simply restores its charge (arginine), rescued the rapamycin phenotype (**Figure 4-1A,** lower panel). The only known function for H3K37 in the cell is to anchor HMGBs to chromatin [252, 253, 316, 317]. In previous work from our laboratory, we hypothesized that the cell death caused by TORC1 inhibition in H3K37A cells was attributable to nuclear delocalization of HMGBs [152]. Given the findings presented in Chapter 3, we sought to expand on this previous work to probe whether TORC1-regulated histone acetylation may contribute to the binding of HMGBs to chromatin.

Initially, we screened for other HMGB proteins that may behave similarly to the previously characterized Nhp10 [152]. We found that Nhp6a is also displaced from the nucleus in H3K37A cells following transient low dose exposure to rapamycin (**Figure 4-1B**). Nhp6a delocalization does not occur in an H3K37R mutant (**Figure 4-1B**), which fits with the fact that H3K37R cells are not sensitive to TORC1 inhibition (**Figure 4-1A)**. Together, this shows that there is a strong correlation between HMGB delocalization and the overall health of the cells under TORC1-limiting conditions. Critically, while HMGB release into the cytoplasm occurred 60 minutes post-rapamycin treatment (**Figure 4-1B**), a significant increase in cell death was not observed until between 60 and 90 minutes post-rapamycin (**Figure 4-1C**). These data support our hypothesis that HMGB nuclear delocalization may drive induction of apoptosis/necrosis under TORC1-limiting conditions, rather than simply occurring as a consequence of cell death. We next asked whether H3K37A mutants would be less sensitive to rapamycin if Hst4 (the sirtuin opposing TORC1-dependent histone acetylation) or Sap4 (one of the ancillary PP6 subunits critical for stabilizing Hst4 under TORC1-repressive conditions) were deleted. *hst4Δ* had no effect on Nhp6a localization (**Figure 4-2A**), nor did *hst4Δ* or *sap4Δ* restore cellular viability following rapamycin treatment (**Figure 4-2B**). Additionally, there was no significant growth advantage for the H3K37A *hst4Δ* or the H3K37A *sap4Δ* during transient or long-term rapamycin exposure (**Figure B-4A** and **B-4B** respectively). And finally, H3K37A mutants plated on media containing both nicotinamide and rapamycin did not show improved growth compared to rapamycin alone (**Figure B-4C**).

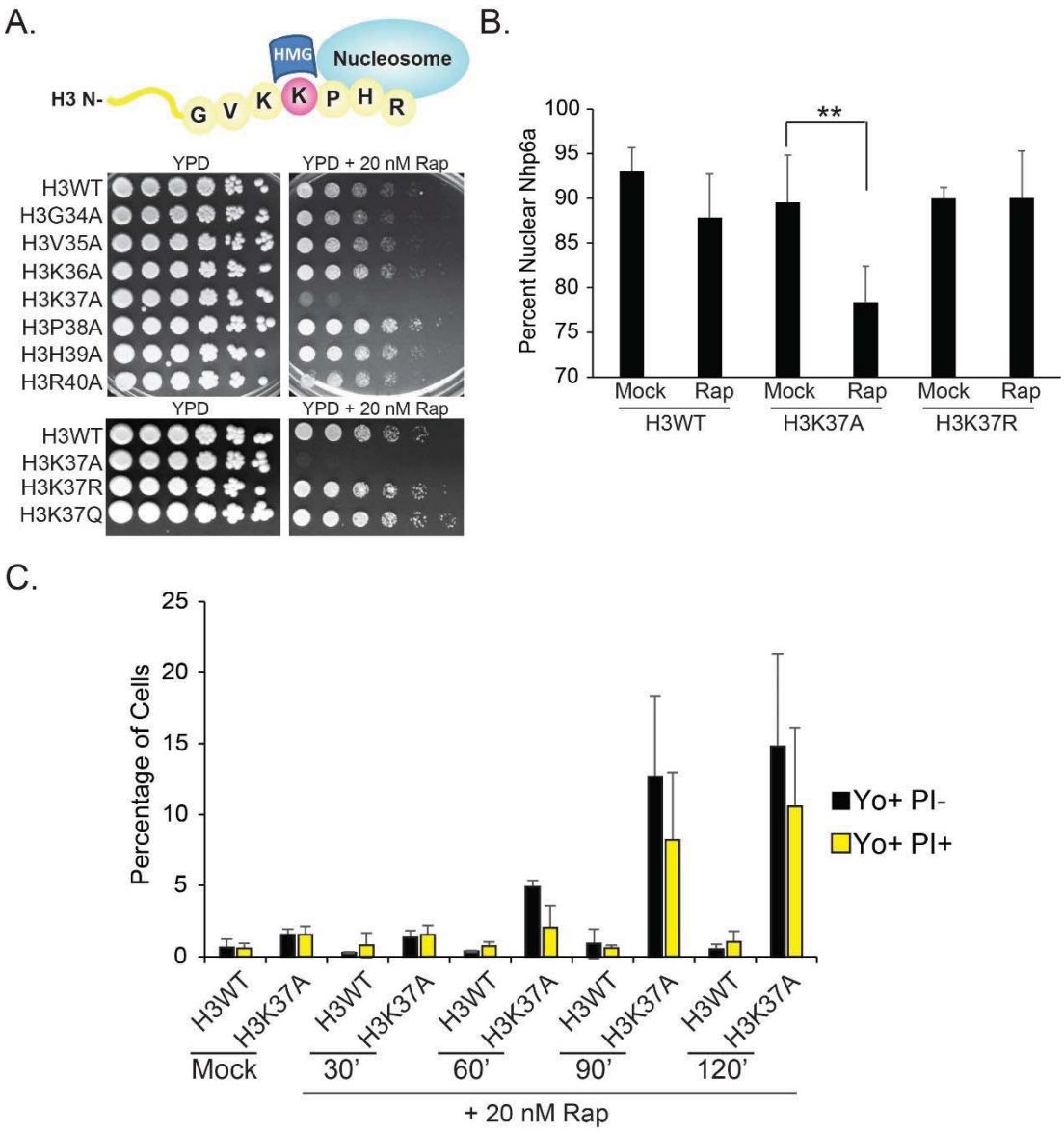

Figure 4-1. The H3K37A mutation correlates with HMGB nuclear delocalization and converts rapamycin from a cytostatic to cytotoxic agent.
A. Strains from a previously described histone mutant library [315] were grown to saturation, five-fold serially diluted, and spotted onto YPD control plates or YPD + 20 nM rapamycin. A cartoon illustrating relevant H3 N-terminal tail residues is provided, and H3K37 is highlighted in pink. See text for more details. **B.** H3WT and H3K37A cells expressing Nhp6a-EGFP were either mock or 20 nM rapamycin treated for one hour. Confocal microscopy images were obtained and analyzed as described in Chapter 2. Quantification of this data is provided, with means and SDs plotted. Significance was determined by pairwise Student's t-test. **-$p<0.01$. **C.** H3WT and H3K37A were cultured to log phase and then mock or 20 nM rapamycin treated for increasing lengths of time as denoted below. Cells were stained with YO-PRO-1 and PI and analyzed by flow cytometry. Averages and SDs are representative of three independent experiments. *Data source: personal communication with Dr. Hongfeng Chen, May 2016.*

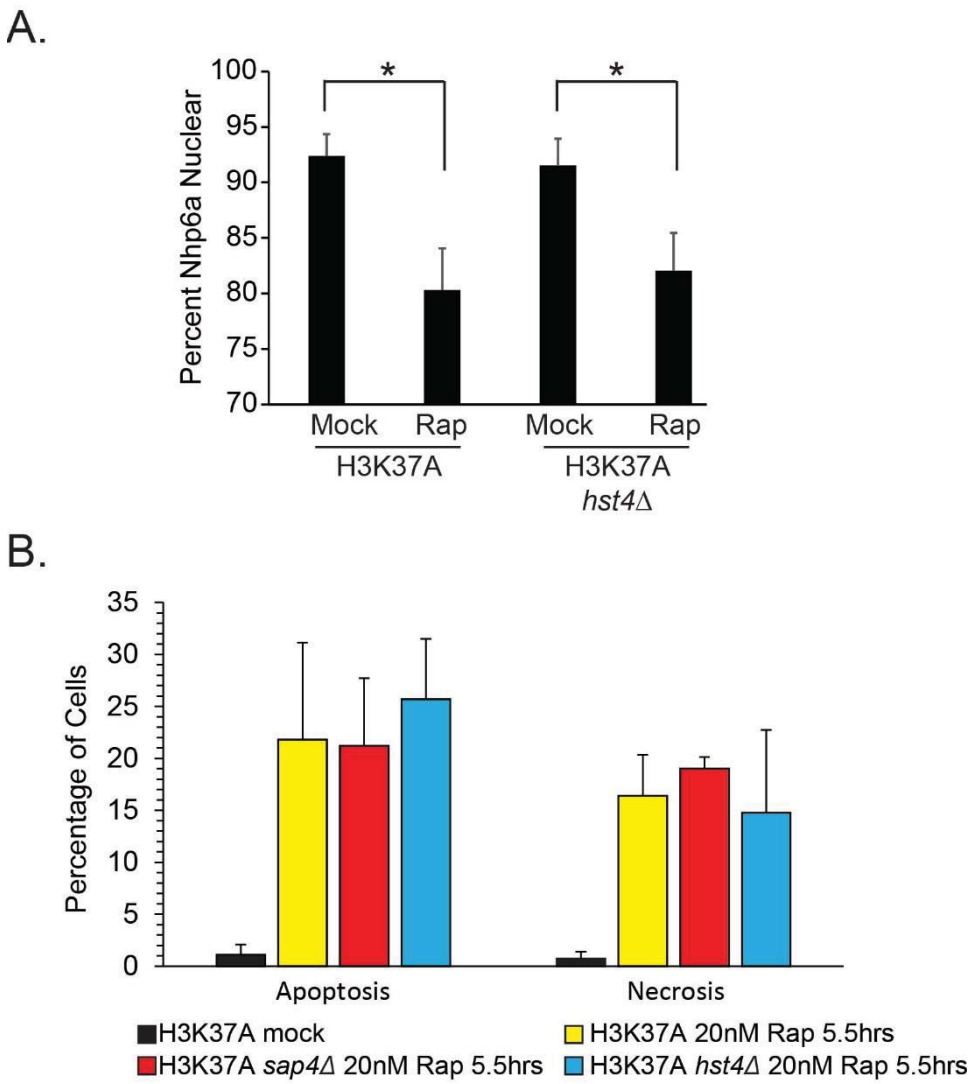

Figure 4-2. Partial restoration of TORC1 responsive histone H3/H4 acetylation does not reverse Nhp6A nuclear delocalization or cell death.
A. H3WT and H3K37A expressing Nhp6a-EGFP, and the matched *hst4Δ* mutants, were either mock or 20 nM rapamycin treated for one hour. Confocal microscopy images were taken and analyzed as described in Chapter 2. Averages and standard deviations are presented, and are representative of at least 3 independent biological replicates. Significance was determined by pairwise Student's t-test. *-$p<0.05$. **B.** H3K37A, H3K37A *hst4Δ* and H3K37A *sap4Δ* were cultured to log phase and then mock or 20 nM rapamycin treated for one hour prior to staining with YO-PRO-1 and PI and FACS analysis. The data are the average and SD of three independent experiments. Matched H3WT samples were analyzed in parallel (including *sap4Δ* and *hst4Δ* strains), however there was not any detectible apoptosis or necrosis in those samples. *Data source for Figure 4-2A: personal communication with Dr. Hongfeng Chen, May 2016.*

Overall, while these data do support a functional role for H3K37 as a vital contact residue for HMGB-chromatin binding under conditions of TORC1 inhibition, they argue against the hypothesis that TORC1-dependent acetylation contributes to this association. An alternative possibility could be that the TORC1-dependent chromatin changes detailed in Chapter 3 may function in parallel with H3K37 to suppress cell death. It is important to emphasize that we have demonstrated there is some functional redundancy amongst the sirtuins and Saps in their effects on histone acetylation. Therefore, in the absence of Hst4 or Sap4, additional Saps or sirtuins may partially compensate and thus, mask their potential contributions to this process. We chose to use these strains as we were unable to create an H3K37A *sit4Δ* mutant, which presumably would have had a greater effect on acetylation, and possibly rapamycin sensitivity.

Aberrant HMGB Expression and Localization Result in Vacuolar Acidification and Apoptotic and Necrotic Cell Death through a Novel Death Pathway

We next investigated the cell death mechanism triggered by HMGB displacement in H3K37A mutants following TORC1 inhibition. Previously, we noticed that the H3K37A cells displayed abnormal vacuolar morphology even prior to TORC1 suppression [152]. It was unclear at the time whether these vacuoles were dysfunctional, or if this was simply a sign of a compensatory increase in autophagy. We speculated that these changes in vacuole morphology may be linked to the cell death phenotype observed in TORC1-suppressed H3K37A cells. To explore this concept, H3 wild-type (H3WT) and H3K37A mutants were stained with CFDA, a dye which is used to visualize changes in vacuolar pH. Confocal microscopy analysis identified significant vacuole acidification in H3K37A mutants following 60 minute rapamycin exposure, whereas no change in pH was detected in similarly treated H3WT cells (**Figure 4-3A**). Importantly, the timing of acidification correlates with the nuclear release of HMGBs, which again, occurs prior to significant cell death (**Figure 4-1C**). Vacuole acidity was quantified by flow cytometry and steadily increased for hours in the rapamycin-treated H3K37A mutant (**Figure 4-3B**). There was no discernible change in the rapamycin-treated H3WT cells over this same period. Together, these results would suggest that cytoplasmic HMGBs may be promoting cell death, in part, via vacuolar dysfunction.

To demonstrate this vacuolar acidification is directly attributable to HMGB delocalization, we next asked whether aberrant HMGB expression caused a similar constellation of vacuolar effects in an otherwise wild-type cell. To accomplish this, we transformed H3WT cells with galactose-inducible Nhp6a or Hmo1 expression vectors. Cells were cultured in raffinose, treated with 2% galactose for 20 minutes, and then stained with CFDA and quantified by flow cytometry analysis. Unfortunately because vacuolar pH is highly responsive to metabolic changes, even transient galactose induction in minimal raffinose media led to increased acidity in the control cells, thus confounding data analysis (data not shown). Still, because the galactose-inducible promoter is leaky, confirmed by immunostaining for HMGB expression in the absence of galactose (**Figure B-5**), we attempted the experiment in minimal raffinose media without galactose induction. Excitingly, we were able to recapitulate the decrease in vacuolar pH by simply

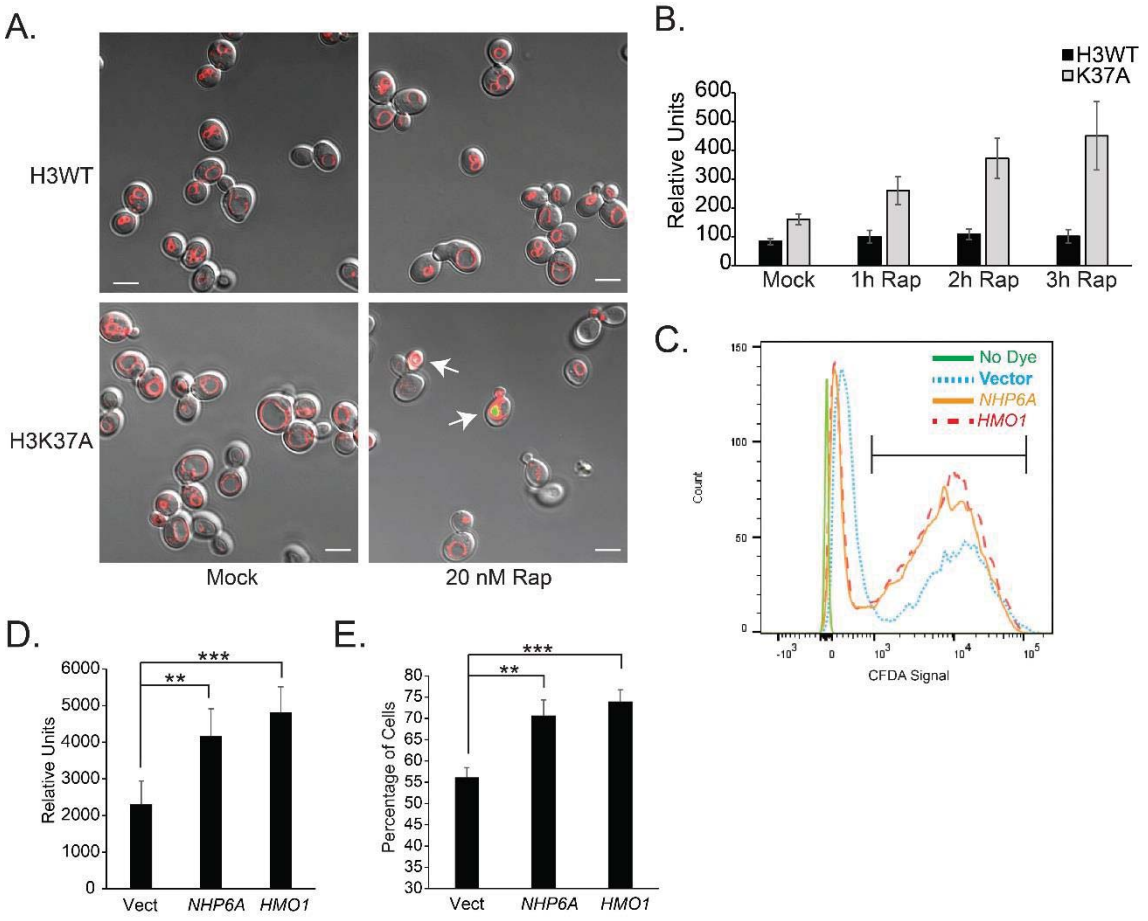

Figure 4-3. Aberrant HMGB localization results in vacuolar acidification. **A.** H3WT and H3K37A cells were grown to log phase in YPD and then mock or 20 nM rapamycin treated for 20 minutes. Cells were stained with CFDA and imaged via direct confocal microscopy as described in Chapter 2. Arrows denote cells with increased vacuolar acidity. **B.** As in (A), except rapamycin treatment was extended to 1-3 hours and analysis was conducted by flow cytometry. **C.** H3WT cells transformed with control vector or galactose-inducible NHP6A or HMO1 vectors were grown to log phase in YP-Raffinose. Cells were then stained with CFDA and analyzed by flow cytometry. **D.** Quantification of the average and SD of the peak CFDA fluorescence of the entire gated population shown in (C). **E.** Quantification of the average cell number and SD of the bracketed population in (C). Data are representative of five independent experiments. Significance was determined by pairwise Student's T-test. **-p<0.01; ***-p<0.001. *Data source for Figure 4-3A: personal communication with Dr. Hongfeng Chen, May 2016.*

deregulating HMGB expression/subcellular distribution in an otherwise wild-type cell (**Figure 4-3C, D** and **E**). We identified a shift in total CFDA signal (**Figure 4-3C,** quantified in **4-3D**), indicative of a decrease in the average vacuolar pH. Additionally, we observed a change in the overall population distribution toward a more acidic pH (denoted by bracketed population in **Figure 4-3C,** quantified in **Figure 4-3E**).

Our time course experiments suggested that vacuole acidification occurred prior to any significant loss of viability (**Figure 4-3B**). However, it remained unclear whether the cell death downstream of TORC1-dependent HMGB displacement was directly caused by the decrease in vacuolar pH. To address this point, we incorporated MES into our plate media to ask whether pH buffering could rescue the H3K37A rapamycin phenotype. We found that the H3K37A cells were significantly less sensitive to rapamycin when cellular pH was buffered (**Figure 4-4**). These results further support our hypothesis that TORC1 inhibition in H3K37A, and the resulting HMGB delocalization, is an initiator of cell death through aberrant vacuolar acidification.

H3K37A Mutants Display Increased TORC1 Activity, Which Correlates with Displacement of HMGBs and Can Be Reversed by HMGB Deletion

Our findings to this point illustrate a strong correlation between HMGB delocalization and vacuolar dysfunction. We previously hypothesized that one reason the H3K37A mutant is hypersensitive to rapamycin is that, while H3K37 serves as the main chromatin docking site for HMGBs, TORC1-dependent histone acetylation states may contribute to HMGB chromatin binding as well. However, the data presented in **Figure 4-2** would suggest instead that TORC1 signaling and HMGB binding may function in parallel to synergistically regulate cell survival. In the process of performing the experiments with the H3K37A *hst4Δ* and H3K37A *sap4Δ* strains (**Figure 4-2)**, we serendipitously discovered that H3K37A mutants have a dramatic increase in basal TORC1 activity as demonstrated by S6 phosphorylation (**Figure 4-5A**).

Recently an insightful review was published by Eltschinger and Loewith [318] describing a series of feedback loops centered around TORC1. Given that TORC1 complex activation is tightly linked to vacuolar processes, we speculated that the nuclear displacement of these HMGs downstream of TORC1 might alter vacuole function to feedback and affect complex activity. Strikingly, wild-type cells transformed with galactose-inducible HMG plasmids exhibited significantly elevated TORC1 signaling relative to control vector expressing cells (**Figure 4-5B**). Additionally, we found that genomic deletion of the HMGs previously identified as having TORC1-responsive cytoplasmic localization (Nhp6a and Nhp10) was sufficient to reduce TORC1 signaling in both H3WT and H3K37A backgrounds (**Figure 4-5C**). This effect is specific as deletion of *HMO1*, a gene encoding an HMG whose nuclear localization was unaffected by both H3K37A and TORC1 inhibition [152], had no effect on TORC1 function (**Figure 4-5C)**. Altogether, these findings confirm that delocalization of HMGs in both H3WT and H3K37A backgrounds, particularly the nuclear to cytoplasmic translocation of

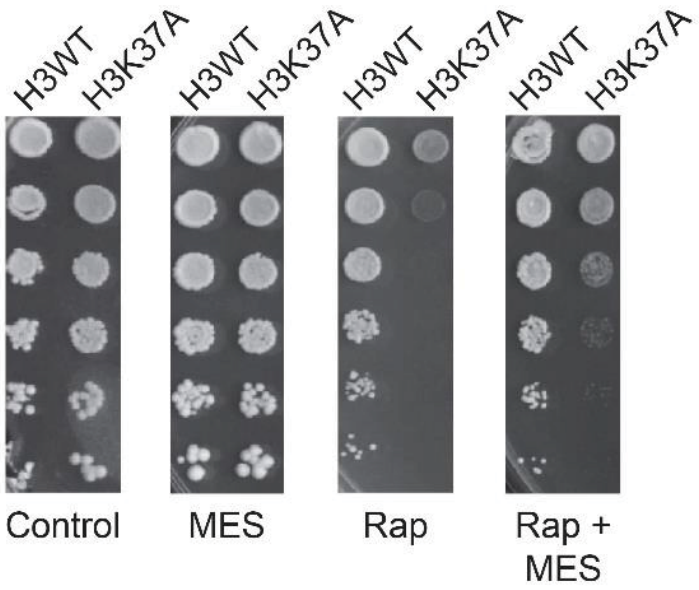

Figure 4-4. Buffering intracellular pH is sufficient to partially reverse the rapamycin sensitivity of an H3K37A mutant.
H3WT and H3K37A cells were grown to log phase, five-fold serially diluted, and spotted to indicated media conditions. *Data source: personal communication with Dr. Hongfeng Chen, May 2016.*

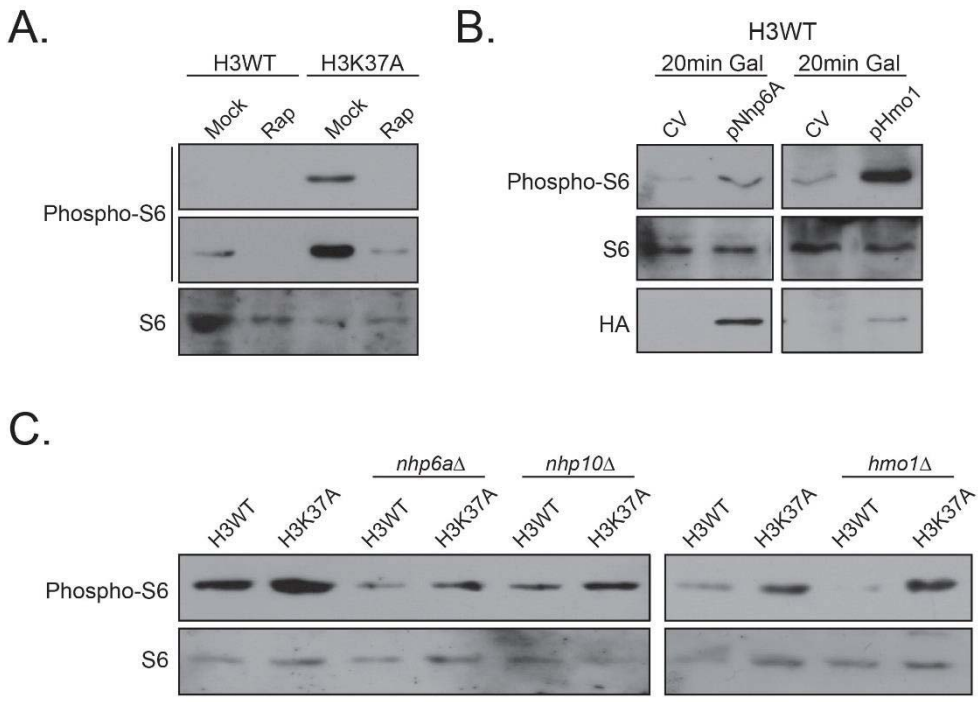

Figure 4-5. H3K37A mutants display increased TORC1 activity that depends on the presence of specific HMGB factors.
A. H3WT and H3K37A cells were grown to log phase and mock or rapamycin treated (20 nM) for 60 minutes. Extracts were prepared and analyzed by IB as indicated. **B.** H3WT cells transformed with galactose-inducible, HA-tagged, HMGB expression vectors were grown to log phase in raffinose media prior to 2% galactose induction for 20 minutes. Samples were processed and analyzed as in (A). **C.** H3WT and H3K37A strains were constructed in which the indicated individual HMGB genes were deleted. Strains were grown up to log phase in YPD and analyzed by IB as in (A).

Nhp6a and Nhp10, is sufficient to promote vacuolar dysfunction and an overall increase in TORC1 activity.

In all, the work presented in this chapter suggests that H3K37 does indeed serve as a docking site for high-mobility group proteins *in vivo*, though whether TORC1-responsive acetylation states contribute to HMGB chromatin binding is questionable. Disruption of HMGB chromatin association results in apoptotic and necrotic cell death marked by aberrant vacuolar pH and elevated TORC1 function.

CHAPTER 5. INVESTIGATING THE ROLE OF TCO89 IN TORC1

Identification of the Domain Necessary for Tco89-Dependent TORC1 Functions

Very little is known about the function of the *S. cerevisiae* TORC1 subunit Tco89, and structurally, we know virtually nothing. As was mentioned in Chapter 1, homologs have been identified in *S. pombe* and *C. albicans,* though curiously, it is currently the only yeast TORC1 subunit without an obvious mammalian ortholog [52, 53]. There is evidence that Tco89 bridges TORC1 and the vacuole [49], coordinates vacuolar function via Vac8 [62], and also regulates site-specific histone acetylation [66]. Previous studies summarized on the Saccharomyces Genome Database demonstrate that *tco89Δ* cells have abnormal cellular physiology and budding patterns, as well as dramatically increased sensitivity to heat, caffeine, MMS, rapamycin and salt [52, 54-60]. Allowing *tco89Δ* cells to reach stationary phase where nutrients are limiting, or treating them with rapamycin, results in an irreversible cell-cycle arrest [49, 61]. These effects demonstrate that loss of this subunit enhances cellular sensitivity to TORC1 inhibition. Interestingly, these mutants are also described as having a decreased rate of carbon and nitrogen metabolism [319]. We believe a better understanding of Tco89's role within the complex could provide insight into whether a similar subunit exists within mammals. If so, targeting such a factor pharmacologically could greatly enhance the clinical efficacy of mTORC1 inhibitors.

We first wanted to identify the key domains of the protein required for its function. We constructed a series of N-terminal Tco89 truncation mutants, each displaying a C-terminal FLAG epitope tag. Very little is currently known about the structure of Tco89, so we utilized the PSI-PRED prediction profiling software as a guide for where to draw our boundaries between clones (**Figure 5-1A**) [302]. It was our hope that with this information we could avoid truncating in the middle of a domain, which would likely confound our analysis. Our cloning strategy is shown in full in **Figure 5-1A**. We demonstrated that all of our truncations are stable and expressed at approximately equal levels in **Figure 5-1B**. While the particular blot presented in **Figure 5-1B** appears to have less of clone B present, we note that this is not a consistent result. There seemed to be a degree of fluctuation across the independent transformations which is not currently understood, but we never observed a pattern that would suggest one clone is more or less stable than the rest, nor did these fluctuations ever seem to correlate to a difference in screened phenotypes.

Wild-type and *tco89Δ* cells transformed with control vector, a vector expressing full-length Tco89, or various Tco89 truncations, were grown overnight to saturation. Equivalent numbers of cells were then serially diluted and spotted onto control selection plates, and selection plates containing rapamycin or caffeine (**Figure 5-2A**). The phenotype of each mutant grown on these various TORC1 inhibitors was qualitatively scored using a previously described method [152]. These values were averaged and are shown in heat map format in **Figure 5-2B**. Clearly, there is a dramatic difference in rapamycin sensitivity comparing fragment C to fragment D, which would indicate that

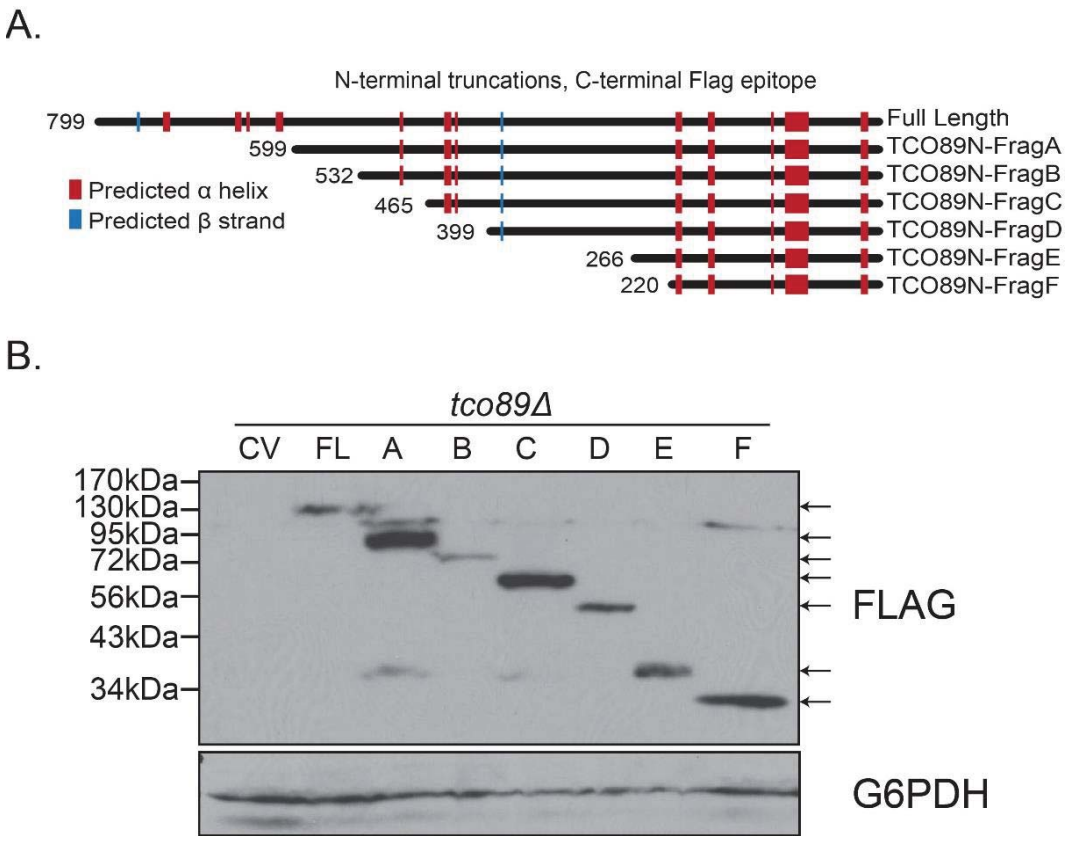

Figure 5-1. Construction of Tco89 mutant expression vectors.
A. Diagram of cloning strategy used to create a series of N-terminal truncations of the TORC1 subunit Tco89. Constructs contain a C-terminal FLAG epitope for visualization. PSI/PRED prediction software was used to locate probable secondary structure, and the software profile information is provided [302]. Predicted α helices are denoted in red and β strands in blue. **B.** *tco89Δ* cells were transformed with control vector (CV), or vectors containing full-length Tco89 (FL) and the truncations (A-F). Transformants were grown to log phase under selection, and whole cell extracts were prepared and blotted for FLAG to confirm expression. Arrows denote the seven Tco89 truncation fragments. G6PDH is provided as a loading control.

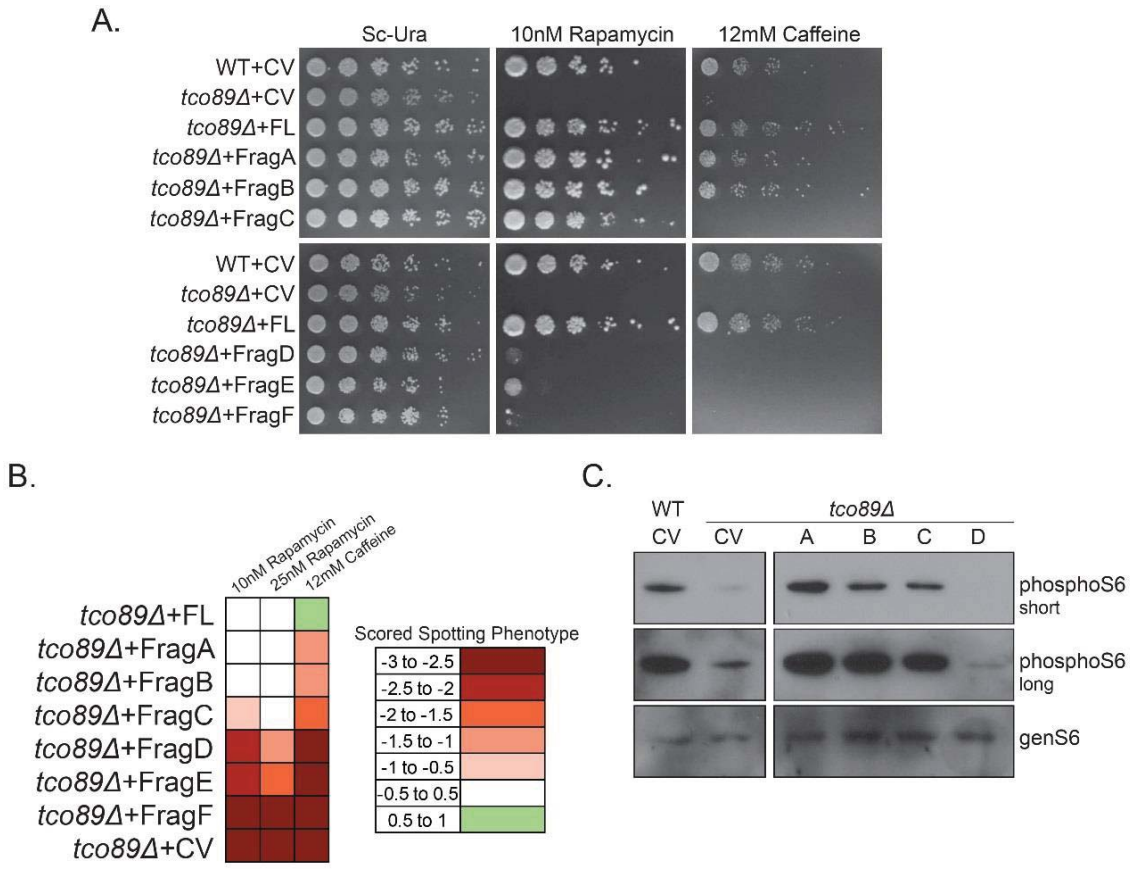

Figure 5-2. Identification of the functional domain necessary for Tco89-dependent TORC1 functions.

A. WT cells transformed with control vector, and *tco89Δ* strains expressing the series of Tco89 truncation vectors, were grown to stationary phase, five-fold serially diluted and spotted to TORC1 inhibitory conditions as indicated. Images are representative of growth following four days incubation. Growth on various conditions was scored on a -3 to 3 scale as described previously [305], and in Chapter 2. **B.** Quantification of growth phenotype scores from (A). Data is presented as a heat map, with red indicating decreased growth compared to wild-type, white indicating no change, and green representing an increase in viability. Scores are the average obtained from at least five independent transformations. **C.** Strains of interest from (A) were grown to log phase and extracts were prepared. Samples were analyzed by immunoblot as indicated.

amino acids 465-399 are critical for maintaining the cell's ability to grow when TORC1 activity is reduced. Interestingly, a similar effect is seen with caffeine between fragments B and C, suggesting that Tco89 may mediate the cellular response to rapamycin and caffeine in different ways. Although fascinating, this result is not entirely surprising given previous work that indicated rapamycin and caffeine affect TORC1 function disparately [320], and that caffeine may inhibit TORC1 in a Tco89-dependent fashion [62].

Finally, we explored whether the dramatic shift in spotting phenotypes observed between fragments C and D correlated with a decline in TORC1 activity. Cells from **Figure 5-2A** were grown to log phase, WCEs were prepared, and TORC1 signaling was assessed by blotting for phosphoS6. In **Figure 5-2C**, we demonstrated that indeed there is an almost complete loss of steady state TORC1 function from fragment C to fragment D, which correlates nicely with the significant increase in sensitivity to rapamycin and caffeine (**Figure 5-2A** and **5-2B).** We had hoped to utilize these truncation mutants for further phenotypic evaluation, however given that our selectable marker was auxotrophic, and all of our processes of interest are highly responsive to nutrients, the necessity of growing cells on defined media to select for the plasmids led to confounding results (data not shown).

The Observed Cell Cycle Arrest in *tco89Δ* Upon TORC1 Limitation Is Not Attributable to Dysregulation of Reactive Oxygen Production

We next wondered whether *tco89Δ*'s dramatic sensitivity to TORC1 inhibitors could be partially alleviated by removal of an upstream negative regulator of TORC1. To assess this possibility, we deleted the gene encoding *NPR3,* a Gtr1 GTPase that suppresses TORC1 signaling. We found that loss of this negative regulator was not sufficient to overcome the observed rapamycin sensitivity, as *tco89Δ npr3Δ* grew just as poorly as *tco89Δ* (**Figure 5-3A**). This likely means that Npr3 inhibition of TORC1 occurs upstream of *tco89Δ*.

Given the reported nutrient utilization phenotypes of a *tco89Δ* [319], and considering that TORC1's effect on lifespan has been suggested to occur, in part, through mediation of mitochondrial ROS signaling [321-325], we next examined the effect loss of Tco89 has on mitochondrial function. Previous findings demonstrated that in wild-type cells, the transition from log phase to stationary phase is marked by a dramatic increase in ROS levels [321]. Interestingly, *tor1Δ* displays increased basal levels of ROS, though there is a negligible effect on cellular ROS as this mutant transitions from log phase to stationary phase [321]. Early exposure to ROS in the *tor1Δ* is suggested to "toughen up" the cells, a phenomena known as hormesis [326]. The combination of hormesis and the reduction in stationary phase ROS has been hypothesized as one of the ways *tor1Δ*, and TORC1 suppression in general, contributes to an increase in lifespan.

We knew that in *tco89Δ,* nutrient limitation, TORC1 inhibition, or simply growing cells to saturation (late log phase) resulted in a permanent exit from the cell

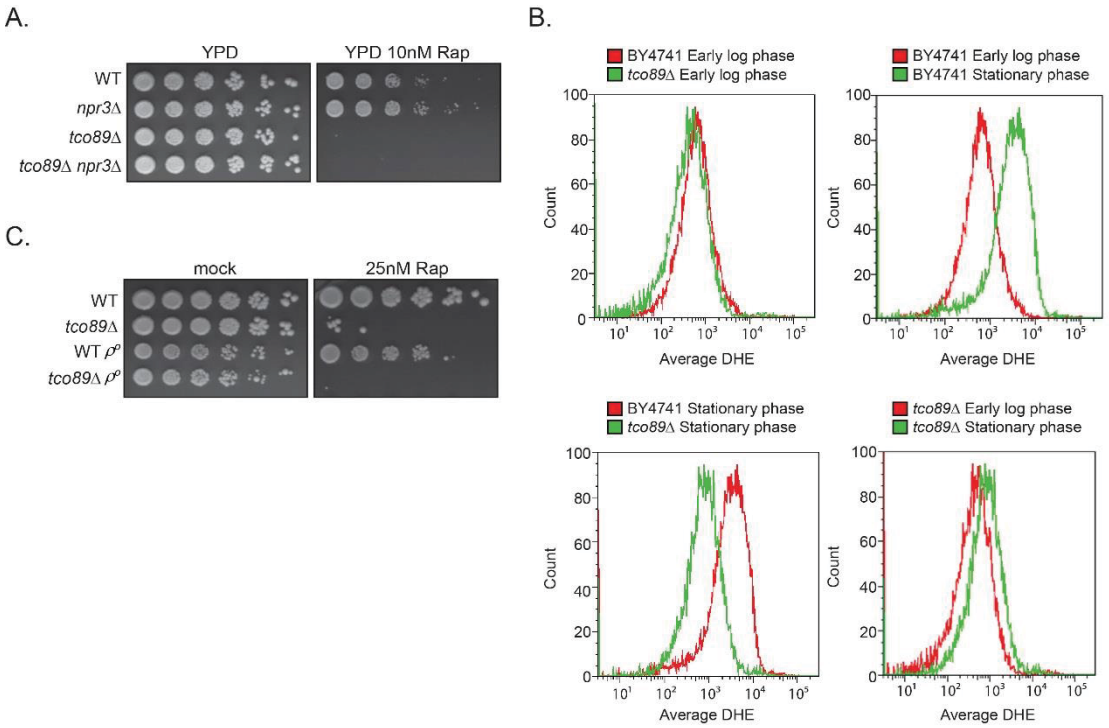

Figure 5-3. Loss of Tco89 results in adaptive ROS response similar to that observed in *tor1Δ*.

A. Wild-type (WT), *npr3Δ*, *tco89Δ* and *tco89Δ npr3Δ* cells were grown to stationary phase, five-fold serially diluted, and spotted onto YPD and YPD + 10 nM rapamycin. Photos provided are representative of growth after 3 days. **B.** WT and *tco89Δ* cells were grown to early log phase (OD~0.4) and mid stationary phase (OD~15). At both points, aliquots of cells were stained with DHE for 20 minutes followed by flow cytometry analysis. **C.** WT, *tco89Δ* and their corresponding mitochondrial-deficient strains (denoted ρ^0) were grown to log phase, mock treated or treated with 25 nM rapamycin for 5.5 hours, washed, and spotted onto YPD.

cycle [43, 49]. This led us to wonder what the ROS profile in a *tco89Δ* would look like as the strain transitioned from log phase to stationary phase, and whether dysfunction in the regulation of ROS production could possibly explain these cell cycle defects. Unlike *tor1Δ*, the *tco89Δ* displayed no significant increase in log phase ROS, though it did have a significant reduction in stationary phase ROS when compared to the wild-type cells (**Figure 5-3B**). The nature of the difference between *tor1Δ* and *tco89Δ* is not readily apparent, though given that log phase and stationary phase *tco89Δ* cells have nearly identical ROS levels, we can say that the observed cell cycle exit is not due to an inability to coordinate these ROS pathways.

Finally, we wondered whether compromising the mitochondrial genome (denoted ρ^0) would have an effect on the normal growth of *tco89Δ*, or its response to transient TORC1 inhibition. Wild-type, *tco89Δ*, and their corresponding ρ^0 mutants were grown to log phase, mock treated or treated with rapamycin for 5.5 hours, washed and spotted onto YPD. The mock treated ρ^0 mutants do tend to grow slower than the paired controls. However there does not appear to be any TORC1-dependent difference, as the *tco89Δ* ρ^0 mutant is equally as sensitive to transient rapamycin treatment as *tco89Δ* (**Figure 5-3C**).

In total, this chapter represents the first structural assessment of the role of the Tco89 subunit within the TORC1 complex. Through construction of a series of truncation mutants, we identify the specific domain that is critical to allow cells to grow in the presence of TORC1 inhibition, and demonstrate that this domain is also critical for steady state TORC1 function. We report that the irreversible cell cycle arrest observed in nutrient deprived *tco89Δ* cannot be explained solely through defects in ROS signaling as cells transition from log phase to stationary phase. We believe these findings and tools will inform future studies to wholly characterize Tco89, and to determine whether it has a functional mammalian counterpart.

CHAPTER 6. DISCUSSION AND FUTURE DIRECTIONS

It is critical for eukaryotes, whether they are single-celled yeast or multicellular organisms, to rapidly adjust their growth and proliferative profiles in response to intracellular deficits or changes in their extracellular environment. Studies from a number of labs suggest a regulatory link exists between TORC1 and the epigenome, including work in which we characterized the TORC1-responsive acetylation of H3K56 [66]. Additionally, we know from prior studies that a correlation exists between TORC1 activity, histone acetylation, and HMGB chromatin binding [152]. At the outset of this study, we speculated that TORC1 signaling likely regulates other histone modifications besides H3K56ac, as it was demonstrated to mediate pan-H4 acetylation at the ribosomal protein genes [12], and that these modifications may contribute to anchoring HMGBs to chromatin.

TORC1 and Histone Acetylation

In Chapter 3, we significantly expanded our understanding of the upstream stimuli linking TORC1 to the control of histone acetylation, and we gained an appreciation of the breadth of TORC1-responsive histone modifications. Foundational studies in the field utilized pan-H3 and pan-H4 acetyl antibodies to identify gross acetylation loss in response to TORC1 inhibition [12, 13]. But here we characterized for the first time the TORC1-mediated acetylation of H3K18, H3K23 and H4K12 (**Figure 3-1**). The specificity we observed is quite interesting and suggests inhibition of TORC1 is not promoting a global decrease in histone acetylation, nor is it a massive non-specific effect due to loss of all transcription-coupled marks (H3K4me3 is intact).

One possible explanation could be that inhibition of TORC1 results in a shift in metabolic intermediate availability, including acetyl CoA and NAD^+, which feed into the acetylation and deacetylation reactions respectively. However, we would expect that if this were the case, the effects would be more universally observed across a multitude of histone residues. Rather this hypoacetylation appears to be a specific, site-directed response to decreased TORC1 function, as low-level pharmacological inhibition for a short time (20 minutes) is sufficient to induce the effect. Considering the existing link between TORC1 and the post-translational modification of H2A in the DNA damage response [327], it would be fascinating to probe other acetylation states such as H2AK7, H2AK21, H2BK11, and H2BK16, to see whether TORC1-responsive acetylation exists on H2A or H2B as well. We believe it is likely that TORC1-dependent histone modifications extend beyond acetylation, possibly to acylation (sirtuin substrate), phosphorylation, methylation, sumolyation, neddylation and others. Incorporation of mass-spectrometry based histone proteomics would provide us a more complete understanding of the diversity of the histone post translational modifications downstream of TORC1.

TORC1 occupies a critical point in a pair of nutrient sensing axes. Amino acids and carbon both feed into the TORC1 signaling pathway, and each appears to do so, in part, through adaptive intracellular pH mechanisms [49, 80, 328]. Prior to this work, TORC1-responsive acetylation has been investigated exclusively by using the direct pharmacological TORC1 inhibitor, rapamycin. And while we also utilize rapamycin for this purpose, we extend our analyses to include several additional means of suppressing TORC1 activity. These stimuli are likely more physiologically relevant and thus, we examined their influence on our chromatin modifications of interest.

We provide striking evidence that not all TORC1 inhibition is equivalent at the level of acetylation, finding that nitrogen metabolism disruption (MSX), but not carbon limitation, led to decreased acetylation of a model TORC1 residue (**Figure 3-2**). The data presented argues against the previous claims that crosstalk between carbon metabolism and TORC1 signaling is responsible for our observed epigenetic effects [328, 329]. Instead, they suggest an interesting regulatory bifurcation through which cells may tailor their epigenome based on the specific nutrient they are lacking. There is likely a degree of overlap between nitrogen and carbon metabolism, as inhibition of TORC1 did not result in total ablation of our modifications of interest. Still, these findings illustrate that nitrogen signaling plays a vital and distinct role in the dynamic regulation of key acetylation sites. Additionally, they imply that signaling between vacuolar components (v-ATPase, EGO complex) and TORC1 is vital for the relay of environmental energy states to chromatin-based processes. Indeed a previous genetic screen of the yeast deletion collection found that a number of vacuole mutants display acetylation phenotypes [330]. We speculate that functions previously attributed to TORC1-mediated histone acetylation, including rDNA stability and regulation of RP gene expression [12, 13], are also nitrogen specific given that the need for ribosomes and anabolic flux is reduced under starvation conditions. However, because these studies only utilized rapamycin to inhibit TORC1, it is impossible to be sure without delving back into those questions using specific amino acid starvation or suppression of general nitrogen metabolism via MSX.

In Chapter 3 we also present findings demonstrating that TORC1-dependent histone acetylation is regulated by sirtuin histone deacetylases. This corroborates our previous observation that deletion of *HST3* and *HST4* in the *tco89Δ* background is sufficient to rescue H3K56ac [66]. The connection between TORC1 and the sirtuins makes sense considering how intimately each is tied to cellular energy states. TORC1 activity is most robust during times of nutrient abundance when cell growth and proliferation would be appropriate and advantageous, while sirtuins are most active when energy availability is limited (low NADH concentration, elevated NAD^+/NADH ratio) [291]. The reciprocal arrangement between TORC1 and the sirtuins reported in yeast appears to be evolutionarily conserved, as mTORC1 suppression in metazoans promotes transcription of the SIRT4 gene [184].

Within our sirtuin results (**Figure 3-10**), we reported several previously unidentified, candidate substrates for each of the enzymes: Hst1 (H4K12ac), Hst2 (H3K18ac), Hst3 (H3K18ac, H4K12ac), Hst4 (H3K18ac, H3K23ac, H4K12ac) and Sir2

(H4K12ac). Looking over these acetyl sites, we recognized several that are downstream of sirtuins in higher order organisms as well, including H3K18ac (deacetylated by SIRT6 and SIRT7) and H3K56ac (deacetylated by SIRT6). SIRT6 regulation of H3K18ac was only recently identified, and was shown to occur at pericentric heterochromatin [237]. Hyperacetylation of H3K18ac in the absence of SIRT6 (which will also increase H3K56ac) leads to transcriptional activation of the otherwise silent pericentric chromatin, and accumulation of centromeric transcripts causes mitotic defects, genomic instability and cellular senescence. This is fascinating considering our data linking the yeast sirtuin Hst4, a regulator of H3K18ac, and the ability of *tco89Δ* cells to re-engage the cell cycle (or evade arrest entirely) in response to TORC1 inhibition. Additionally, the SIRT7-dependent regulation of H3K18ac has been reported to promote oncogenic transformation and maintain tumorigenicity by disabling transcription of tumor suppressor genes [240, 331, 332]. Notably, it was previously reported that overexpression of SIRT1 could complement loss of Sir2 in yeast [177].

We believe future complementation studies using vector-based human sirtuins in yeast deletion mutants could flesh out whether the human sirtuins are also responsive to TORC1, while highlighting which enzymes are most functionally conserved between humans and yeast. This would also provide significant evidence of mechanistic conservation of our described mechanism. A shortcoming of this portion is that to this point, all of the data linking TORC1 and specific acetylation states has been genetic in nature. Considering all the different pieces of evidence we have obtained, we are extremely confident that this observed phenomena is biologically real. Still, our stance would be significantly strengthened if we were to use biotinylated recombinant histones in *in vitro* deacetylation assays (such as the *Fluor de Lys*™ assay from Enzo Life Sciences [159]) to confirm that the sirtuins do in fact target these residues.

The PP6 Phosphatase Complex and the TORC1-Dependent "Acetylome"

Our data demonstrate that when ample nitrogen is available, TORC1 regulates sirtuin-dependent site-specific histone H3/H4 acetylation through the suppression of the Sit4/PP6 complex and subsequently, enhanced Hst4 protein levels. One of the most compelling parts of this work involves how PP6 activation triggers this increase in Hst4 expression. We first investigated whether *HST4* gene transcription is regulated through the Sit4-mediated NCR stress response by deleting the Sit4-responsive transcription factors Gln3 and Gat1. The rationale being that if Hst4 protein levels are tied to Gln3 and/or Gat1 function, deletion of these NCR components should result in a decrease in Hst4 protein and an increase in histone acetylation. It was clear however, that this was not the case. Loss of these transcriptional regulators did not have a positive effect on acetylation. Likewise, deletion of the cytoplasmic anchor that mediates their cytoplasmic localization upon nutrient stress did not promote a decrease in acetylation. We also find that TORC1 inhibition does not result in any increase in *HST4* mRNA expression, all together suggesting that the elevated Hst4 protein levels that occur in response to TORC1 inhibition occurs independent of *HST4* transcriptional regulation or changes to *HST4* mRNA stability. Instead, we report a mechanism in which Sit4 activation promotes a

rapid, cytoplasmic to nuclear redistribution of Hst4, resulting in protein stabilization and a site-specific decrease in histone acetylation. The most important take away is timing, as we demonstrate that maximal nuclear accumulation occurs within 20 minutes (**Figure 3-16**). Presumably, it is this population of Hst4 that promotes the immediate deacetylation observed upon acute rapamycin treatment. The subsequent increase in protein levels does not occur until some 40 minutes later (**Figure 3-11**), and we believe this stabilization sustains the hypoacetylation phenotype until TORC1 activity is restored.

In situations where we find a TORC1-dependent increase in Hst4 levels, we also observe a corresponding decrease in Hst3, which could suggest a regulatory balance exists between the amount of Hst3 and Hst4 in the cell. This possibility has already been hinted at in a work which demonstrated that the replication origin deficiencies observed in an *hst3Δ* cell could be overcome by expressing Hst4 under the control of the Hst3 promoter [333]. Still, it is currently unclear as to how Sit4-PP6 activation results in Hst4 nuclear accumulation (denoted by question marks in **Figure 6-1**). Our Phos-tag results (**Figure 3-15**) would suggest that this stabilization is not directly attributable to Sit4-mediated sirtuin phosphorylation. However, we have only addressed this hypothesis with the Phos-tag approach, as our attempts to incorporate pan-phosphorylation antibodies and phosphostains were unsuccessful (data not shown). As a consequence, given what is known about the turnover of Hst3, we cannot yet exclude the possibility that Sit4-dependent dephosphorylation of Hst3 or Hst4 does indeed regulate their function. Still, this leaves us to wonder about alternative explanations. Such as whether the phosphatase may coordinate sirtuin nuclear localization through regulation of importin (Srp1) and exportin (Xpo1) factors; the yeast carrier proteins responsible for actively chaperoning cargo proteins in and out of the nucleus. There is precedent for this as Hst2 shuttling is known to be regulated by Xpo1 [164]. Further, the import capacity of a mammalian ortholog of Srp1, importin α1, has been shown to be responsive to phosphorylation and acetylation [334].

Interestingly, it would appear that the identity of the Sit4-associated protein may confer an additional layer of specificity to the acetylation response, as we find that loss of Sap4 or Sap185 leads to a reduction in H3K18ac rapamycin sensitivity (**Figure 3-6**). Previous work examining rapamycin and zymocin sensitivity in yeast also identified dramatic phenotypic differences attributed to Sap association [100], though it is unclear what exactly the Saps contribute to these processes. Given the partial rescue observed in the *sap4Δ* and the *sap185Δ*, we speculate that these regulatory subunits are functioning at least somewhat redundantly to bridge the interaction between the Sit4 phosphatase and its downstream targets. Considering the high degree of conservation across this pathway, and that mammalian sirtuins are known to actively shuttle from the nucleus to the cytoplasm, we propose that future studies include pilot experiments asking whether exogenous human Sit4 (PPP6C) could complement Hst4 stability and localization in a *sit4Δ* cell. A similar approach could be conducted using the human Sap orthologs (PPP6R1/2/3). If it appears these mechanisms are indeed conserved, we could attempt to replicate these findings by monitoring acetylation in human cells with RNAi knockdown of PPP6C, PPP6R1/2/3, or the sirtuins which have been shown to shuttle intracellularly (SIRT1/2/3).

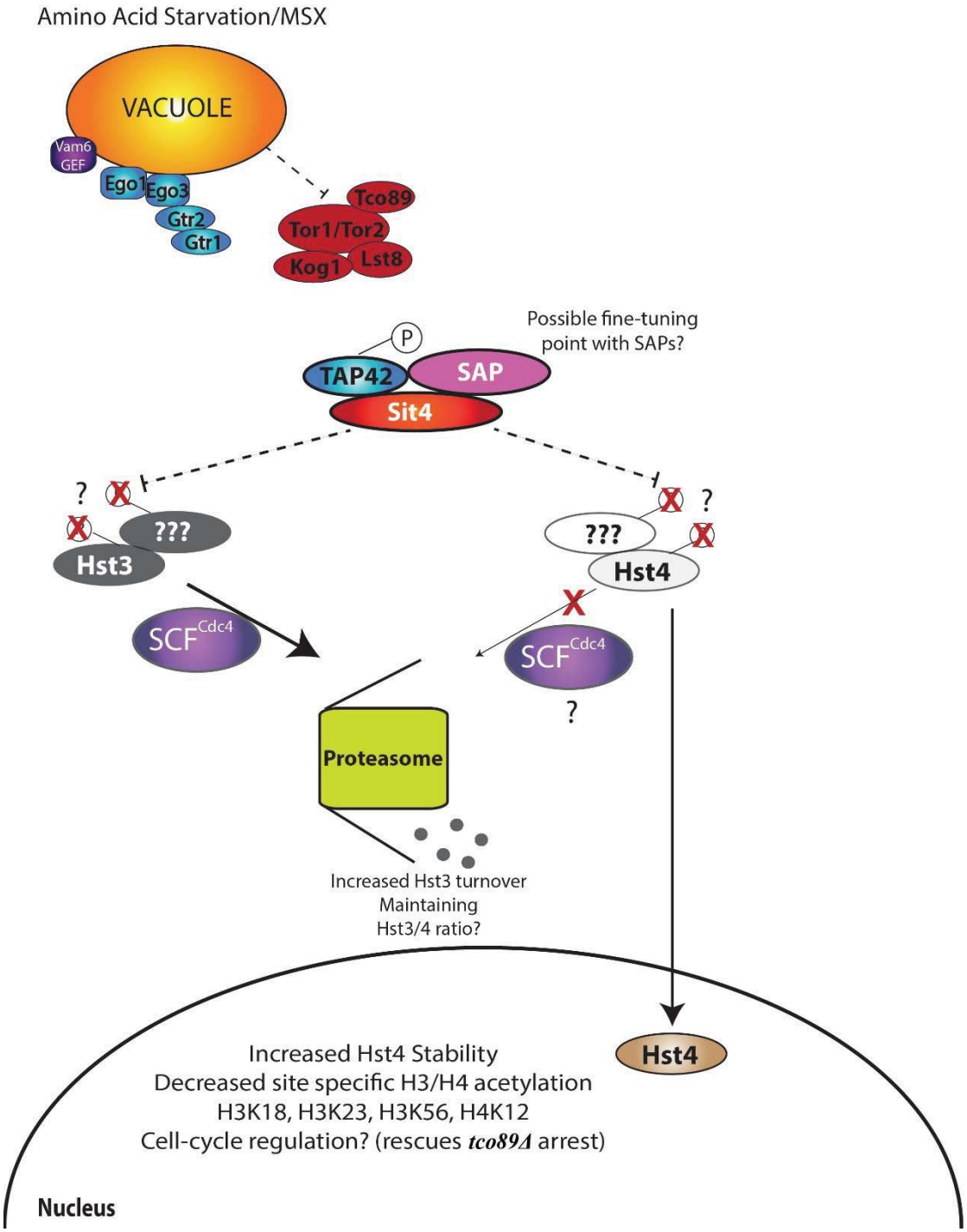

Figure 6-1. Proposed mechanism.
Summary of work presented in Chapter 3 as discussed in Chapter 6. Areas requiring further study are denoted by question marks. See text for more details.

Finally, it seems likely that TORC1 regulation of sirtuin function could contribute to changes in acetylation of non-histone substrates as well. The mammalian sirtuins, and particularly SIRT1, have been shown to target chromatin-modifying enzymes (p300, MOF, Tip60), as well as proteins involved in autophagy (FOXO1, FOXO3, LC3, Atg5/7/8), the stress-response (NF-κB, c-Myc, HIF-1α), metabolism (LKB1, PGC-1α) and DNA repair (Ku70, PARP1). Can we build on this information to define a TORC1-responsive acetylome to better understand how aberrant mTORC1 signaling promotes disease? Could some of mTORC1's canonical functions (anabolism, autophagy, and ribosome biogenesis) be partially attributed to mTORC1-dependent sirtuin localization? In addition to the yeast orthologs of the proteins mentioned above, there are a few other yeast candidate factors we propose evaluating in future studies.

Spt7

Previous studies identified a replicative lifespan increase in mutants of the Gcn5-containing SAGA histone acetyltransferase complex [335]. This observed lifespan extension could implicate TORC1 in coordination of SAGA function, and the fact that this effect requires Sir2 suggests the possibility that TORC1-dependent sirtuin activity could feed into SAGA. The Pep4-dependent processing of the SAGA subunit, Spt7, determines whether SAGA exists as a holocomplex or a subcomplex (also known as SLIK/SALSA) lacking Spt8 [336]. Spt7 has been shown to possess a bromodomain whose chromatin binding is sensitive to histone acetylation [337], and Spt7 has itself been suggested to be acetylated [163].

We speculate that TORC1 may participate in regulating SAGA chromatin binding through coordination of H3 acetylation (Chapter 3). However, it is also possible that TORC1 may affect Spt7 acetylation via sirtuin stabilization to influence Spt7 processing, and SAGA composition or localization. It would be fascinating to utilize the previously described multi-epitope Spt7 strains [338] to assess TORC1 contributions to these SAGA dynamics. Further, we could immunoprecipitate Spt7 under same conditions and immunoblot to determine if its acetylation state is dependent on TORC1 activity. Either of these proposed mechanisms (histone acetylation dependent, direct effects on SAGA via Spt7) would enable TORC1 suppression to promote initial histone deacetylation through nuclear accumulation of Hst4, and also to feed back onto SAGA to prevent the incorporation of new histone acetyl marks. Together, these effects maintain a transcriptionally repressive chromatin state until environmental conditions improve.

Ifh1

Ifh1is a coactivator of ribosomal protein gene transcription, and it is found at the RP promoters when environmental nutrient availability is sufficient to sustain growth. It is an essential gene that, when partially inactivated, results in an extension of lifespan marked by increased sensitivity to rapamycin and DNA damage. Gcn5 acetylates Ifh1 in a TORC1-responsive fashion, which allows for a RP transcriptional burst following

refeeding. Importantly, these Gcn5-dependent modifications are opposed by a subset of sirtuins. Together, this suggests the possibility that sirtuin localization/stabilization may communicate changes in TORC1 activity to ribosome biogenesis via Ifh1 acetylation or SAGA function (see above). If TORC1 regulates Ifh1 acetylation through a Sit4-sirtuin pathway, we would expect that loss of the phosphatase would render Ifh1 marks irresponsive to rapamycin. Similarly, if the hypothesis is correct, Ifh1 acetylation should fluctuate with MSX or nicotinamide treatment as well.

Mitochondrial proteins

Lastly, we propose examining the acetylation state of mitochondrial proteins in response to TORC1 activity. We presented evidence in Chapter 3 that localization of Hst4 shifts toward a more nuclear distribution upon inactivation of TORC1. At the time we did not attempt to categorize where in the cytoplasm the mobilized Hst4 was coming from. However, we were inspired by a recent work that demonstrated Hst4 can localize to the mitochondria in a dynamic fashion and deacetylate mitoproteins [176], drawing parallels between yeast Hst4 and mammalian SIRT3 (see **Table 1-2**).

We speculate that when TORC1 is inhibited, mitochondrial Hst4 localizes to the nucleus. This means that not only does amino acid starvation promote deacetylation of nuclear proteins, but it also may result in an indirect increase in acetylation of mitochondrial proteins as a consequence of a depletion of mitochondrial-localized sirtuins. This could have a significant consequence on cellular metabolism, oxidative stress and mitochondrial efficiency. The possibility of a multi-organellar signaling web connecting the vacuole, the mitochondria, and the nucleus is tantalizing. Incorporating MitoTracker (Life Technologies) into our Hst4-9xMyc confocal studies (**Figure 3-15**), or immunoprecipitating mitochondrial proteins and evaluating whether they display TORC1-responsive acetylation, are comparatively quick and easy ways to determine whether the proposed connection would be worth pursuing. The aforementioned biotin study from Madsen *et al.* does provide us with a few candidates to work with, as they characterized the dynamic acetylation states of specific mitoproteins in the absence of Hst2, Hst4, or Sir2 [176]. We were able to use this data to determine which proteins are most highly responsive to Hst4 activity, and then stratify further by which targets' acetylation seems to be specific for Hst4 (since we know only Hst4 is significantly relocalizing). There were a few hits that were particularly interesting and could warrant further study.

Asparagine synthetase displayed the greatest increase in acetylation in response to *hst4Δ* (30 fold), which would make sense if the TORC1-regulation of sirtuins promotes amino acid biosynthesis to attempt to overcome starvation. Fumarate reductase was also an interesting find as it functions in the electron transport chain, meaning that affecting its acetylation could result in changes in ATP production from mitochondria. And finally, isocitrate dehydrogenase is a possible candidate as well, as its *p*-value was very high and it plays a critical role in the TCA cycle. TORC1-regulated acetylation of either fumarate reductase or isocitrate dehydrogenase would suggest a linkage between environmental nutrient status and cellular bioenergetics at the mitochondria anchored by TORC1.

TORC1-Dependent Histone Acetylation and Anabolic Gene Transcription

TORC1 signaling is known to promote transcription of an array of anabolic genes involved in cellular growth and proliferation. Inactivation of TORC1 during starvation leads to reduced expression of these genes. However, the extent to which TORC1-responsive histone acetylation contributes to these transcriptional dynamics remains unclear. To date, the most well-defined links between TORC1 and anabolic gene transcription are Sch9-dependent, yet we know that the histone acetylation response occurs through the Tap42-associated phosphatases, specifically PP6. We wondered then whether deleting components of our signaling pathway would result in changes to RP gene expression.

Somewhat surprisingly, in a TORC1 mutant (*tco89Δ*) where we have identified global acetylation defects, mRNA levels of select ribosomal protein genes are unaffected. Chen et al. provide a possible explanation for this, as they report that TORC1 regulation of the RP genes occurs in parallel with PKA [339]. This type of dual input allows for proper coordination of ribosome biogenesis with both carbon and amino acid availability, but also suggests that in *tco89Δ*, the low-level TORC1 activity (**Figure B-1**) paired with functional PKA may be sufficient to maintain RP gene expression. In our previous work characterizing TORC1-dependent rDNA transcription, we utilized H3K56A mutants, which would theoretically ablate all H3K56 acetylation in the cell. Therefore, another possible explanation for the lack of effect on RP gene expression could be that the low level of basal TORC1 activity retained in *tco89Δ* may be able to sustain local acetylation, and as a consequence transcription, despite the overwhelming global changes. This hypothesis is supported by the fact that the cells show no obvious growth deficiency under steady state conditions.

It is important to remember that TORC1's transcriptional regulation reaches beyond just RP genes, so it is possible that other genes will be responsive to the reduced histone acetylation described here. Future studies incorporating ChIP-seq technology (identify genes with TORC1-responsive acetylation) and RNA-seq (quantify changes in gene expression in response to TORC1 inhibition) will be the foundation for examining how these modifications influence the transcriptional process. These data sets can be overlaid to identify genes whose acetylation patterns are TORC1-dependent and correlate with gene expression. Single gene ChIP and RT-qPCR analysis would confirm these findings, while also determining where on the gene (promoter/body) these modifications are occurring. Altered histone lysine acetylation may contribute to gene expression generally, by loosening the DNA-nucleosome contacts and enabling chromatin decondensation. But acetylation changes may also alter the docking of chromatin modifying complexes containing bromodomains or YEATS-domains [340, 341]. Gaining a greater understanding of how the chromatin association of these ancillary factors changes in response to TORC1 activity will be critical to defining how environmental nutrient availability influence anabolism at the level of transcription. Altogether, this information would provide significant insight into how these TORC1-responsive histone acetylation states affect chromatin-based processes.

Interplay between Histone Acetylation and Sensitivity to TORC1 Inhibition

tco89Δ cells are acutely sensitive to rapamycin and arsenic trioxide. Importantly, while these compounds are often grouped together as "TORC1 inhibitors", the cellular response they elicit, and the way in which these signals are relayed throughout the cell, can vary significantly [314]. The effect of rapamycin on yeast TORC1 is well understood. FK506-associated rapamycin directly binds the Tor1 kinase via its FKBP-rapamycin binding domain. Short term exposure results in transient G_1-S cell cycle arrest, while long term TORC1 inhibition results in a G_0 (or quiescence) response which proves inescapable if TORC1 function is compromised (i.e. *tco89Δ*). Arsenic trioxide's effect on TORC1 is more unclear, though the majority of its phenotypes appear to be Sch9-dependent [313]. The metalloid has been reported to promote a G2-M cell cycle arrest in cell culture models [342].

Interestingly, we demonstrate that the TORC1-PP6-sirtuin cascade delineated in Chapter 3 may contribute to cell-cycle re-entry following certain types of TORC1 stress, as *tco89Δ hst3Δ* and *tco89Δ hst4Δ* mutants are able to escape their reported arrests and grow similar to wild-type cells on both rapamycin and arsenic. We note that there are likely many other signaling molecules feeding into these processes, as *tco89Δ hst3Δ* or *tco89Δ hst4Δ* mutants are still sensitive to higher doses of rapamycin (10 nM, **Figure 3-18**, top right panel). There is a precedent for Tap42-associated phosphatases regulating the cell cycle, as it was previously shown that the nitrogen responsive, Rim15-dependent phosphorylation of PP2A plays a critical role in cell entry and exit from quiescence [343]. We propose that sirtuin stabilization downstream of TORC1 inhibition may reinforce the cell-cycle exit observed in *tco89Δ* cells exposed to arsenic or rapamycin, in part through chromatin deacetylation. Further, we believe that the deletion of *HST3* or *HST4* in the *tco89Δ* background enables re-entry by promoting a hyperacetylated, transcriptionally permissive chromatin structure, devoid of barriers to the induction of genes required to exit cell-cycle arrest. Support for such a mechanism exists, as a similar observation was recently described in which carbon-responsive histone acetylation regulates transcription of the *CLN3* cyclin to mediate reentry into the cell-cycle following glucose starvation [151]. A second explanation for the phenotypic rescue observed in the *tco89Δ hst3Δ* and *tco89Δ hst4Δ* is that, rather than loss of the sirtuins promoting exit from the transient cell-cycle arrest, the strains may simply be unable to initiate the arrest without these sirtuins. Previous reports have demonstrated that *tco89Δ* cells are also sensitive to the DNA damaging agent hydroxyurea [57], though the high throughput nature of the study makes it unclear as to whether treatment induces a cell cycle arrest similar to rapamycin, or if it promotes cell death. Similar to the findings with rapamycin and arsenic, the *tco89Δ hst3Δ* and *tco89Δ hst4Δ* strains show little sensitivity to hydroxyurea, which we hypothesize may be explained by restoration of H3K56ac, a chromatin mark essential for DNA repair. Indeed it has been previously shown that mimicking H3K56ac promotes resistance to DNA damaging agents [153]. In all, we find that preventing sirtuin activation downstream of TORC1 inhibition is sufficient to rescue sensitivity to rapamycin, arsenic trioxide and hydroxyurea, though likely through distinct mechanisms.

Deletion of *SIT4*, the phosphatase identified as a regulator of sirtuin localization and stabilization, was sufficient to rescue *tco89Δ*'s growth on hydroxyurea and arsenic oxide. Unexpectedly though, it had no effect on rapamycin sensitivity. Resistance to hydroxyurea is likely due once again to H3K56ac, as was alluded to above. A previous work demonstrated that Sit4's function in response to rapamycin is dependent on the identity of the associated Sap protein, which certainly implies the possibility of context-specific functions [100]. To our knowledge, nobody has ever looked at how various TORC1 stressors affect Sit4-Sap interactions, but if arsenic and rapamycin have distinct effects on these dynamics, it could explain the observed plating phenotypes. Another possible explanation is that the Sit4 phosphatase, which is known to exist outside of Tap42, has both positive and negative functions in TORC1-dependent cell growth and the necessity of each depends on the nature of the stress. We speculate that one such positive function may be a feedback signal from the Tap42-phosphatases, or the downstream sirtuins, to Sch9. Indeed a similar mechanism has been identified in mammals, albeit for a different downstream mTORC1 effector, as SIRT1 activation in response to caloric restriction regulates the acetylation, and subsequent TORC1-dependent phosphorylation, of S6K1 (Ypk3 in yeast) [344-347]. Sch9 activity is known to be responsive to NAD^+ homeostasis [348] (an essential co-factor for sirtuins), acetylation of its upstream regulator Sip2 [349], as well as direct phosphorylation by TORC1 [80]. Considering aforementioned evidence, we wonder whether in response to starvation, the activation of the Tap42-associated PP6 complex, and subsequent stabilization of sirtuins, may feedback onto Sch9 to silence any TORC1-independent activity that may arise while nutrients are limiting. If this were the case, in our *tco89Δ sit4Δ* strain, in addition to preventing the nuclear accumulation and stabilization of the sirtuins (reversing the hypoacetylation response), we are also allowing for low-level TORC1-independent activation of Sch9. This could enable these mutants to grow on arsenic trioxide since the majority of arsenic effects are Sch9 specific. However the reason why these cells do not grow on rapamycin may be due to the lack of signal continuity, as a cell's ability to grow in the presence of rapamycin requires coordination of Sch9 and Tap42-associated phosphatases. Each of these effectors are known to regulate critical responses downstream of starvation.

In summary, the findings in Chapter 3 identify a novel signaling mechanism through which amino acid availability is sensed by TORC1 and relayed to chromatin in two parts. The initial PP6-dependent nuclear accumulation of Hst4 prompts rapid changes in site-specific acetylation of H3 and H4. The subsequent increase in Hst4 protein stability suggests that nuclear localization may shield Hst4 from proteasomal turnover. We believe that this influx of Hst4 sustains the hypoacetylation response until the environment is permissive for growth. Coordination of these dynamics appears to play a vital role in at least a subset of TORC1's biological functions.

Epigenetic Dysfunction and Cellular Transformation

It has been widely reported that a vast array of cancers display aberrant mTORC1 function. This may occur in response to loss of function in the tumor suppressor PTEN,

hyperactivation of PI3K, deletion of TSC1/2, or other genetic lesions that act to impair normal mTORC1 regulation. Accordingly, a sizable arsenal of mTORC1 inhibitors ("rapalogs") have been developed and paired with just about every therapeutic imaginable in clinical trials. In addition to mTORC1 dysfunction, many tumors also display altered cellular metabolism and increased nitrogen requirements [350]. These changes would likely feed into sustaining mTORC1 activity and involve the amino acid sensing machinery at the lysosome. With this in mind, a new approach that is gaining traction involves targeting v-ATPase function to overcome drug resistance and prevent metastasis in a subset of cancers, including breast, non-small-cell lung, leukemia and sarcoma [351-357]. We speculate that at least some of the benefit observed from inhibition of the v-ATPase results from the corresponding reduction in mTORC1 function. However our data also indicates that mTORC1-responsive acetylation is strictly downstream of amino acids, meaning that inhibiting the v-ATPase, rather than mTORC1, may produce discernible differences in the downstream cellular phenotype.

Indeed, a recent publication found that overexpression of the E2F1 transcription factor results in stimulation of v-ATPase activity, lysosomal reorganization, mTORC1 activation and autophagic inhibition [358]. Interestingly however, these functions do not overlap substantially. Activation of mTORC1 involves altered lysosomal trafficking, while the activation of v-ATPase activity involves promoting the association of the V_0 and V_1 subunits [358]. The authors speculate that pharmacological inhibition of the v-ATPase may be beneficial in curbing metastasis in tumors overexpressing E2F1. This study beautifully illustrates how fully understanding a signaling pathway enables a more targeted therapeutic approach.

Considering what we now know about TORC1-mediated histone acetylation, and given that these modifications have been tied to transcription, chromatin remodeling, bromodomain docking, DNA repair, cell cycle progression and genomic stability, it is clear that epigenetic dysregulation downstream of hyperactive mTORC1 could play a significant role in disease pathogenesis. Such a relationship would explain the efficacy of combinatorial therapies pairing mTORC1 inhibitors with sirtuin activators [359-361]. It would be interesting to compare the epigenetic response elicited by rapamycin, bafilomycin A1 (v-ATPase inhibitor), or a combination of the two. We believe this area of study deserves considerable attention, as it would provide significant insight into downstream consequences of mTORC1 dysfunction while also illuminating a poorly understood molecular mechanism of cancer progression.

TORC1-Dependent Acetylation Does Not Contribute to HMGB Chromatin Binding

In Chapter 4, we investigated whether the TORC1-PP6-Hst4 cascade described in Chapter 3 contributed to the seemingly TORC1-dependent chromatin association of HMGB proteins. Previous works demonstrated that H3K36 and H3K37, on the N-terminal tail of histone H3, were critical for HMGB chromatin binding [252, 253]. We also knew that disruption of this site in yeast (H3K37A) paired with TORC1 inhibition led to dramatic HMGB (Nhp10) displacement and cell death [152]. We confirmed here

that this biological response also occurs with other HMGBs, as Nhp6a shuttles to the cytoplasm in response to rapamycin in the H3K37A strain, but not in the H3WT or H3K37R (restores protein-protein interactions) strains. This movement precedes the observed apoptotic and necrotic cell death, and similar timing was described for Nhp10 [152]. To this point, the behavior of Nhp6a and Nhp10 in response to H3K37 mutation and TORC1 inhibition appear to mirror one and other.

We hypothesized that one reason TORC1 inhibition disrupts the chromatin binding of HMGBs is that the corresponding loss of acetylation, described in Chapter 3, may destabilize the association between HMGBs and the histone tail. Surprisingly though, combining H3K37A with *hst4Δ* or *sap4Δ* was not sufficient to suppress the HMG displacement or the apoptotic/necrotic cell death. We believe this is explainable by the fact that neither of these deletions completely restore acetylation under TORC1-suppressive conditions (**Figures 3-6, 3-10**). Unfortunately, we were unable to create an H3K37A *sit4Δ* mutant, which is the combination which likely would have been the most promising given that acetylation in a *sit4Δ* is almost completely irresponsive to TORC1 (**Figure 3-5**). It is possible that if we were to pre-treat H3K37A with nicotinamide prior to rapamycin exposure, we may see a reduction in HMG relocalization and/or cell death. We could pursue creating an H3K37A *hst3Δ hst4Δ* as well.

An important note to discuss is that until recently, HMGB1 nuclear release in mammals was believed to occur as a consequence of necrotic cell death. Once in the extracellular space, these proteins would function as signaling molecules to stimulate macrophage recruitment to clear the necrotic cells [251]. However, our timing experiments demonstrate that HMGB displacement in yeast occurs **prior** to induction of apoptosis and necrosis. This result leads us to propose that the nuclear to cytoplasmic movement of HMGs could be a contributing cause, rather than an effect, of cell death. With this new paradigm in mind, there are suddenly many new areas of study, including determining how the HMGs are inducing cell death (next section), and evaluating other potential intracellular signaling functions (e.g. bioenergetics, metabolism [255]) these molecules may possess. We can now begin to visualize a complex intracellular signaling web, centered on TORC1, which coordinates communication between the vacuole, the nucleus and the mitochondria to affect cell viability and lifespan.

One of the weaknesses of this section is that we do not provide unequivocal mechanistic evidence that the HMGBs are binding H3K37. Such experimental evidence could likely be achieved using recombinant wild-type or H3K37A containing nucleosomes and *in vitro* binding assays. Additionally, we do not understand yet where the HMGBs relocalize to following their exit from the nucleus, although this is an area we are currently pursuing. We propose future studies examining how cells respond to constitutively cytoplasmic/nuclear versions of these HMGBs to directly ask whether their altered subcellular distribution is causing the cell death observed in the rapamycin treated H3K37A cells. It would also be fascinating to pursue defining how decreased TORC1 signaling synergizes with H3K37A to cause selective cytoplasmic localization of specific HMGBs. We have not completely ruled out the contribution of TORC1-dependent chromatin modifications, though it seems equally plausible that localization of the

HMGBs may be mediated via direct modification (TORC1-dependent phosphorylation, sirtuin-dependent deacetylation, etc.); a phenomena that has already been reported in metazoan cells [362].

Cells with Aberrant HMG Localization Undergo Massive Cell Death Characterized by Vacuolar Dysfunction and Hyperactive TORC1

Despite finding that the TORC1-dependent histone acetylation marks likely do not contribute directly to the association of HMGBs and the H3 N-terminal tail, we were still very interested in characterizing the cell death that appears to be triggered in response to their nuclear displacement. After all, these dynamics proved capable of turning low levels of rapamycin from a cytostatic agent to a cytotoxic agent. The potential therapeutic benefit of targeting the chromatin association of HMGBs was apparent, and served as a driving factor for the inquiries that followed.

We first demonstrated that the cell death response triggered by HMGB dislodgement is preceded by significant acidification of the vacuole (**Figure 4-3**). This was most clearly observable in rapamycin treated H3K37A cells, however there was an approximate two-fold increase in CFDA staining of mock treated H3K37A cells compared to the wild type control. A similar response was observed in H3WT cells expressing exogenous Nhp6a and Hmo1 from a plasmid. We subsequently found that mock treated H3K37A cells, and the Nhp6a/Hmo1-expressing H3WT cells, also display a somewhat surprising increase in TORC1 activity. It is clear this is an HMGB-dependent response, as the H3K37A *nhp6aΔ* and the H3K37A *nhp10Δ* do not display substantially increased TORC1 function. The idea that aberrant vacuolar pH and elevated TORC1 signaling contributes to induction of cell death is supported by the fact that buffering the growth media was sufficient to reverse sensitivity to rapamycin (**Figure 4-4**).

We speculate that loss of vacuolar membrane integrity, leading to release of hydrolases/proteases and cellular acidification, may contribute to this HMGB-triggered programmed cell death. With the above concepts in mind, we propose that one possible destination for these displaced HMGBs may be the vacuole. There is, in fact, precedent for this concept. Mammalian inflammatory cells actively secrete HMGB1, and this process involves HMGB translocation from the nucleus to the lysosome in response to its acetylation [363, 364]. This intracellular shuttling is not limited to inflammatory cells though, as HMGB1 has also been shown to relocalize from the nucleus to the lysosome in the human peritoneal mesothelial cell line (HMrSV5), particularly in response to the availability of lipopolysaccharides [365]. These parallels provide support for the possibility that displaced yeast HMGBs are shuttling to the vacuole. This hypothesis is readily testable through co-localization studies incorporating fluorescent HMGB tags and vacuolar stains (FM4-64). Conversely, we could attempt to co-immunoprecipitate vacuole surface proteins and HMGBs. It is important to note that HMGB1 movement in mammals appears to be tied more to the secretory nature, rather than the pH, of the lysosome. However whether these functions are truly mutually exclusive remains to be seen.

If we assume for a moment that the HMGBs are functioning as signaling molecules as they move from chromatin to the vacuole, we are still left to wonder what exactly they are doing to promote vacuole acidification and TORC1 function. One consideration is that the activation of TORC1 could simply be a physiological response to HMGB-mediated pH changes, which likely occur through modulation of the v-ATPase. We believe that fluctuations in pH, to an extent, may optimize conditions for the vacuolar proteases leading to a more active enzymatic compartment, increased protein breakdown and nitrogen availability, and enhanced TORC1 function. And while plausible, this hypothesis would seem to contradict work from Hughes et al. which demonstrated that as cells replicatively age, increased TORC1 signaling results in a more basic vacuolar pH [366]. This increase in pH, which can be reversed by inhibiting TOR, PKA or Sch9, contributes to cellular aging and mitochondrial dysfunction as a result of defective amino acid storage. We note that Hughes is presenting this data in a different model of aging (replicative vs. chronological), however the link between TORC1 and vacuolar pH is striking. Considering this, we propose an alternative explanation. The observed increase in TORC1 signaling may be a compensatory mechanism to prevent the apoptosis and necrosis that occurs as a result of HMGB displacement. This concept would be consistent with our results which demonstrate that buffering the growth media partially suppresses the cell death phenotype of H3K37A mutants treated with rapamycin. This would also be supported by the fact that H3K37A cells grow very much like wild-type under steady state conditions, despite vacuole morphological differences and modest HMGB displacement.

If HMGB release from chromatin proves to be a cell-death initiation signal in mammalian cells like it appears to be in yeast, it would certainly be an attractive pharmaceutical target. Displacement of HMGBs at low levels appears to be tolerable, but when paired with low-dose rapamycin, it initiates a cell death response. This observation suggests that if HMGB1 chromatin binding could be interrupted, it may allow for administration of reduced doses of rapamycin, which could hopefully circumvent some of the most compromising side effects.

Mapping the Functional Domains of Tco89

In Chapter 5, we made significant strides toward understanding the yeast TORC1 subunit, Tco89. The severe rapamycin sensitivity in *tco89Δ* cells is marked by a permanent exit from the cell cycle, as was discussed previously [43], and it is our hope that a more complete understanding of the subunit's role in the complex will lead to the identification of a mammalian ortholog. Existence of such an ortholog seems likely given that every other yeast TORC1 component has a mammalian counterpart. The mammalian equivalent of Tco89 would be an attractive therapeutic target to sensitize cells with hyper mTORC1 function to TORC1 inhibitors.

Using vectors expressing the different Tco89 fragments proved challenging when mapping the region required for particular TORC1-dependent functions. This was due to the need to culture the cells in nutrient-defined media to select for the plasmids. The fact

that TORC1 activity is so heavily impacted by availability of nutrients means that many of our phenotypes are not nearly as pronounced in synthetic complete media as they are in nutrient rich media. This makes observing differences, and attributing them to particular protein fragments, quite arduous. If these obstacles could be overcome, by tweaking media conditions or integrating our mutants into the genomic locus, there are a number of very interesting studies that could be conducted. The most straightforward of which involve utilizing our different fragments to map Tco89's structural and functional contributions to TORC1. We could use co-immunoprecipitation to assess which domain is required for Tco89 incorporation into TORC1, as well as to investigate how Tco89 affects TORC1 complex stability by using Kog1 association with Lst8 as a readout. We have already mapped which portion is critical for regulating TORC1 function (via pS6 blot) and growth on rapamycin (**Figure 5-2**), and it would be interesting to follow up and ask whether this same region (demarcated between fragments C and D) is involved in coordinating TORC1-dependent histone modifications. Notably, an earlier study utilizing much larger Tco89 fragments reported that residues 799-388 were responsible for interacting with Vac8 to promote the turnover of non-preferred carbon utilization enzymes [62]. This overlaps with our region of interest (532-399), and could provide insight as to how Tco89 coordinates the TORC1-dependent nutrient stress response.

We are enthusiastic about the identification of this minimal portion of Tco89 as we believe it can enlighten us to what its true function is, while also aiding in determining which downstream proteins are participating in this diverse signal relay system. Immunoprecipitation of a few different fragments (i.e. one that does rescue on rapamycin compared to one that does not) paired with mass spectrometric analysis could be incredibly powerful, enabling us to identify the physical interactions necessary for these phenotypes. Likely hits would include members of the TORC1 complex and EGO complex, but we speculate there are additional, yet to be determined binding partners of significant biological relevance.

tco89Δ mutants growth arrest at the G1-S boundary and enter a permanent quiescence-like state (yet remain viable) when exposed to rapamycin, and we would like to understand how this response is initiated and sustained. We first wondered whether the cell cycle defect could be explained by an inability to manage ROS production as metabolic requirements shifted. The *tor1Δ* mutant is known to decrease TORC1 activity and extend lifespan. It displays a distinct increase in log phase basal ROS but a significant reduction (compared to wild-type) in stationary phase ROS. These effects on reactive oxygen have been identified as potential explanations for the observed increase in lifespan of TORC1 mutants, which led us to investigate whether *tco89Δ* was deficient in these mitochondrial-based processes. Our data demonstrate that unlike *tor1Δ*, *tco89Δ* does not undergo a significant increase in log phase ROS. Though both mutants share a significant reduction in stationary phase ROS compared to the wild-type. It is currently unclear what is occurring in the *tco89Δ* strain, as it appears that ROS levels have been completely uncoupled from these metabolically distinct stages of growth. We speculate that deregulation of sirtuin-dependent acetylation of mitochondrial proteins, as discussed earlier in this chapter, may contribute to the relatively stagnant ROS production in

tco89Δ. This would be consistent with our previous result that showed TORC1-dependent H3K56ac is responsive to deletion of *TCO89* but not *TOR1* [66].

Looking ahead, we are interested in investigating whether cellular growth and proliferation is sensitive to nutrients throughout the cell cycle, or if there is a defined window of time to arrest, after which the cell is committed to division regardless of nutrient availability. If we used α-factor (G1) and nocodazole (G2-M) to arrest cells, then released them into media containing rapamycin and analyzed their cell cycle profile via flow cytometry, we could begin to understand this TORC1-dependent regulatory signal. For example, following α-factor arrest, if *tco89Δ* cells exposed to rapamycin pass through S-phase and G2-M to finish their current cell division, it would suggest a brief window between mitosis and G1 at which cells assess their environmental conditions. If true, we would expect that cells arrested with nocodazole and released into rapamycin would complete mitosis and then enter G_0.

In terms of sustaining the arrest, one possible explanation is that Tco89 coordinates the dynamic association of Rho1 and Tap42 to TORC1. This intricate relationship is known to regulate the stress response [50]. In the absence of Tco89, cells grow normally under steady state conditions, but we speculate that once the stress response is initiated (i.e. rapamycin), it cannot be turned off. This leads to the permanent cell cycle arrest, despite cells retaining viability. This could be studied by labeling and co-immunoprecipitating Kog1 and Rho1, and Kog1 and Tap42 in the absence and presence of Tco89. We could then ask whether disruption of the Rho1 stress response prevents rapamycin effects on acetylation. Finally, we could examine how the sirtuins fit into all of these functions since we know deletion of *HST3* and *HST4* is sufficient to promote growth on low-level rapamycin.

We acknowledge there is still considerable work to be done, but the potential of this project excites us. Undoubtedly, with persistence this avenue will prove fruitful. The trials outlined here have equipped our lab with a unique set of tools and information that we believe will soon lead us to the most comprehensive mechanistic and structural understanding of Tco89 to date.

Closing Remarks

It is becoming increasingly clear that the pathologies attributed to mTORC1 dysfunction, including metabolic disorders, cancer, and cardiovascular disease, likely possess a degree of epigenetic deregulation that far exceeds what was previously known. While this dissertation focused on a single post-translational modification, on a defined series of histone substrates, there are almost certainly many more TORC1-dependent histone post-translational modifications that have yet to be discovered. We have speculated on a few potential non-histone acetylation targets earlier in this chapter as well (Ifh1, Spt7, mitochondrial proteins). Given the involvement of PP6, a phosphatase known to regulate a number of downstream TORC1 effectors, there is a likelihood that TORC1

activity could be translated into any number of epigenetic modifications beyond just acetylation, including methylation, phosphorylation, and ubiquitination.

The scientific funding and publishing bodies in this country have embraced high-throughput sequencing techniques, which are costly, laborious to interpret for non-bioinformaticians, and the results of which are often difficult to independently replicate. These technologies are immensely powerful, and they have led to some of the most compelling evidence of an epigenetic component to cancer; somatic mutations leading to an H3K27M substitution that drives gliomagenesis [367]. But the work presented in this dissertation illustrates how molecular biology is still a critical piece of the puzzle. There are reasons why combinatorial therapeutic approaches work but often times in the world of chemical screening and mouse modeling, the actual biology gets lost. If we understand how a signaling mechanism works under physiologically normal conditions, we know where to look when things begin to go awry.

It has truly been an honor working in such an elite, dynamic, rapidly expanding field with fantastic colleagues over the past five years. I look forward to seeing where the epigenetic community goes in the months and years to come.

LIST OF REFERENCES

1. Kornberg, R.D. and J.O. Thomas, *Chromatin structure; oligomers of the histones.* Science, 1974. **184**(4139): p. 865-8.
2. Luger, K., et al., *Crystal structure of the nucleosome core particle at 2.8 A resolution.* Nature, 1997. **389**(6648): p. 251-60.
3. Finch, J.T., M. Noll, and R.D. Kornberg, *Electron microscopy of defined lengths of chromatin.* Proc Natl Acad Sci U S A, 1975. **72**(9): p. 3320-2.
4. Gayatri, S. and M.T. Bedford, *Readers of histone methylarginine marks.* Biochim Biophys Acta, 2014. **1839**(8): p. 702-10.
5. Rothbart, S.B., et al., *Multivalent histone engagement by the linked tandem Tudor and PHD domains of UHRF1 is required for the epigenetic inheritance of DNA methylation.* Genes Dev, 2013. **27**(11): p. 1288-98.
6. Zhang, Q., et al., *Biochemical profiling of histone binding selectivity of the yeast bromodomain family.* PLoS One, 2010. **5**(1): p. e8903.
7. Adams-Cioaba, M.A., et al., *Structural studies of the tandem Tudor domains of fragile X mental retardation related proteins FXR1 and FXR2.* PLoS One, 2010. **5**(11): p. e13559.
8. Adams-Cioaba, M.A. and J. Min, *Structure and function of histone methylation binding proteins.* Biochem Cell Biol, 2009. **87**(1): p. 93-105.
9. Cheng, H., X. He, and C. Moore, *The essential WD repeat protein Swd2 has dual functions in RNA polymerase II transcription termination and lysine 4 methylation of histone H3.* Mol Cell Biol, 2004. **24**(7): p. 2932-43.
10. Friesen, W.J., et al., *A novel WD repeat protein component of the methylosome binds Sm proteins.* J Biol Chem, 2002. **277**(10): p. 8243-7.
11. Liu, Z., et al., *RTG-dependent mitochondria to nucleus signaling is negatively regulated by the seven WD-repeat protein Lst8p.* EMBO J, 2001. **20**(24): p. 7209-19.
12. Rohde, J.R. and M.E. Cardenas, *The tor pathway regulates gene expression by linking nutrient sensing to histone acetylation.* Mol Cell Biol, 2003. **23**(2): p. 629-35.
13. Ha, C.W. and W.K. Huh, *Rapamycin increases rDNA stability by enhancing association of Sir2 with rDNA in Saccharomyces cerevisiae.* Nucleic Acids Res, 2011. **39**(4): p. 1336-50.
14. van Otterdijk, S.D. and K.B. Michels, *Transgenerational epigenetic inheritance in mammals: how good is the evidence?* FASEB J, 2016.
15. Nestler, E.J., *Transgenerational Epigenetic Contributions to Stress Responses: Fact or Fiction?* PLoS Biol, 2016. **14**(3): p. e1002426.
16. Nagy, C. and G. Turecki, *Transgenerational epigenetic inheritance: an open discussion.* Epigenomics, 2015. **7**(5): p. 781-90.
17. Trerotola, M., et al., *Epigenetic inheritance and the missing heritability.* Hum Genomics, 2015. **9**: p. 17.
18. Ptashne, M., *Epigenetics: core misconcept.* Proc Natl Acad Sci U S A, 2013. **110**(18): p. 7101-3.

19. Ptashne, M., *Faddish stuff: epigenetics and the inheritance of acquired characteristics.* FASEB J, 2013. **27**(1): p. 1-2.
20. *DNA Packaging - Shmoop Biology*. 2008 [cited 2016 May 11]; Available from: http://www.shmoop.com/dna/dna-packaging.html.
21. Marzluff, W.F., et al., *The human and mouse replication-dependent histone genes.* Genomics, 2002. **80**(5): p. 487-98.
22. Hake, S.B., et al., *Expression patterns and post-translational modifications associated with mammalian histone H3 variants.* J Biol Chem, 2006. **281**(1): p. 559-68.
23. Botstein, D. and G.R. Fink, *Yeast: an experimental organism for 21st Century biology.* Genetics, 2011. **189**(3): p. 695-704.
24. Petersen, J. and P. Nurse, *TOR signalling regulates mitotic commitment through the stress MAP kinase pathway and the Polo and Cdc2 kinases.* Nat Cell Biol, 2007. **9**(11): p. 1263-72.
25. Matsui, A., Y. Kamada, and A. Matsuura, *The role of autophagy in genome stability through suppression of abnormal mitosis under starvation.* PLoS Genet, 2013. **9**(1): p. e1003245.
26. Jorgensen, P., et al., *A dynamic transcriptional network communicates growth potential to ribosome synthesis and critical cell size.* Genes Dev, 2004. **18**(20): p. 2491-505.
27. Jorgensen, P. and M. Tyers, *How cells coordinate growth and division.* Curr Biol, 2004. **14**(23): p. R1014-27.
28. Lloyd, A.C., *The regulation of cell size.* Cell, 2013. **154**(6): p. 1194-205.
29. Laplante, M. and D.M. Sabatini, *mTOR signaling in growth control and disease.* Cell. **149**(2): p. 274-93.
30. Vezina, C., A. Kudelski, and S.N. Sehgal, *Rapamycin (AY-22,989), a new antifungal antibiotic. I. Taxonomy of the producing streptomycete and isolation of the active principle.* J Antibiot (Tokyo), 1975. **28**(10): p. 721-6.
31. Benjamin, D., et al., *Rapamycin passes the torch: a new generation of mTOR inhibitors.* Nat Rev Drug Discov. **10**(11): p. 868-80.
32. Siekierka, J.J., et al., *The cytosolic-binding protein for the immunosuppressant FK-506 is both a ubiquitous and highly conserved peptidyl-prolyl cis-trans isomerase.* J Biol Chem, 1990. **265**(34): p. 21011-5.
33. Bierer, B.E., et al., *Two distinct signal transmission pathways in T lymphocytes are inhibited by complexes formed between an immunophilin and either FK506 or rapamycin.* Proc Natl Acad Sci U S A, 1990. **87**(23): p. 9231-5.
34. Harding, M.W., et al., *A receptor for the immunosuppressant FK506 is a cis-trans peptidyl-prolyl isomerase.* Nature, 1989. **341**(6244): p. 758-60.
35. Heitman, J., N.R. Movva, and M.N. Hall, *Targets for cell cycle arrest by the immunosuppressant rapamycin in yeast.* Science, 1991. **253**(5022): p. 905-9.
36. Sabatini, D.M., et al., *RAFT1: a mammalian protein that binds to FKBP12 in a rapamycin-dependent fashion and is homologous to yeast TORs.* Cell, 1994. **78**(1): p. 35-43.
37. Chiu, M.I., H. Katz, and V. Berlin, *RAPT1, a mammalian homolog of yeast Tor, interacts with the FKBP12/rapamycin complex.* Proc Natl Acad Sci U S A, 1994. **91**(26): p. 12574-8.

38. Brown, E.J., et al., *A mammalian protein targeted by G1-arresting rapamycin-receptor complex.* Nature, 1994. **369**(6483): p. 756-8.
39. Loewith, R., et al., *Two TOR complexes, only one of which is rapamycin sensitive, have distinct roles in cell growth control.* Mol Cell, 2002. **10**(3): p. 457-68.
40. Jacinto, E., et al., *Mammalian TOR complex 2 controls the actin cytoskeleton and is rapamycin insensitive.* Nat Cell Biol, 2004. **6**(11): p. 1122-8.
41. Wedaman, K.P., et al., *Tor kinases are in distinct membrane-associated protein complexes in Saccharomyces cerevisiae.* Mol Biol Cell, 2003. **14**(3): p. 1204-20.
42. Loewith, R. and M.N. Hall, *Target of rapamycin (TOR) in nutrient signaling and growth control.* Genetics, 2011. **189**(4): p. 1177-201.
43. Reinke, A., et al., *TOR complex 1 includes a novel component, Tco89p (YPL180w), and cooperates with Ssd1p to maintain cellular integrity in Saccharomyces cerevisiae.* J Biol Chem, 2004. **279**(15): p. 14752-62.
44. Araki, T., et al., *LAS24/KOG1, a component of the TOR complex 1 (TORC1), is needed for resistance to local anesthetic tetracaine and normal distribution of actin cytoskeleton in yeast.* Genes Genet Syst, 2005. **80**(5): p. 325-43.
45. Adami, A., et al., *Structure of TOR and its complex with KOG1.* Mol Cell, 2007. **27**(3): p. 509-16.
46. Dennis, M.D., S.R. Kimball, and L.S. Jefferson, *Mechanistic target of rapamycin complex 1 (mTORC1)-mediated phosphorylation is governed by competition between substrates for interaction with raptor.* J Biol Chem, 2013. **288**(1): p. 10-9.
47. Rapley, J., et al., *The mechanism of insulin-stimulated 4E-BP protein binding to mammalian target of rapamycin (mTOR) complex 1 and its contribution to mTOR complex 1 signaling.* J Biol Chem, 2011. **286**(44): p. 38043-53.
48. Kira, S., et al., *Reciprocal conversion of Gtr1 and Gtr2 nucleotide-binding states by Npr2-Npr3 inactivates TORC1 and induces autophagy.* Autophagy, 2014. **10**(9): p. 1565-78.
49. Binda, M., et al., *The Vam6 GEF controls TORC1 by activating the EGO complex.* Mol Cell, 2009. **35**(5): p. 563-73.
50. Yan, G., Y. Lai, and Y. Jiang, *The TOR complex 1 is a direct target of Rho1 GTPase.* Mol Cell, 2012. **45**(6): p. 743-53.
51. Hu, K., et al., *Ubiquitin regulates TORC1 in yeast Saccharomyces cerevisiae.* Mol Microbiol, 2016. **100**(2): p. 303-14.
52. Zheng, C., et al., *Identification and characterization of a functional Candida albicans homolog of the Saccharomyces cerevisiae TCO89 gene.* FEMS Yeast Res, 2007. **7**(4): p. 558-68.
53. Hayashi, T., et al., *Rapamycin sensitivity of the Schizosaccharomyces pombe tor2 mutant and organization of two highly phosphorylated TOR complexes by specific and common subunits.* Genes Cells, 2007. **12**(12): p. 1357-70.
54. Tekletsadik, Y.K., R. Sonn, and M.A. Osman, *A conserved role of IQGAP1 in regulating TOR complex 1.* J Cell Sci, 2012. **125**(Pt 8): p. 2041-52.
55. Sinha, H., et al., *Sequential elimination of major-effect contributors identifies additional quantitative trait loci conditioning high-temperature growth in yeast.* Genetics, 2008. **180**(3): p. 1661-70.

56. Dudley, A.M., et al., *A global view of pleiotropy and phenotypically derived gene function in yeast.* Mol Syst Biol, 2005. **1**: p. 2005 0001.
57. Kapitzky, L., et al., *Cross-species chemogenomic profiling reveals evolutionarily conserved drug mode of action.* Mol Syst Biol, 2010. **6**: p. 451.
58. Hoepfner, D., et al., *High-resolution chemical dissection of a model eukaryote reveals targets, pathways and gene functions.* Microbiol Res, 2014. **169**(2-3): p. 107-20.
59. Parsons, A.B., et al., *Integration of chemical-genetic and genetic interaction data links bioactive compounds to cellular target pathways.* Nat Biotechnol, 2004. **22**(1): p. 62-9.
60. Huber, A., et al., *Characterization of the rapamycin-sensitive phosphoproteome reveals that Sch9 is a central coordinator of protein synthesis.* Genes Dev, 2009. **23**(16): p. 1929-43.
61. Dubouloz, F., et al., *The TOR and EGO protein complexes orchestrate microautophagy in yeast.* Mol Cell, 2005. **19**(1): p. 15-26.
62. Tang, F., et al., *Vac8p, an armadillo repeat protein, coordinates vacuole inheritance with multiple vacuolar processes.* Traffic, 2006. **7**(10): p. 1368-77.
63. Yan, Y. and B. Kang, *Regulation of Vid-dependent degradation of FBPase by TCO89, a component of TOR Complex 1.* Int J Biol Sci, 2010. **6**(4): p. 361-70.
64. Robinson, L.C., et al., *Suppressors of ipl1-2 in components of a Glc7 phosphatase complex, Cdc48 AAA ATPase, TORC1, and the kinetochore.* G3 (Bethesda), 2012. **2**(12): p. 1687-701.
65. Tatchell, K., et al., *Temperature-sensitive ipl1-2/Aurora B mutation is suppressed by mutations in TOR complex 1 via the Glc7/PP1 phosphatase.* Proc Natl Acad Sci U S A, 2011. **108**(10): p. 3994-9.
66. Chen, H., et al., *The histone H3 lysine 56 acetylation pathway is regulated by target of rapamycin (TOR) signaling and functions directly in ribosomal RNA biogenesis.* Nucleic Acids Res, 2012. **40**(14): p. 6534-46.
67. Medvedik, O., et al., *MSN2 and MSN4 link calorie restriction and TOR to sirtuin-mediated lifespan extension in Saccharomyces cerevisiae.* PLoS Biol, 2007. **5**(10): p. e261.
68. Anderson, R.M., et al., *Nicotinamide and PNC1 govern lifespan extension by calorie restriction in Saccharomyces cerevisiae.* Nature, 2003. **423**(6936): p. 181-5.
69. Gallo, C.M., D.L. Smith, Jr., and J.S. Smith, *Nicotinamide clearance by Pnc1 directly regulates Sir2-mediated silencing and longevity.* Mol Cell Biol, 2004. **24**(3): p. 1301-12.
70. Powers, R.W., 3rd, et al., *Extension of chronological life span in yeast by decreased TOR pathway signaling.* Genes Dev, 2006. **20**(2): p. 174-84.
71. Kaeberlein, M., et al., *Regulation of yeast replicative life span by TOR and Sch9 in response to nutrients.* Science, 2005. **310**(5751): p. 1193-6.
72. Fabrizio, P., et al., *Regulation of longevity and stress resistance by Sch9 in yeast.* Science, 2001. **292**(5515): p. 288-90.
73. Kapahi, P., et al., *Regulation of lifespan in Drosophila by modulation of genes in the TOR signaling pathway.* Curr Biol, 2004. **14**(10): p. 885-90.

74. Jia, K., D. Chen, and D.L. Riddle, *The TOR pathway interacts with the insulin signaling pathway to regulate C. elegans larval development, metabolism and life span.* Development, 2004. **131**(16): p. 3897-906.
75. Beck, T. and M.N. Hall, *The TOR signalling pathway controls nuclear localization of nutrient-regulated transcription factors.* Nature, 1999. **402**(6762): p. 689-92.
76. Morita, M., et al., *mTORC1 controls mitochondrial activity and biogenesis through 4E-BP-dependent translational regulation.* Cell Metab, 2013. **18**(5): p. 698-711.
77. Jia, Y., et al., *Cap-dependent translation initiation factor eIF4E: an emerging anticancer drug target.* Med Res Rev, 2012. **32**(4): p. 786-814.
78. Dowling, R.J., et al., *mTORC1-mediated cell proliferation, but not cell growth, controlled by the 4E-BPs.* Science, 2010. **328**(5982): p. 1172-6.
79. Gonzalez, A., et al., *TORC1 promotes phosphorylation of ribosomal protein S6 via the AGC kinase Ypk3 in Saccharomyces cerevisiae.* PLoS One, 2015. **10**(3): p. e0120250.
80. Urban, J., et al., *Sch9 is a major target of TORC1 in Saccharomyces cerevisiae.* Mol Cell, 2007. **26**(5): p. 663-74.
81. Swinnen, E., et al., *Molecular mechanisms linking the evolutionary conserved TORC1-Sch9 nutrient signalling branch to lifespan regulation in Saccharomyces cerevisiae.* FEMS Yeast Res, 2014. **14**(1): p. 17-32.
82. Smets, B., et al., *Genome-wide expression analysis reveals TORC1-dependent and -independent functions of Sch9.* FEMS Yeast Res, 2008. **8**(8): p. 1276-88.
83. Roelants, F.M., P.D. Torrance, and J. Thorner, *Differential roles of PDK1- and PDK2-phosphorylation sites in the yeast AGC kinases Ypk1, Pkc1 and Sch9.* Microbiology, 2004. **150**(Pt 10): p. 3289-304.
84. Voordeckers, K., et al., *Yeast 3-phosphoinositide-dependent protein kinase-1 (PDK1) orthologs Pkh1-3 differentially regulate phosphorylation of protein kinase A (PKA) and the protein kinase B (PKB)/S6K ortholog Sch9.* J Biol Chem, 2011. **286**(25): p. 22017-27.
85. Liu, K., et al., *The sphingoid long chain base phytosphingosine activates AGC-type protein kinases in Saccharomyces cerevisiae including Ypk1, Ypk2, and Sch9.* J Biol Chem, 2005. **280**(24): p. 22679-87.
86. Huber, A., et al., *Sch9 regulates ribosome biogenesis via Stb3, Dot6 and Tod6 and the histone deacetylase complex RPD3L.* EMBO J, 2011. **30**(15): p. 3052-64.
87. Wei, Y. and X.F. Zheng, *Sch9 partially mediates TORC1 signaling to control ribosomal RNA synthesis.* Cell Cycle, 2009. **8**(24): p. 4085-90.
88. Yorimitsu, T., et al., *Protein kinase A and Sch9 cooperatively regulate induction of autophagy in Saccharomyces cerevisiae.* Mol Biol Cell, 2007. **18**(10): p. 4180-9.
89. Michels, A.A., *MAF1: a new target of mTORC1.* Biochem Soc Trans, 2011. **39**(2): p. 487-91.
90. Cocklin, R. and M. Goebl, *Nutrient sensing kinases PKA and Sch9 phosphorylate the catalytic domain of the ubiquitin-conjugating enzyme Cdc34.* PLoS One, 2011. **6**(11): p. e27099.

91. Jin, Y. and L.S. Weisman, *The vacuole/lysosome is required for cell-cycle progression.* Elife, 2015. **4**.
92. Cai, Y. and Y.H. Wei, *Distinct regulation of Maf1 for lifespan extension by Protein kinase A and Sch9.* Aging (Albany NY), 2015. **7**(2): p. 133-43.
93. Zabrocki, P., et al., *Protein phosphatase 2A on track for nutrient-induced signalling in yeast.* Mol Microbiol, 2002. **43**(4): p. 835-42.
94. Lillo, C., et al., *Protein phosphatases PP2A, PP4 and PP6: mediators and regulators in development and responses to environmental cues.* Plant Cell Environ, 2014. **37**(12): p. 2631-48.
95. Cohen, P.T., A. Philp, and C. Vazquez-Martin, *Protein phosphatase 4--from obscurity to vital functions.* FEBS Lett, 2005. **579**(15): p. 3278-86.
96. Wang, H., X. Wang, and Y. Jiang, *Interaction with Tap42 is required for the essential function of Sit4 and type 2A phosphatases.* Mol Biol Cell, 2003. **14**(11): p. 4342-51.
97. Luke, M.M., et al., *The SAP, a new family of proteins, associate and function positively with the SIT4 phosphatase.* Mol Cell Biol, 1996. **16**(6): p. 2744-55.
98. Fernandez-Sarabia, M.J., et al., *SIT4 protein phosphatase is required for the normal accumulation of SWI4, CLN1, CLN2, and HCS26 RNAs during late G1.* Genes Dev, 1992. **6**(12A): p. 2417-28.
99. Sutton, A., D. Immanuel, and K.T. Arndt, *The SIT4 protein phosphatase functions in late G1 for progression into S phase.* Mol Cell Biol, 1991. **11**(4): p. 2133-48.
100. Jablonowski, D., et al., *Distinct subsets of Sit4 holophosphatases are required for inhibition of Saccharomyces cerevisiae growth by rapamycin and zymocin.* Eukaryot Cell, 2009. **8**(11): p. 1637-47.
101. Rohde, J.R., et al., *TOR controls transcriptional and translational programs via Sap-Sit4 protein phosphatase signaling effectors.* Mol Cell Biol, 2004. **24**(19): p. 8332-41.
102. Morales-Johansson, H., et al., *Human protein phosphatase PP6 regulatory subunits provide Sit4-dependent and rapamycin-sensitive sap function in Saccharomyces cerevisiae.* PLoS One, 2009. **4**(7): p. e6331.
103. Tate, J.J., R. Rai, and T.G. Cooper, *Ammonia-specific regulation of Gln3 localization in Saccharomyces cerevisiae by protein kinase Npr1.* J Biol Chem, 2006. **281**(38): p. 28460-9.
104. Merhi, A. and B. Andre, *Internal amino acids promote Gap1 permease ubiquitylation via TORC1/Npr1/14-3-3-dependent control of the Bul arrestin-like adaptors.* Mol Cell Biol, 2012. **32**(22): p. 4510-22.
105. Di Como, C.J. and K.T. Arndt, *Nutrients, via the Tor proteins, stimulate the association of Tap42 with type 2A phosphatases.* Genes Dev, 1996. **10**(15): p. 1904-16.
106. Chen, J., R.T. Peterson, and S.L. Schreiber, *Alpha 4 associates with protein phosphatases 2A, 4, and 6.* Biochem Biophys Res Commun, 1998. **247**(3): p. 827-32.
107. Nanahoshi, M., et al., *Regulation of protein phosphatase 2A catalytic activity by alpha4 protein and its yeast homolog Tap42.* Biochem Biophys Res Commun, 1998. **251**(2): p. 520-6.

108. Jiang, Y. and J.R. Broach, *Tor proteins and protein phosphatase 2A reciprocally regulate Tap42 in controlling cell growth in yeast.* EMBO J, 1999. **18**(10): p. 2782-92.
109. Hardwick, J.S., et al., *Rapamycin-modulated transcription defines the subset of nutrient-sensitive signaling pathways directly controlled by the Tor proteins.* Proc Natl Acad Sci U S A, 1999. **96**(26): p. 14866-70.
110. Duvel, K., et al., *Multiple roles of Tap42 in mediating rapamycin-induced transcriptional changes in yeast.* Mol Cell, 2003. **11**(6): p. 1467-78.
111. Yan, G., X. Shen, and Y. Jiang, *Rapamycin activates Tap42-associated phosphatases by abrogating their association with Tor complex 1.* EMBO J, 2006. **25**(15): p. 3546-55.
112. Kong, M., et al., *Alpha4 is an essential regulator of PP2A phosphatase activity.* Mol Cell, 2009. **36**(1): p. 51-60.
113. Jacinto, E., et al., *TIP41 interacts with TAP42 and negatively regulates the TOR signaling pathway.* Mol Cell, 2001. **8**(5): p. 1017-26.
114. Zhang, T., et al., *Ego3 functions as a homodimer to mediate the interaction between Gtr1-Gtr2 and Ego1 in the ego complex to activate TORC1.* Structure, 2012. **20**(12): p. 2151-60.
115. Kira, S., et al., *Dynamic relocation of the TORC1-Gtr1/2-Ego1/2/3 complex is regulated by Gtr1 and Gtr2.* Mol Biol Cell, 2016. **27**(2): p. 382-96.
116. Panchaud, N., M.P. Peli-Gulli, and C. De Virgilio, *SEACing the GAP that nEGOCiates TORC1 activation: Evolutionary conservation of Rag GTPase regulation.* Cell Cycle, 2013. **12**(18).
117. Peli-Gulli, M.P., et al., *Amino Acids Stimulate TORC1 through Lst4-Lst7, a GTPase-Activating Protein Complex for the Rag Family GTPase Gtr2.* Cell Rep, 2015.
118. Gong, R., et al., *Crystal structure of the Gtr1p-Gtr2p complex reveals new insights into the amino acid-induced TORC1 activation.* Genes Dev, 2011. **25**(16): p. 1668-73.
119. Sancak, Y., et al., *Ragulator-Rag complex targets mTORC1 to the lysosomal surface and is necessary for its activation by amino acids.* Cell, 2010. **141**(2): p. 290-303.
120. Nada, S., et al., *The novel lipid raft adaptor p18 controls endosome dynamics by anchoring the MEK-ERK pathway to late endosomes.* EMBO J, 2009. **28**(5): p. 477-89.
121. Wunderlich, W., et al., *A novel 14-kilodalton protein interacts with the mitogen-activated protein kinase scaffold mp1 on a late endosomal/lysosomal compartment.* J Cell Biol, 2001. **152**(4): p. 765-76.
122. Schaeffer, H.J., et al., *MP1: a MEK binding partner that enhances enzymatic activation of the MAP kinase cascade.* Science, 1998. **281**(5383): p. 1668-71.
123. Bar-Peled, L., et al., *Ragulator is a GEF for the rag GTPases that signal amino acid levels to mTORC1.* Cell, 2012. **150**(6): p. 1196-208.
124. Zoncu, R., et al., *mTORC1 senses lysosomal amino acids through an inside-out mechanism that requires the vacuolar H(+)-ATPase.* Science, 2011. **334**(6056): p. 678-83.

125. Bar-Peled, L., et al., *A Tumor suppressor complex with GAP activity for the Rag GTPases that signal amino acid sufficiency to mTORC1.* Science, 2013. **340**(6136): p. 1100-6.
126. Tsun, Z.Y., et al., *The Folliculin Tumor Suppressor Is a GAP for the RagC/D GTPases That Signal Amino Acid Levels to mTORC1.* Mol Cell, 2013.
127. Jeong, J.H., et al., *Crystal structure of the Gtr1p(GTP)-Gtr2p(GDP) protein complex reveals large structural rearrangements triggered by GTP-to-GDP conversion.* J Biol Chem, 2012. **287**(35): p. 29648-53.
128. Sancak, Y., et al., *The Rag GTPases bind raptor and mediate amino acid signaling to mTORC1.* Science, 2008. **320**(5882): p. 1496-501.
129. Inoki, K., et al., *Rheb GTPase is a direct target of TSC2 GAP activity and regulates mTOR signaling.* Genes Dev, 2003. **17**(15): p. 1829-34.
130. Fawal, M.A., M. Brandt, and N. Djouder, *MCRS1 binds and couples Rheb to amino acid-dependent mTORC1 activation.* Dev Cell, 2015. **33**(1): p. 67-81.
131. Jung, J., H.M. Genau, and C. Behrends, *Amino Acid-Dependent mTORC1 Regulation by the Lysosomal Membrane Protein SLC38A9.* Mol Cell Biol, 2015. **35**(14): p. 2479-94.
132. Rebsamen, M., et al., *SLC38A9 is a component of the lysosomal amino acid sensing machinery that controls mTORC1.* Nature, 2015. **519**(7544): p. 477-81.
133. Wang, S., et al., *Metabolism. Lysosomal amino acid transporter SLC38A9 signals arginine sufficiency to mTORC1.* Science, 2015. **347**(6218): p. 188-94.
134. Thomas, J.D., et al., *Rab1A is an mTORC1 activator and a colorectal oncogene.* Cancer Cell, 2014. **26**(5): p. 754-69.
135. Sturgill, T.W., et al., *TOR1 and TOR2 have distinct locations in live cells.* Eukaryot Cell, 2008. **7**(10): p. 1819-30.
136. Kim, J.E. and J. Chen, *Cytoplasmic-nuclear shuttling of FKBP12-rapamycin-associated protein is involved in rapamycin-sensitive signaling and translation initiation.* Proc Natl Acad Sci U S A, 2000. **97**(26): p. 14340-5.
137. Li, H., et al., *Nutrient regulates Tor1 nuclear localization and association with rDNA promoter.* Nature, 2006. **442**(7106): p. 1058-61.
138. Bachmann, R.A., et al., *A nuclear transport signal in mammalian target of rapamycin is critical for its cytoplasmic signaling to S6 kinase 1.* J Biol Chem, 2006. **281**(11): p. 7357-63.
139. Vazquez-Martin, A., et al., *Raptor, a positive regulatory subunit of mTOR complex 1, is a novel phosphoprotein of the rDNA transcription machinery in nucleoli and chromosomal nucleolus organizer regions (NORs).* Cell Cycle, 2011. **10**(18): p. 3140-52.
140. Tsang, C.K., et al., *Chromatin-mediated regulation of nucleolar structure and RNA Pol I localization by TOR.* EMBO J, 2003. **22**(22): p. 6045-56.
141. Humphrey, E.L., et al., *Rpd3p relocation mediates a transcriptional response to rapamycin in yeast.* Chem Biol, 2004. **11**(3): p. 295-9.
142. Tsang, C.K., H. Li, and X.S. Zheng, *Nutrient starvation promotes condensin loading to maintain rDNA stability.* EMBO J, 2007. **26**(2): p. 448-58.
143. Sandmeier, J.J., et al., *RPD3 is required for the inactivation of yeast ribosomal DNA genes in stationary phase.* EMBO J, 2002. **21**(18): p. 4959-68.

144. Dilova, I., et al., *Tor signaling and nutrient-based signals converge on Mks1p phosphorylation to regulate expression of Rtg1.Rtg3p-dependent target genes.* J Biol Chem, 2004. **279**(45): p. 46527-35.
145. Cardenas, M.E., et al., *The TOR signaling cascade regulates gene expression in response to nutrients.* Genes Dev, 1999. **13**(24): p. 3271-9.
146. Vannini, A., et al., *Molecular basis of RNA polymerase III transcription repression by Maf1.* Cell, 2010. **143**(1): p. 59-70.
147. Kantidakis, T., et al., *mTOR associates with TFIIIC, is found at tRNA and 5S rRNA genes, and targets their repressor Maf1.* Proc Natl Acad Sci U S A, 2010. **107**(26): p. 11823-8.
148. Wei, Y., C.K. Tsang, and X.F. Zheng, *Mechanisms of regulation of RNA polymerase III-dependent transcription by TORC1.* EMBO J, 2009. **28**(15): p. 2220-30.
149. Oficjalska-Pham, D., et al., *General repression of RNA polymerase III transcription is triggered by protein phosphatase type 2A-mediated dephosphorylation of Maf1.* Mol Cell, 2006. **22**(5): p. 623-32.
150. Cai, L., et al., *Acetyl-CoA induces cell growth and proliferation by promoting the acetylation of histones at growth genes.* Mol Cell, 2011. **42**(4): p. 426-37.
151. Shi, L. and B.P. Tu, *Acetyl-CoA induces transcription of the key G1 cyclin CLN3 to promote entry into the cell division cycle in Saccharomyces cerevisiae.* Proc Natl Acad Sci U S A, 2013. **110**(18): p. 7318-23.
152. Chen, H., et al., *Target of rapamycin signaling regulates high mobility group protein association to chromatin, which functions to suppress necrotic cell death.* Epigenetics Chromatin, 2013. **6**(1): p. 29.
153. Chen, C.C., et al., *Acetylated lysine 56 on histone H3 drives chromatin assembly after repair and signals for the completion of repair.* Cell, 2008. **134**(2): p. 231-43.
154. Maas, N.L., et al., *Cell cycle and checkpoint regulation of histone H3 K56 acetylation by Hst3 and Hst4.* Mol Cell, 2006. **23**(1): p. 109-19.
155. Altschul, S.F., et al., *Basic local alignment search tool.* J Mol Biol, 1990. **215**(3): p. 403-10.
156. Cornu, M., V. Albert, and M.N. Hall, *mTOR in aging, metabolism, and cancer.* Curr Opin Genet Dev, 2013. **23**(1): p. 53-62.
157. Valenzano, D.R., et al., *Resveratrol prolongs lifespan and retards the onset of age-related markers in a short-lived vertebrate.* Curr Biol, 2006. **16**(3): p. 296-300.
158. Wood, J.G., et al., *Sirtuin activators mimic caloric restriction and delay ageing in metazoans.* Nature, 2004. **430**(7000): p. 686-9.
159. Howitz, K.T., et al., *Small molecule activators of sirtuins extend Saccharomyces cerevisiae lifespan.* Nature, 2003. **425**(6954): p. 191-6.
160. Huh, W.K., et al., *Global analysis of protein localization in budding yeast.* Nature, 2003. **425**(6959): p. 686-91.
161. Li, M., et al., *Genome-wide analysis of functional sirtuin chromatin targets in yeast.* Genome Biol, 2013. **14**(5): p. R48.
162. Guillemette, B., et al., *H3 lysine 4 is acetylated at active gene promoters and is regulated by H3 lysine 4 methylation.* PLoS Genet, 2011. **7**(3): p. e1001354.

163. Downey, M., et al., *Gcn5 and sirtuins regulate acetylation of the ribosomal protein transcription factor Ifh1.* Curr Biol, 2013. **23**(17): p. 1638-48.
164. Wilson, J.M., et al., *Nuclear export modulates the cytoplasmic Sir2 homologue Hst2.* EMBO Rep, 2006. **7**(12): p. 1247-51.
165. Perrod, S., et al., *A cytosolic NAD-dependent deacetylase, Hst2p, can modulate nucleolar and telomeric silencing in yeast.* EMBO J, 2001. **20**(1-2): p. 197-209.
166. Lamming, D.W., et al., *HST2 mediates SIR2-independent life-span extension by calorie restriction.* Science, 2005. **309**(5742): p. 1861-4.
167. Liu, I.C., et al., *The histone deacetylase Hos2 forms an Hsp42-dependent cytoplasmic granule in quiescent yeast cells.* Mol Biol Cell, 2012. **23**(7): p. 1231-42.
168. Vaquero, A., et al., *SirT2 is a histone deacetylase with preference for histone H4 Lys 16 during mitosis.* Genes Dev, 2006. **20**(10): p. 1256-61.
169. Che, J., et al., *Hyper-Acetylation of Histone H3K56 Limits Break-Induced Replication by Inhibiting Extensive Repair Synthesis.* PLoS Genet, 2015. **11**(2): p. e1004990.
170. Hachinohe, M., F. Hanaoka, and H. Masumoto, *Hst3 and Hst4 histone deacetylases regulate replicative lifespan by preventing genome instability in Saccharomyces cerevisiae.* Genes Cells, 2011. **16**(4): p. 467-77.
171. Yang, B., A. Miller, and A.L. Kirchmaier, *HST3/HST4-dependent deacetylation of lysine 56 of histone H3 in silent chromatin.* Mol Biol Cell, 2008. **19**(11): p. 4993-5005.
172. Jack, C.V., et al., *Regulation of ribosomal DNA amplification by the TOR pathway.* Proc Natl Acad Sci U S A, 2015. **112**(31): p. 9674-9.
173. Brachmann, C.B., et al., *The SIR2 gene family, conserved from bacteria to humans, functions in silencing, cell cycle progression, and chromosome stability.* Genes Dev, 1995. **9**(23): p. 2888-902.
174. Miller, K.M., N.L. Maas, and D.P. Toczyski, *Taking it off: regulation of H3 K56 acetylation by Hst3 and Hst4.* Cell Cycle, 2006. **5**(22): p. 2561-5.
175. Celic, I., et al., *The sirtuins hst3 and Hst4p preserve genome integrity by controlling histone h3 lysine 56 deacetylation.* Curr Biol, 2006. **16**(13): p. 1280-9.
176. Madsen, C.T., et al., *Biotin starvation causes mitochondrial protein hyperacetylation and partial rescue by the SIRT3-like deacetylase Hst4p.* Nat Commun, 2015. **6**: p. 7726.
177. Gaglio, D., A. D'Alfonso, and G. Camilloni, *Functional complementation of sir2Delta yeast mutation by the human orthologous gene SIRT1.* PLoS One, 2013. **8**(12): p. e83114.
178. Choy, J.S., et al., *A role for histone H4K16 hypoacetylation in Saccharomyces cerevisiae kinetochore function.* Genetics, 2011. **189**(1): p. 11-21.
179. Delgoshaie, N., et al., *Regulation of the histone deacetylase Hst3 by cyclin-dependent kinases and the ubiquitin ligase SCFCdc4.* J Biol Chem, 2014. **289**(19): p. 13186-96.
180. Edenberg, E.R., et al., *Hst3 is turned over by a replication stress-responsive SCF(Cdc4) phospho-degron.* Proc Natl Acad Sci U S A, 2014. **111**(16): p. 5962-7.

181. Tang, X., et al., *Genome-wide surveys for phosphorylation-dependent substrates of SCF ubiquitin ligases.* Methods Enzymol, 2005. **399**: p. 433-58.
182. McClure, J.M., et al., *Pnc1p-mediated nicotinamide clearance modifies the epigenetic properties of rDNA silencing in Saccharomyces cerevisiae.* Genetics, 2008. **180**(2): p. 797-810.
183. Sandmeier, J.J., et al., *Telomeric and rDNA silencing in Saccharomyces cerevisiae are dependent on a nuclear NAD(+) salvage pathway.* Genetics, 2002. **160**(3): p. 877-89.
184. Csibi, A., et al., *The mTORC1 pathway stimulates glutamine metabolism and cell proliferation by repressing SIRT4.* Cell, 2013. **153**(4): p. 840-54.
185. Ghosh, H.S., M. McBurney, and P.D. Robbins, *SIRT1 negatively regulates the mammalian target of rapamycin.* PLoS One, 2010. **5**(2): p. e9199.
186. Kokkonen, P., et al., *Studying SIRT6 regulation using H3K56 based substrate and small molecules.* Eur J Pharm Sci, 2014. **63**: p. 71-6.
187. Michishita, E., et al., *Evolutionarily conserved and nonconserved cellular localizations and functions of human SIRT proteins.* Mol Biol Cell, 2005. **16**(10): p. 4623-35.
188. Tanno, M., et al., *Nucleocytoplasmic shuttling of the NAD+-dependent histone deacetylase SIRT1.* J Biol Chem, 2007. **282**(9): p. 6823-32.
189. Hajji, N., et al., *Opposing effects of hMOF and SIRT1 on H4K16 acetylation and the sensitivity to the topoisomerase II inhibitor etoposide.* Oncogene, 2010. **29**(15): p. 2192-204.
190. Vaquero, A., R. Sternglanz, and D. Reinberg, *NAD+-dependent deacetylation of H4 lysine 16 by class III HDACs.* Oncogene, 2007. **26**(37): p. 5505-20.
191. Mulligan, P., et al., *A SIRT1-LSD1 corepressor complex regulates Notch target gene expression and development.* Mol Cell, 2011. **42**(5): p. 689-99.
192. Guo, Y.J., et al., *Resveratrol alleviates MPTP-induced motor impairments and pathological changes by autophagic degradation of alpha-synuclein via SIRT1-deacetylated LC3.* Mol Nutr Food Res, 2016.
193. Huang, R. and W. Liu, *Identifying an essential role of nuclear LC3 for autophagy.* Autophagy, 2015. **11**(5): p. 852-3.
194. Lee, I.H., et al., *A role for the NAD-dependent deacetylase Sirt1 in the regulation of autophagy.* Proc Natl Acad Sci U S A, 2008. **105**(9): p. 3374-9.
195. Bouras, T., et al., *SIRT1 deacetylation and repression of p300 involves lysine residues 1020/1024 within the cell cycle regulatory domain 1.* J Biol Chem, 2005. **280**(11): p. 10264-76.
196. Lu, L., et al., *Modulations of hMOF autoacetylation by SIRT1 regulate hMOF recruitment and activities on the chromatin.* Cell Res, 2011. **21**(8): p. 1182-95.
197. Wang, J. and J. Chen, *SIRT1 regulates autoacetylation and histone acetyltransferase activity of TIP60.* J Biol Chem, 2010. **285**(15): p. 11458-64.
198. Yamagata, K. and I. Kitabayashi, *Sirt1 physically interacts with Tip60 and negatively regulates Tip60-mediated acetylation of H2AX.* Biochem Biophys Res Commun, 2009. **390**(4): p. 1355-60.
199. Peck, B., et al., *SIRT inhibitors induce cell death and p53 acetylation through targeting both SIRT1 and SIRT2.* Mol Cancer Ther, 2010. **9**(4): p. 844-55.

200. Langley, E., et al., *Human SIR2 deacetylates p53 and antagonizes PML/p53-induced cellular senescence.* EMBO J, 2002. **21**(10): p. 2383-96.
201. Vaziri, H., et al., *hSIR2(SIRT1) functions as an NAD-dependent p53 deacetylase.* Cell, 2001. **107**(2): p. 149-59.
202. Motta, M.C., et al., *Mammalian SIRT1 represses forkhead transcription factors.* Cell, 2004. **116**(4): p. 551-63.
203. Kobayashi, Y., et al., *SIRT1 is critical regulator of FOXO-mediated transcription in response to oxidative stress.* Int J Mol Med, 2005. **16**(2): p. 237-43.
204. Yeung, F., et al., *Modulation of NF-kappaB-dependent transcription and cell survival by the SIRT1 deacetylase.* EMBO J, 2004. **23**(12): p. 2369-80.
205. Mao, B., et al., *Sirt1 deacetylates c-Myc and promotes c-Myc/Max association.* Int J Biochem Cell Biol, 2011. **43**(11): p. 1573-81.
206. Dioum, E.M., et al., *Regulation of hypoxia-inducible factor 2alpha signaling by the stress-responsive deacetylase sirtuin 1.* Science, 2009. **324**(5932): p. 1289-93.
207. Joo, H.Y., et al., *SIRT1 deacetylates and stabilizes hypoxia-inducible factor-1alpha (HIF-1alpha) via direct interactions during hypoxia.* Biochem Biophys Res Commun, 2015. **462**(4): p. 294-300.
208. Lim, J.H., et al., *Sirtuin 1 modulates cellular responses to hypoxia by deacetylating hypoxia-inducible factor 1alpha.* Mol Cell, 2010. **38**(6): p. 864-78.
209. Nemoto, S., M.M. Fergusson, and T. Finkel, *SIRT1 functionally interacts with the metabolic regulator and transcriptional coactivator PGC-1{alpha}.* J Biol Chem, 2005. **280**(16): p. 16456-60.
210. Lan, F., et al., *SIRT1 modulation of the acetylation status, cytosolic localization, and activity of LKB1. Possible role in AMP-activated protein kinase activation.* J Biol Chem, 2008. **283**(41): p. 27628-35.
211. Cohen, H.Y., et al., *Calorie restriction promotes mammalian cell survival by inducing the SIRT1 deacetylase.* Science, 2004. **305**(5682): p. 390-2.
212. Rajamohan, S.B., et al., *SIRT1 promotes cell survival under stress by deacetylation-dependent deactivation of poly(ADP-ribose) polymerase 1.* Mol Cell Biol, 2009. **29**(15): p. 4116-29.
213. Kolthur-Seetharam, U., et al., *Control of AIF-mediated cell death by the functional interplay of SIRT1 and PARP-1 in response to DNA damage.* Cell Cycle, 2006. **5**(8): p. 873-7.
214. North, B.J. and E. Verdin, *Interphase nucleo-cytoplasmic shuttling and localization of SIRT2 during mitosis.* PLoS One, 2007. **2**(8): p. e784.
215. Inoue, T., et al., *SIRT2, a tubulin deacetylase, acts to block the entry to chromosome condensation in response to mitotic stress.* Oncogene, 2007. **26**(7): p. 945-57.
216. van Leeuwen, I.M., et al., *Modulation of p53 C-terminal acetylation by mdm2, p14ARF, and cytoplasmic SirT2.* Mol Cancer Ther, 2013. **12**(4): p. 471-80.
217. Wang, F., et al., *Deacetylation of FOXO3 by SIRT1 or SIRT2 leads to Skp2-mediated FOXO3 ubiquitination and degradation.* Oncogene, 2012. **31**(12): p. 1546-57.
218. Wang, F., et al., *SIRT2 deacetylates FOXO3a in response to oxidative stress and caloric restriction.* Aging Cell, 2007. **6**(4): p. 505-14.

219. Onyango, P., et al., *SIRT3, a human SIR2 homologue, is an NAD-dependent deacetylase localized to mitochondria.* Proc Natl Acad Sci U S A, 2002. **99**(21): p. 13653-8.
220. Schwer, B., et al., *The human silent information regulator (Sir)2 homologue hSIRT3 is a mitochondrial nicotinamide adenine dinucleotide-dependent deacetylase.* J Cell Biol, 2002. **158**(4): p. 647-57.
221. Huang, J.Y., et al., *Mitochondrial sirtuins.* Biochim Biophys Acta, 2010. **1804**(8): p. 1645-51.
222. Scher, M.B., A. Vaquero, and D. Reinberg, *SirT3 is a nuclear NAD+-dependent histone deacetylase that translocates to the mitochondria upon cellular stress.* Genes Dev, 2007. **21**(8): p. 920-8.
223. Schwer, B., et al., *Reversible lysine acetylation controls the activity of the mitochondrial enzyme acetyl-CoA synthetase 2.* Proc Natl Acad Sci U S A, 2006. **103**(27): p. 10224-9.
224. Hallows, W.C., S. Lee, and J.M. Denu, *Sirtuins deacetylate and activate mammalian acetyl-CoA synthetases.* Proc Natl Acad Sci U S A, 2006. **103**(27): p. 10230-5.
225. Xue, L., et al., *Acetylation-dependent regulation of mitochondrial ALDH2 activation by SIRT3 mediates acute ethanol-induced eNOS activation.* FEBS Lett, 2012. **586**(2): p. 137-42.
226. Finley, L.W., et al., *Succinate dehydrogenase is a direct target of sirtuin 3 deacetylase activity.* PLoS One, 2011. **6**(8): p. e23295.
227. Cimen, H., et al., *Regulation of succinate dehydrogenase activity by SIRT3 in mammalian mitochondria.* Biochemistry, 2010. **49**(2): p. 304-11.
228. Sundaresan, N.R., et al., *SIRT3 is a stress-responsive deacetylase in cardiomyocytes that protects cells from stress-mediated cell death by deacetylation of Ku70.* Mol Cell Biol, 2008. **28**(20): p. 6384-401.
229. Ahuja, N., et al., *Regulation of insulin secretion by SIRT4, a mitochondrial ADP-ribosyltransferase.* J Biol Chem, 2007. **282**(46): p. 33583-92.
230. Haigis, M.C., et al., *SIRT4 inhibits glutamate dehydrogenase and opposes the effects of calorie restriction in pancreatic beta cells.* Cell, 2006. **126**(5): p. 941-54.
231. Ogura, M., et al., *Overexpression of SIRT5 confirms its involvement in deacetylation and activation of carbamoyl phosphate synthetase 1.* Biochem Biophys Res Commun, 2010. **393**(1): p. 73-8.
232. Nakagawa, T., et al., *SIRT5 Deacetylates carbamoyl phosphate synthetase 1 and regulates the urea cycle.* Cell, 2009. **137**(3): p. 560-70.
233. Liszt, G., et al., *Mouse Sir2 homolog SIRT6 is a nuclear ADP-ribosyltransferase.* J Biol Chem, 2005. **280**(22): p. 21313-20.
234. Kawahara, T.L., et al., *SIRT6 links histone H3 lysine 9 deacetylation to NF-kappaB-dependent gene expression and organismal life span.* Cell, 2009. **136**(1): p. 62-74.
235. Michishita, E., et al., *SIRT6 is a histone H3 lysine 9 deacetylase that modulates telomeric chromatin.* Nature, 2008. **452**(7186): p. 492-6.
236. Schwer, B., et al., *Neural sirtuin 6 (Sirt6) ablation attenuates somatic growth and causes obesity.* Proc Natl Acad Sci U S A, 2010. **107**(50): p. 21790-4.

237. Tasselli, L., et al., *SIRT6 deacetylates H3K18ac at pericentric chromatin to prevent mitotic errors and cellular senescence.* Nat Struct Mol Biol, 2016. **23**(5): p. 434-40.
238. Kaidi, A., et al., *Human SIRT6 promotes DNA end resection through CtIP deacetylation.* Science, 2010. **329**(5997): p. 1348-53.
239. Ford, E., et al., *Mammalian Sir2 homolog SIRT7 is an activator of RNA polymerase I transcription.* Genes Dev, 2006. **20**(9): p. 1075-80.
240. Barber, M.F., et al., *SIRT7 links H3K18 deacetylation to maintenance of oncogenic transformation.* Nature, 2012. **487**(7405): p. 114-8.
241. Hargreaves, D.C. and G.R. Crabtree, *ATP-dependent chromatin remodeling: genetics, genomics and mechanisms.* Cell Res, 2011. **21**(3): p. 396-420.
242. Das, C., J.K. Tyler, and M.E. Churchill, *The histone shuffle: histone chaperones in an energetic dance.* Trends Biochem Sci, 2010. **35**(9): p. 476-89.
243. Nightingale, K., et al., *Evidence for a shared structural role for HMG1 and linker histones B4 and H1 in organizing chromatin.* EMBO J, 1996. **15**(3): p. 548-61.
244. Varga-Weisz, P., K. van Holde, and J. Zlatanova, *Competition between linker histones and HMG1 for binding to four-way junction DNA: implications for transcription.* Biochem Biophys Res Commun, 1994. **203**(3): p. 1904-11.
245. Kohlstaedt, L.A., et al., *Non-histone chromosomal protein HMG1 modulates the histone H1-induced condensation of DNA.* J Biol Chem, 1987. **262**(2): p. 524-6.
246. Bianchi, M.E., et al., *The DNA binding site of HMG1 protein is composed of two similar segments (HMG boxes), both of which have counterparts in other eukaryotic regulatory proteins.* EMBO J, 1992. **11**(3): p. 1055-63.
247. Najima, Y., et al., *High mobility group protein-B1 interacts with sterol regulatory element-binding proteins to enhance their DNA binding.* J Biol Chem, 2005. **280**(30): p. 27523-32.
248. Dasgupta, A. and W.M. Scovell, *TFIIA abrogates the effects of inhibition by HMGB1 but not E1A during the early stages of assembly of the transcriptional preinitiation complex.* Biochim Biophys Acta, 2003. **1627**(2-3): p. 101-10.
249. Das, D. and W.M. Scovell, *The binding interaction of HMG-1 with the TATA-binding protein/TATA complex.* J Biol Chem, 2001. **276**(35): p. 32597-605.
250. Lu, W., et al., *Influence of HMG-1 and adenovirus oncoprotein E1A on early stages of transcriptional preinitiation complex assembly.* J Biol Chem, 2000. **275**(45): p. 35006-12.
251. Scaffidi, P., T. Misteli, and M.E. Bianchi, *Release of chromatin protein HMGB1 by necrotic cells triggers inflammation.* Nature, 2002. **418**(6894): p. 191-5.
252. Ueda, T., et al., *Acidic C-tail of HMGB1 is required for its target binding to nucleosome linker DNA and transcription stimulation.* Biochemistry, 2004. **43**(30): p. 9901-8.
253. Kawase, T., et al., *Distinct domains in HMGB1 are involved in specific intramolecular and nucleosomal interactions.* Biochemistry, 2008. **47**(52): p. 13991-6.
254. Park, J.S., et al., *Involvement of toll-like receptors 2 and 4 in cellular activation by high mobility group box 1 protein.* J Biol Chem, 2004. **279**(9): p. 7370-7.

255. Kang, R., et al., *The HMGB1/RAGE inflammatory pathway promotes pancreatic tumor growth by regulating mitochondrial bioenergetics.* Oncogene, 2014. **33**(5): p. 567-77.
256. Salminen, A., A. Kauppinen, and K. Kaarniranta, *Emerging role of NF-kappaB signaling in the induction of senescence-associated secretory phenotype (SASP).* Cell Signal, 2012. **24**(4): p. 835-45.
257. Tsaponina, O., et al., *Ixr1 is required for the expression of the ribonucleotide reductase Rnr1 and maintenance of dNTP pools.* PLoS Genet, 2011. **7**(5): p. e1002061.
258. Castro-Prego, R., et al., *Regulatory factors controlling transcription of Saccharomyces cerevisiae IXR1 by oxygen levels: a model of transcriptional adaptation from aerobiosis to hypoxia implicating ROX1 and IXR1 cross-regulation.* Biochem J, 2010. **425**(1): p. 235-43.
259. McA'Nulty, M.M. and S.J. Lippard, *The HMG-domain protein Ixr1 blocks excision repair of cisplatin-DNA adducts in yeast.* Mutat Res, 1996. **362**(1): p. 75-86.
260. Klinkenberg, L.G., et al., *Combinatorial repression of the hypoxic genes of Saccharomyces cerevisiae by DNA binding proteins Rox1 and Mot3.* Eukaryot Cell, 2005. **4**(4): p. 649-60.
261. Ter Linde, J.J. and H.Y. Steensma, *A microarray-assisted screen for potential Hap1 and Rox1 target genes in Saccharomyces cerevisiae.* Yeast, 2002. **19**(10): p. 825-40.
262. Balasubramanian, B., C.V. Lowry, and R.S. Zitomer, *The Rox1 repressor of the Saccharomyces cerevisiae hypoxic genes is a specific DNA-binding protein with a high-mobility-group motif.* Mol Cell Biol, 1993. **13**(10): p. 6071-8.
263. Sia, R.A., et al., *Loss of the mitochondrial nucleoid protein, Abf2p, destabilizes repetitive DNA in the yeast mitochondrial genome.* Genetics, 2009. **181**(1): p. 331-4.
264. Cho, J.H., Y.K. Lee, and C.B. Chae, *The modulation of the biological activities of mitochondrial histone Abf2p by yeast PKA and its possible role in the regulation of mitochondrial DNA content during glucose repression.* Biochim Biophys Acta, 2001. **1522**(3): p. 175-86.
265. MacAlpine, D.M., P.S. Perlman, and R.A. Butow, *The high mobility group protein Abf2p influences the level of yeast mitochondrial DNA recombination intermediates in vivo.* Proc Natl Acad Sci U S A, 1998. **95**(12): p. 6739-43.
266. Diffley, J.F. and B. Stillman, *A close relative of the nuclear, chromosomal high-mobility group protein HMG1 in yeast mitochondria.* Proc Natl Acad Sci U S A, 1991. **88**(17): p. 7864-8.
267. Bauerle, K.T., E. Kamau, and A. Grove, *Interactions between N- and C-terminal domains of the Saccharomyces cerevisiae high-mobility group protein HMO1 are required for DNA bending.* Biochemistry, 2006. **45**(11): p. 3635-45.
268. Kamau, E., K.T. Bauerle, and A. Grove, *The Saccharomyces cerevisiae high mobility group box protein HMO1 contains two functional DNA binding domains.* J Biol Chem, 2004. **279**(53): p. 55234-40.

269. Hepp, M.I., et al., *Nucleosome remodeling by the SWI/SNF complex is enhanced by yeast high mobility group box (HMGB) proteins.* Biochim Biophys Acta, 2014. **1839**(9): p. 764-72.
270. Xiao, L., A.M. Williams, and A. Grove, *The C-terminal domain of yeast high mobility group protein HMO1 mediates lateral protein accretion and in-phase DNA bending.* Biochemistry, 2010. **49**(19): p. 4051-9.
271. Knight, B., et al., *Two distinct promoter architectures centered on dynamic nucleosomes control ribosomal protein gene transcription.* Genes Dev, 2014. **28**(15): p. 1695-709.
272. Xiao, L. and A. Grove, *Coordination of Ribosomal Protein and Ribosomal RNA Gene Expression in Response to TOR Signaling.* Curr Genomics, 2009. **10**(3): p. 198-205.
273. Merz, K., et al., *Actively transcribed rRNA genes in S. cerevisiae are organized in a specialized chromatin associated with the high-mobility group protein Hmo1 and are largely devoid of histone molecules.* Genes Dev, 2008. **22**(9): p. 1190-204.
274. Hall, D.B., J.T. Wade, and K. Struhl, *An HMG protein, Hmo1, associates with promoters of many ribosomal protein genes and throughout the rRNA gene locus in Saccharomyces cerevisiae.* Mol Cell Biol, 2006. **26**(9): p. 3672-9.
275. Albert, B., et al., *Structure-function analysis of Hmo1 unveils an ancestral organization of HMG-Box factors involved in ribosomal DNA transcription from yeast to human.* Nucleic Acids Res, 2013. **41**(22): p. 10135-49.
276. Stillman, D.J., *Nhp6: a small but powerful effector of chromatin structure in Saccharomyces cerevisiae.* Biochim Biophys Acta, 2010. **1799**(1-2): p. 175-80.
277. Kolodrubetz, D., M. Kruppa, and A. Burgum, *Gene dosage affects the expression of the duplicated NHP6 genes of Saccharomyces cerevisiae.* Gene, 2001. **272**(1-2): p. 93-101.
278. Mahapatra, S., et al., *Yeast H2A.Z, FACT complex and RSC regulate transcription of tRNA gene through differential dynamics of flanking nucleosomes.* Nucleic Acids Res, 2011. **39**(10): p. 4023-34.
279. Dowell, N.L., et al., *Chromatin-dependent binding of the S. cerevisiae HMGB protein Nhp6A affects nucleosome dynamics and transcription.* Genes Dev, 2010. **24**(18): p. 2031-42.
280. Formosa, T., et al., *Spt16-Pob3 and the HMG protein Nhp6 combine to form the nucleosome-binding factor SPN.* EMBO J, 2001. **20**(13): p. 3506-17.
281. Brewster, N.K., G.C. Johnston, and R.A. Singer, *A bipartite yeast SSRP1 analog comprised of Pob3 and Nhp6 proteins modulates transcription.* Mol Cell Biol, 2001. **21**(10): p. 3491-502.
282. Rhoades, A.R., S. Ruone, and T. Formosa, *Structural features of nucleosomes reorganized by yeast FACT and its HMG box component, Nhp6.* Mol Cell Biol, 2004. **24**(9): p. 3907-17.
283. Eisenberg, T., et al., *Induction of autophagy by spermidine promotes longevity.* Nat Cell Biol, 2009. **11**(11): p. 1305-14.
284. Morrison, A.J., et al., *INO80 and gamma-H2AX interaction links ATP-dependent chromatin remodeling to DNA damage repair.* Cell, 2004. **119**(6): p. 767-75.

285. Kashiwaba, S., et al., *The mammalian INO80 complex is recruited to DNA damage sites in an ARP8 dependent manner.* Biochem Biophys Res Commun, 2010. **402**(4): p. 619-25.
286. van Attikum, H., O. Fritsch, and S.M. Gasser, *Distinct roles for SWR1 and INO80 chromatin remodeling complexes at chromosomal double-strand breaks.* EMBO J, 2007. **26**(18): p. 4113-25.
287. Ray, S. and A. Grove, *The yeast high mobility group protein HMO2, a subunit of the chromatin-remodeling complex INO80, binds DNA ends.* Nucleic Acids Res, 2009. **37**(19): p. 6389-99.
288. Sekiguchi, T., et al., *Genetic evidence that Ras-like GTPases, Gtr1p, and Gtr2p, are involved in epigenetic control of gene expression in Saccharomyces cerevisiae.* Biochem Biophys Res Commun, 2008. **368**(3): p. 748-54.
289. Dazert, E. and M.N. Hall, *mTOR signaling in disease.* Curr Opin Cell Biol, 2011. **23**(6): p. 744-55.
290. Sinclair, D.A., *Toward a unified theory of caloric restriction and longevity regulation.* Mech Ageing Dev, 2005. **126**(9): p. 987-1002.
291. Imai, S.I. and L. Guarente, *NAD and sirtuins in aging and disease.* Trends Cell Biol.
292. Kang, W.K., et al., *Sir2 phosphorylation through cAMP-PKA and CK2 signaling inhibits the lifespan extension activity of Sir2 in yeast.* Elife, 2015. **4**.
293. Jurk, D., et al., *Postmitotic neurons develop a p21-dependent senescence-like phenotype driven by a DNA damage response.* Aging Cell, 2012. **11**(6): p. 996-1004.
294. Thakurela, S., et al., *Dynamics and function of distal regulatory elements during neurogenesis and neuroplasticity.* Genome Res, 2015. **25**(9): p. 1309-24.
295. Maze, I., et al., *Critical Role of Histone Turnover in Neuronal Transcription and Plasticity.* Neuron, 2015. **87**(1): p. 77-94.
296. Atwood, C.S. and R.L. Bowen, *The endocrine dyscrasia that accompanies menopause and andropause induces aberrant cell cycle signaling that triggers re-entry of post-mitotic neurons into the cell cycle, neurodysfunction, neurodegeneration and cognitive disease.* Horm Behav, 2015. **76**: p. 63-80.
297. Raina, A.K., et al., *Neurons in Alzheimer disease emerge from senescence.* Mech Ageing Dev, 2001. **123**(1): p. 3-9.
298. Gong, H., et al., *Histone modifications change with age, dietary restriction and rapamycin treatment in mouse brain.* Oncotarget, 2015. **6**(18): p. 15882-90.
299. Liu, L., et al., *Chromatin modifications as determinants of muscle stem cell quiescence and chronological aging.* Cell Rep, 2013. **4**(1): p. 189-204.
300. Janke, C., et al., *A versatile toolbox for PCR-based tagging of yeast genes: new fluorescent proteins, more markers and promoter substitution cassettes.* Yeast, 2004. **21**(11): p. 947-62.
301. Mumberg, D., R. Muller, and M. Funk, *Yeast vectors for the controlled expression of heterologous proteins in different genetic backgrounds.* Gene, 1995. **156**(1): p. 119-22.
302. Jones, D.T., *Protein secondary structure prediction based on position-specific scoring matrices.* J Mol Biol, 1999. **292**(2): p. 195-202.

303. Laribee, R.N., et al., *Ccr4-not regulates RNA polymerase I transcription and couples nutrient signaling to the control of ribosomal RNA biogenesis.* PLoS Genet, 2015. **11**(3): p. e1005113.
304. Workman, J.J., H. Chen, and R.N. Laribee, *Saccharomyces cerevisiae TORC1 Controls Histone Acetylation by Signaling Through the Sit4/PP6 Phosphatase To Regulate Sirtuin Deacetylase Nuclear Accumulation.* Genetics, 2016.
305. Rizzardi, L.F., et al., *DNA replication origin function is promoted by H3K4 di-methylation in Saccharomyces cerevisiae.* Genetics, 2012. **192**(2): p. 371-84.
306. Friis, R.M., et al., *A glycolytic burst drives glucose induction of global histone acetylation by picNuA4 and SAGA.* Nucleic Acids Res, 2009. **37**(12): p. 3969-80.
307. Crespo, J.L., et al., *The TOR-controlled transcription activators GLN3, RTG1, and RTG3 are regulated in response to intracellular levels of glutamine.* Proc Natl Acad Sci U S A, 2002. **99**(10): p. 6784-9.
308. Magasanik, B., *Ammonia assimilation by Saccharomyces cerevisiae.* Eukaryot Cell, 2003. **2**(5): p. 827-9.
309. Yorimitsu, T., et al., *Tap42-associated protein phosphatase type 2A negatively regulates induction of autophagy.* Autophagy, 2009. **5**(5): p. 616-24.
310. Hombauer, H., et al., *Generation of active protein phosphatase 2A is coupled to holoenzyme assembly.* PLoS Biol, 2007. **5**(6): p. e155.
311. Hasmann, M. and I. Schemainda, *FK866, a highly specific noncompetitive inhibitor of nicotinamide phosphoribosyltransferase, represents a novel mechanism for induction of tumor cell apoptosis.* Cancer Res, 2003. **63**(21): p. 7436-42.
312. Hisahara, S., et al., *Histone deacetylase SIRT1 modulates neuronal differentiation by its nuclear translocation.* Proc Natl Acad Sci U S A, 2008. **105**(40): p. 15599-604.
313. Hosiner, D., et al., *Arsenic toxicity to Saccharomyces cerevisiae is a consequence of inhibition of the TORC1 kinase combined with a chronic stress response.* Mol Biol Cell, 2009. **20**(3): p. 1048-57.
314. Tate, J.J. and T.G. Cooper, *Five conditions commonly used to down-regulate tor complex 1 generate different physiological situations exhibiting distinct requirements and outcomes.* J Biol Chem, 2013. **288**(38): p. 27243-62.
315. Dai, J., et al., *Probing nucleosome function: a highly versatile library of synthetic histone H3 and H4 mutants.* Cell, 2008. **134**(6): p. 1066-78.
316. Watson, M., et al., *Characterization of the interaction between HMGB1 and H3-a possible means of positioning HMGB1 in chromatin.* Nucleic Acids Res, 2014. **42**(2): p. 848-59.
317. Watson, M., K. Stott, and J.O. Thomas, *Mapping intramolecular interactions between domains in HMGB1 using a tail-truncation approach.* J Mol Biol, 2007. **374**(5): p. 1286-97.
318. Eltschinger, S. and R. Loewith, *TOR Complexes and the Maintenance of Cellular Homeostasis.* Trends Cell Biol, 2015.
319. VanderSluis, B., et al., *Broad metabolic sensitivity profiling of a prototrophic yeast deletion collection.* Genome Biol, 2014. **15**(4): p. R64.

320. Reinke, A., et al., *Caffeine targets TOR complex I and provides evidence for a regulatory link between the FRB and kinase domains of Tor1p.* J Biol Chem, 2006. **281**(42): p. 31616-26.
321. Pan, Y., et al., *Regulation of yeast chronological life span by TORC1 via adaptive mitochondrial ROS signaling.* Cell Metab, 2011. **13**(6): p. 668-78.
322. Barbato, D.L., et al., *Mitochondrial Hormesis links nutrient restriction to improved metabolism in fat cell.* Aging (Albany NY), 2015. **7**(10): p. 869-81.
323. Raffaello, A. and R. Rizzuto, *Mitochondrial longevity pathways.* Biochim Biophys Acta, 2011. **1813**(1): p. 260-8.
324. Pan, Y. and G.S. Shadel, *Extension of chronological life span by reduced TOR signaling requires down-regulation of Sch9p and involves increased mitochondrial OXPHOS complex density.* Aging (Albany NY), 2009. **1**(1): p. 131-45.
325. Bonawitz, N.D., et al., *Reduced TOR signaling extends chronological life span via increased respiration and upregulation of mitochondrial gene expression.* Cell Metab, 2007. **5**(4): p. 265-77.
326. Blagosklonny, M.V., *Hormesis does not make sense except in the light of TOR-driven aging.* Aging (Albany NY), 2011. **3**(11): p. 1051-62.
327. Anandharaj, A., S. Cinghu, and W.Y. Park, *Rapamycin-mediated mTOR inhibition attenuates survivin and sensitizes glioblastoma cells to radiation therapy.* Acta Biochim Biophys Sin (Shanghai), 2011. **43**(4): p. 292-300.
328. Dechant, R., et al., *Cytosolic pH regulates cell growth through distinct GTPases, Arf1 and Gtr1, to promote Ras/PKA and TORC1 activity.* Mol Cell, 2014. **55**(3): p. 409-21.
329. Schmelzle, T., et al., *Activation of the RAS/cyclic AMP pathway suppresses a TOR deficiency in yeast.* Mol Cell Biol, 2004. **24**(1): p. 338-51.
330. Peng, W., et al., *Regulators of cellular levels of histone acetylation in Saccharomyces cerevisiae.* Genetics, 2008. **179**(1): p. 277-89.
331. Li, L. and R. Bhatia, *The controversial role of Sirtuins in tumorigenesis - SIRT7 joins the debate.* Cell Res, 2013. **23**(1): p. 10-2.
332. Martinez-Redondo, P., I. Santos-Barriopedro, and A. Vaquero, *A big step for SIRT7, one giant leap for Sirtuins... in cancer.* Cancer Cell, 2012. **21**(6): p. 719-21.
333. Irene, C., et al., *Hst3p, a histone deacetylase, promotes maintenance of Saccharomyces cerevisiae chromosome III lacking efficient replication origins.* Mol Genet Genomics, 2016. **291**(1): p. 271-83.
334. Wang, W., et al., *AMP-activated protein kinase-regulated phosphorylation and acetylation of importin alpha1: involvement in the nuclear import of RNA-binding protein HuR.* J Biol Chem, 2004. **279**(46): p. 48376-88.
335. McCormick, M.A., et al., *The SAGA histone deubiquitinase module controls yeast replicative lifespan via Sir2 interaction.* Cell Rep, 2014. **8**(2): p. 477-86.
336. Spedale, G., et al., *Identification of Pep4p as the protease responsible for formation of the SAGA-related SLIK protein complex.* J Biol Chem, 2010. **285**(30): p. 22793-9.

337. Hassan, A.H., et al., *Selective recognition of acetylated histones by bromodomains in transcriptional co-activators.* Biochem J, 2007. **402**(1): p. 125-33.
338. Hoke, S.M., et al., *C-terminal processing of yeast Spt7 occurs in the absence of functional SAGA complex.* BMC Biochem, 2007. **8**: p. 16.
339. Chen, J.C. and T. Powers, *Coordinate regulation of multiple and distinct biosynthetic pathways by TOR and PKA kinases in S. cerevisiae.* Curr Genet, 2006. **49**(5): p. 281-93.
340. Sanchez, R., J. Meslamani, and M.M. Zhou, *The bromodomain: from epigenome reader to druggable target.* Biochim Biophys Acta, 2014. **1839**(8): p. 676-85.
341. Shanle, E.K., et al., *Association of Taf14 with acetylated histone H3 directs gene transcription and the DNA damage response.* Genes Dev, 2015. **29**(17): p. 1795-800.
342. Jiao, G., et al., *Arsenic trioxide inhibits growth of human chondrosarcoma cells through G2/M arrest and apoptosis as well as autophagy.* Tumour Biol, 2015. **36**(5): p. 3969-77.
343. Bontron, S., et al., *Yeast endosulfines control entry into quiescence and chronological life span by inhibiting protein phosphatase 2A.* Cell Rep, 2013. **3**(1): p. 16-22.
344. Hong, S., et al., *Cross-talk between sirtuin and mammalian target of rapamycin complex 1 (mTORC1) signaling in the regulation of S6 kinase 1 (S6K1) phosphorylation.* J Biol Chem, 2014. **289**(19): p. 13132-41.
345. Fenton, T.R., et al., *S6K1 is acetylated at lysine 516 in response to growth factor stimulation.* Biochem Biophys Res Commun, 2010. **398**(3): p. 400-5.
346. Fenton, T.R., et al., *Histone acetyltransferases interact with and acetylate p70 ribosomal S6 kinases in vitro and in vivo.* Int J Biochem Cell Biol, 2010. **42**(2): p. 359-66.
347. Igarashi, M. and L. Guarente, *mTORC1 and SIRT1 Cooperate to Foster Expansion of Gut Adult Stem Cells during Calorie Restriction.* Cell, 2016.
348. Kato, M. and S.J. Lin, *Regulation of NAD+ metabolism, signaling and compartmentalization in the yeast Saccharomyces cerevisiae.* DNA Repair (Amst), 2014. **23**: p. 49-58.
349. Lu, J.Y., et al., *Acetylation of yeast AMPK controls intrinsic aging independently of caloric restriction.* Cell, 2011. **146**(6): p. 969-79.
350. Pavlova, N.N. and C.B. Thompson, *The Emerging Hallmarks of Cancer Metabolism.* Cell Metab, 2016. **23**(1): p. 27-47.
351. Schneider, L.S., et al., *Vacuolar-ATPase Inhibition Blocks Iron Metabolism to Mediate Therapeutic Effects in Breast Cancer.* Cancer Res, 2015. **75**(14): p. 2863-74.
352. Zhang, S., et al., *Anti-leukemic effects of the V-ATPase inhibitor Archazolid A.* Oncotarget, 2015. **6**(41): p. 43508-28.
353. Schempp, C.M., et al., *V-ATPase inhibition regulates anoikis resistance and metastasis of cancer cells.* Mol Cancer Ther, 2014. **13**(4): p. 926-37.
354. von Schwarzenberg, K., et al., *V-ATPase inhibition overcomes trastuzumab resistance in breast cancer.* Mol Oncol, 2014. **8**(1): p. 9-19.

355. Kobia, F., et al., *Pharmacologic inhibition of vacuolar H+ ATPase reduces physiologic and oncogenic Notch signaling.* Mol Oncol, 2014. **8**(2): p. 207-20.
356. Salerno, M., et al., *Impairment of lysosomal activity as a therapeutic modality targeting cancer stem cells of embryonal rhabdomyosarcoma cell line RD.* PLoS One, 2014. **9**(10): p. e110340.
357. Capecci, J. and M. Forgac, *The function of vacuolar ATPase (V-ATPase) a subunit isoforms in invasiveness of MCF10a and MCF10CA1a human breast cancer cells.* J Biol Chem, 2013. **288**(45): p. 32731-41.
358. Meo-Evoli, N., et al., *V-ATPase: a master effector of E2F1-mediated lysosomal trafficking, mTORC1 activation and autophagy.* Oncotarget, 2015. **6**(29): p. 28057-70.
359. Alayev, A., et al., *The combination of rapamycin and resveratrol blocks autophagy and induces apoptosis in breast cancer cells.* J Cell Biochem, 2015. **116**(3): p. 450-7.
360. Alayev, A., et al., *Effects of combining rapamycin and resveratrol on apoptosis and growth of TSC2-deficient xenograft tumors.* Am J Respir Cell Mol Biol, 2015. **53**(5): p. 637-46.
361. He, X., et al., *Resveratrol enhances the anti-tumor activity of the mTOR inhibitor rapamycin in multiple breast cancer cell lines mainly by suppressing rapamycin-induced AKT signaling.* Cancer Lett, 2011. **301**(2): p. 168-76.
362. Rabadi, M.M., et al., *High-mobility group box 1 is a novel deacetylation target of Sirtuin1.* Kidney Int, 2015. **87**(1): p. 95-108.
363. Bonaldi, T., et al., *Monocytic cells hyperacetylate chromatin protein HMGB1 to redirect it towards secretion.* EMBO J, 2003. **22**(20): p. 5551-60.
364. Gardella, S., et al., *The nuclear protein HMGB1 is secreted by monocytes via a non-classical, vesicle-mediated secretory pathway.* EMBO Rep, 2002. **3**(10): p. 995-1001.
365. Cao, S., et al., *The potential role of HMGB1 release in peritoneal dialysis-related peritonitis.* PLoS One, 2013. **8**(1): p. e54647.
366. Hughes, A.L. and D.E. Gottschling, *An early age increase in vacuolar pH limits mitochondrial function and lifespan in yeast.* Nature, 2012. **492**(7428): p. 261-5.
367. Wu, G., et al., *Somatic histone H3 alterations in pediatric diffuse intrinsic pontine gliomas and non-brainstem glioblastomas.* Nat Genet, 2012. **44**(3): p. 251-3.

APPENDIX A. SUPPLEMENTAL TABLES

Table A-1. List of strains used in this study.

Strain	Genotype	Source
BY4741	MATa *his3Δ1 leu2Δ0 met15Δ0 ura3Δ0* BY4741	OPEN Bio
gat1Δ	BY4741; *gat1Δ::KanMX*	OPEN Bio
gln3 Δ	BY4741; *gln3Δ::KanMX*	OPEN Bio
hda1Δ	BY4741; *hda1Δ::KanMX*	OPEN Bio
npr3Δ	BY4741; *npr3Δ::KanMX*	OPEN Bio
ppg1Δ	BY4741; *ppg1Δ::KanMX*	OPEN Bio
pph3Δ	BY4741; *pph3Δ::KanMX*	OPEN Bio
rpd3Δ	BY4741; *rpd3Δ::KanMX*	OPEN Bio
sap155Δ	BY4741; *sap155Δ::KanMX*	OPEN Bio
sap185Δ	BY4741; *sap185Δ::KanMX*	OPEN Bio
sap190Δ	BY4741; *sap190Δ::KanMX*	OPEN Bio
sap4Δ	BY4741; *sap4Δ::KanMX*	OPEN Bio
sch9Δ	BY4741; *sch9Δ::KanMX*	OPEN Bio
sit4Δ	BY4741; *sit4Δ::KanMX*	OPEN Bio
tco89Δ	BY4741; *tco89Δ::KanMX*	OPEN Bio
tpd3Δ	BY4741; *tpd3Δ::KanMX*	OPEN Bio
ure2Δ	BY4741; *ure2Δ::KanMX*	OPEN Bio
H3G34A	MATa *his3Δ200 leu2Δ0 lys2Δ0 trp1Δ63 ura3Δ0met15Δ0 can1::MFA1pr-HIS3 hht1-hhf1::NatMX4 hht2-hhf2::[HHTS-HHFS]-ura3Δ* H3G34A	[315]
H3V35A	MATa *his3Δ200 leu2Δ0 lys2Δ0 trp1Δ63 ura3Δ0met15Δ0 can1::MFA1pr-HIS3 hht1-hhf1::NatMX4 hht2-hhf2::[HHTS-HHFS]-ura3Δ* H3V35A	[315]
H3K36A	MATa *his3Δ200 leu2Δ0 lys2Δ0 trp1Δ63 ura3Δ0met15Δ0 can1::MFA1pr-HIS3 hht1-hhf1::NatMX4 hht2-hhf2::[HHTS-HHFS]-ura3Δ* H3K36A	[315]
H3K37A	MATa *his3Δ200 leu2Δ0 lys2Δ0 trp1Δ63 ura3Δ0met15Δ0 can1::MFA1pr-HIS3 hht1-hhf1::NatMX4 hht2-hhf2::[HHTS-HHFS]-ura3Δ* H3K37A	[315]
H3K37Q	MATa *his3Δ200 leu2Δ0 lys2Δ0 trp1Δ63 ura3Δ0met15Δ0 can1::MFA1pr-HIS3 hht1-hhf1::NatMX4 hht2-hhf2::[HHTS-HHFS]-ura3Δ* H3K37Q	[315]
H3K37R	MATa *his3Δ200 leu2Δ0 lys2Δ0 trp1Δ63 ura3Δ0met15Δ0 can1::MFA1pr-HIS3 hht1-hhf1::NatMX4 hht2-hhf2::[HHTS-HHFS]-ura3Δ* H3K37R	[315]
H3P38A	MATa *his3Δ200 leu2Δ0 lys2Δ0 trp1Δ63 ura3Δ0met15Δ0 can1::MFA1pr-HIS3 hht1-hhf1::NatMX4 hht2-hhf2::[HHTS-HHFS]-ura3Δ* H3P38A	[315]
H3H39A	MATa *his3Δ200 leu2Δ0 lys2Δ0 trp1Δ63 ura3Δ0met15Δ0 can1::MFA1pr-HIS3 hht1-hhf1::NatMX4 hht2-hhf2::[HHTS-HHFS]-ura3Δ* H3H39A	[315]
H3R40A	MATa *his3Δ200 leu2Δ0 lys2Δ0 trp1Δ63 ura3Δ0met15Δ0 can1::MFA1pr-HIS3 hht1-hhf1::NatMX4 hht2-hhf2::[HHTS-HHFS]-ura3Δ* H3R40A	[315]

Table A-1. (Continued).

Strain	Genotype	Source
H3WT	MATa *his3Δ200 leu2Δ0 lys2Δ0 trp1Δ63 ura3Δ0met15Δ0 can1::MFA1pr-HIS3 hht1-hhf1::NatMX4 hht2-hhf2::[HHTS-HHFS]-ura3Δ* H3WT	[315]
YNL387	MATa *his3Δ1 leu2Δ0 met15Δ0 ura3Δ0 BY4741 tco89Δ::KanMX hst3Δ::NAT*	[66]
YNL389	MATa *his3Δ1 leu2Δ0 met15Δ0 ura3Δ0 BY4741 tco89Δ::KanMX hst4Δ::NAT*	[66]
Y3032	W303-1A *tap42*Δ::*HIS3* pRS415-*tap42-11*	[309]
Y3033	W303-1A *tap42*Δ::*HIS3* pRS414-*TAP42*	[309]
Y3034	W303-1A *tap42*Δ::*HIS3* pRS414-*tap42-106*	[309]
Y3035	W303-1A *tap42*Δ::*HIS3* pRS414-*tap42-109*	[309]
YNL251	MATa *his3Δ1 leu2Δ0 met15Δ0 ura3Δ0* BY4741 *Sch9-6xHA::NAT*	[304]
YNL487	MATa *his3Δ1 leu2Δ0 met15Δ0 ura3Δ0* BY4741 *tco89Δ::NAT*	[304]
YNL502	MATa *his3Δ1 leu2Δ0 met15Δ0 ura3Δ0* BY4741 *tco89Δ::NAT rpd3Δ::KanMX*	[304]
YNL516	MATa *his3Δ1 leu2Δ0 met15Δ0 ura3Δ0* BY4741 *tco89Δ::NAT hst1Δ::KanMX*	[304]
YNL517	MATa *his3Δ1 leu2Δ0 met15Δ0 ura3Δ0* BY4741 *tco89Δ::NAT sir2Δ::KanMX*	[304]
YNL519	MATa *his3Δ1 leu2Δ0 met15Δ0 ura3Δ0* BY4741 *tco89Δ::NAT hst2Δ::KanMX*	[304]
YNL541	MATa *his3Δ1 leu2Δ0 met15Δ0 ura3Δ0* BY4741 *tco89Δ::HphNT1 pnc1Δ::KanMX*	[304]
YNL564	MATa *his3Δ1 leu2Δ0 met15Δ0 ura3Δ0* BY4741 ρ-	[304]
YNL566	MATa *his3Δ1 leu2Δ0 met15Δ0 ura3Δ0* BY4741 *tco89Δ::KanMX* ρ-	[304]
YNL583	MATa *his3Δ1 leu2Δ0 met15Δ0 ura3Δ0* BY4741 *tco89Δ::NAT npr3Δ::KanMX*	[304]
YNL612	MATa *his3Δ1 leu2Δ0 met15Δ0 ura3Δ0* BY4741 *Hst4-9xMyc::KanMX*	[304]
YNL614	MATa *his3Δ1 leu2Δ0 met15Δ0 ura3Δ0* BY4741 *tco89Δ::NAT Hst4-9xMyc::KanMX*	[304]
YNL622	MATa *his3Δ1 leu2Δ0 met15Δ0 ura3Δ0* BY4741 *tco89Δ::NAT sit4Δ::KanMX*	[304]
YNL670	MATa *his3Δ1 leu2Δ0 met15Δ0 ura3Δ0* BY4741 *tco89Δ::NAT hda1Δ::KanMX*	[304]
YNL676	MATa *his3Δ1 leu2Δ0 met15Δ0 ura3Δ0* BY4741 *tco89Δ::NAT Hst3-9xMyc::KanMX*	[304]
YNL678	MATa *his3Δ1 leu2Δ0 met15Δ0 ura3Δ0* BY4741 *Hst1-9xMyc::KanMX*	[304]
YNL681	MATa *his3Δ1 leu2Δ0 met15Δ0 ura3Δ0* BY4741 *tco89Δ::NAT Hst1-9xMyc::KanMX*	[304]
YNL685	MATa *his3Δ1 leu2Δ0 met15Δ0 ura3Δ0* BY4741 *Hst2-9xMyc::KanMX*	[304]
YNL687	MATa *his3Δ1 leu2Δ0 met15Δ0 ura3Δ0* BY4741 *Sir2-9xMyc::KanMX*	[304]
YNL689	MATa *his3Δ1 leu2Δ0 met15Δ0 ura3Δ0* BY4741 *tco89Δ::NAT Sir2-9xMyc::KanMX*	[304]
YNL698	MATa *his3Δ1 leu2Δ0 met15Δ0 ura3Δ0* BY4741 *Hst3-9xMyc::KanMX*	[304]
YNL700	MATa *his3Δ1 leu2Δ0 met15Δ0 ura3Δ0* BY4741 *tco89Δ::NAT Hst2-9xMyc::KanMX*	[304]
YNL714	MATa *his3Δ1 leu2Δ0 met15Δ0 ura3Δ0* BY4741 *Hst4-9xMyc::KanMX tco89Δ::NAT* (MATED HAPLOIDS/SPORULATED)	[304]
YNL716	MATa *his3Δ1 leu2Δ0 met15Δ0 ura3Δ0* BY4741 *Hst4-9xMyc::HYGRO sit4Δ::KANMX*	[304]

Table A-1. (Continued).

Strain	Genotype	Source
YNL718	MATa *his3Δ1 leu2Δ0 met15Δ0 ura3Δ0* BY4741 *Hst4-9xMyc::HYGRO sit4Δ::KANMX tco89Δ:HphNT1*	[304]
YNL775	MATa *his3Δ1 leu2Δ0 met15Δ0 ura3Δ0* BY4741 *Hst4-9xMyc::KANMX sap4Δ::HYGRO*	[304]
YNL776	MATa *his3Δ1 leu2Δ0 met15Δ0 ura3Δ0 BY4741 Hst4-9xMyc::KANMX sap4Δ::HYGRO tco89Δ::NAT*	[304]
YNL778	MATa *his3Δ1 leu2Δ0 met15Δ0 ura3Δ0* BY4741 *Maf1-9xMyc::NAT*	[304]
YNL780	MATa *his3Δ1 leu2Δ0 met15Δ0 ura3Δ0* BY4741 *Maf1-9xMyc::NAT sch9Δ KANMX*	[304]
YNL465	MATa *his3Δ200 leu2Δ0 lys2Δ0 trp1Δ63 ura3Δ0met15Δ0 can1::MFA1pr-HIS3 hht1-hhf1::NatMX4 hht2-hhf2::[HHTS-HHFS]-ura3Δ* H3WT *hmo1Δ::KanMX*	This Study
YNL467	MATa *his3Δ200 leu2Δ0 lys2Δ0 trp1Δ63 ura3Δ0met15Δ0 can1::MFA1pr-HIS3 hht1-hhf1::NatMX4 hht2-hhf2::[HHTS-HHFS]-ura3Δ* H3K37A *hmo1Δ::KanMX*	This Study
YNL490	MATa *his3Δ200 leu2Δ0 lys2Δ0 trp1Δ63 ura3Δ0met15Δ0 can1::MFA1pr-HIS3 hht1-hhf1::NatMX4 hht2-hhf2::[HHTS-HHFS]-ura3Δ* H3WT *nhp10aΔ::KanMX*	This Study
YNL491	MATa *his3Δ200 leu2Δ0 lys2Δ0 trp1Δ63 ura3Δ0met15Δ0 can1::MFA1pr-HIS3 hht1-hhf1::NatMX4 hht2-hhf2::[HHTS-HHFS]-ura3Δ* H3K37A *nhp10aΔ::KanMX*	This Study
YNL512	MATa *his3Δ200 leu2Δ0 lys2Δ0 trp1Δ63 ura3Δ0met15Δ0 can1::MFA1pr-HIS3 hht1-hhf1::NatMX4 hht2-hhf2::[HHTS-HHFS]-ura3Δ* H3WT *nhp6aΔ::KanMX*	This Study
YNL514	MATa *his3Δ200 leu2Δ0 lys2Δ0 trp1Δ63 ura3Δ0met15Δ0 can1::MFA1pr-HIS3 hht1-hhf1::NatMX4 hht2-hhf2::[HHTS-HHFS]-ura3Δ* H3K37A *nhp6aΔ::KanMX*	This Study
YNL595	MATa *his3Δ200 leu2Δ0 lys2Δ0 trp1Δ63 ura3Δ0met15Δ0 can1::MFA1pr-HIS3 hht1-hhf1::NatMX4 hht2-hhf2::[HHTS-HHFS]-ura3Δ* H3WT *NHP6A-EGFP::KanMX*	This Study
YNL596	MATa *his3Δ200 leu2Δ0 lys2Δ0 trp1Δ63 ura3Δ0met15Δ0 can1::MFA1pr-HIS3 hht1-hhf1::NatMX4 hht2-hhf2::[HHTS-HHFS]-ura3Δ* H3K37A *NHP6A-EGFP::KanMX*	This Study
YNL653	MATa *his3Δ200 leu2Δ0 lys2Δ0 trp1Δ63 ura3Δ0met15Δ0 can1::MFA1pr-HIS3 hht1-hhf1::NatMX4 hht2-hhf2::[HHTS-HHFS]-ura3Δ* H3WT *sap4Δ::KanMX*	This Study
YNL655	MATa *his3Δ200 leu2Δ0 lys2Δ0 trp1Δ63 ura3Δ0met15Δ0 can1::MFA1pr-HIS3 hht1-hhf1::NatMX4 hht2-hhf2::[HHTS-HHFS]-ura3Δ* H3K37A *sap4Δ::KanMX*	This Study
YNL671	MATa *his3Δ200 leu2Δ0 lys2Δ0 trp1Δ63 ura3Δ0met15Δ0 can1::MFA1pr-HIS3 hht1-hhf1::NatMX4 hht2-hhf2::[HHTS-HHFS]-ura3Δ* H3K37A *hst4Δ::KanMX*	This Study
YNL674	MATa *his3Δ200 leu2Δ0 lys2Δ0 trp1Δ63 ura3Δ0met15Δ0 can1::MFA1pr-HIS3 hht1-hhf1::NatMX4 hht2-hhf2::[HHTS-HHFS]-ura3Δ* H3WT *hst4Δ::KanMX*	This Study
YNL710	MATa *his3Δ200 leu2Δ0 lys2Δ0 trp1Δ63 ura3Δ0met15Δ0 can1::MFA1pr-HIS3 hht1-hhf1::NatMX4 hht2-hhf2::[HHTS-HHFS]-ura3Δ* H3K37R *NHP6A-EGFP::KanMX*	This Study
YNL722	MATa *his3Δ200 leu2Δ0 lys2Δ0 trp1Δ63 ura3Δ0met15Δ0 can1::MFA1pr-HIS3 hht1-hhf1::NatMX4 hht2-hhf2::[HHTS-HHFS]-ura3Δ* H3WT *NHP6A-yeGFP::HYGRO*	This Study

Table A-1. (Continued).

Strain	Genotype	Source
YNL723	MATa *his3Δ200 leu2Δ0 lys2Δ0 trp1Δ63 ura3Δ0met15Δ0 can1::MFA1pr-HIS3 hht1-hhf1::NatMX4 hht2-hhf2::[HHTS-HHFS]-ura3Δ* H3K37A *NHP6A-yeGFP::HYGRO*	This Study
YNL724	MATa *his3Δ200 leu2Δ0 lys2Δ0 trp1Δ63 ura3Δ0met15Δ0 can1::MFA1pr-HIS3 hht1-hhf1::NatMX4 hht2-hhf2::[HHTS-HHFS]-ura3Δ* H3WT *hst4Δ::KanMX NHP6A-yeGFP::HYGRO*	This Study
YNL725	MATa *his3Δ200 leu2Δ0 lys2Δ0 trp1Δ63 ura3Δ0met15Δ0 can1::MFA1pr-HIS3 hht1-hhf1::NatMX4 hht2-hhf2::[HHTS-HHFS]-ura3Δ* H3K37A *hst4Δ::KanMX NHP6A-yeGFP::HYGRO*	This Study

Table A-2. List of plasmids used in the study.

Parent	Vector/Insert	Source
	pHmo1 Gal-HA	Open Bio GAL1 collection
	pNhp6A Gal-HA	Open Bio GAL1 collection
pRS416	pSCH9-6xHA	[80]
pJU790	pSCH9-6xHA (T723A, S726A, T737A, S758A, S765A)	[80]
pJU855	pSCH9-6xHA (T723D, S726D, T737E, S758E, S765E)	[80]
pRS416	pSit4FL FLAG	This study
pRS416	pTco89 N-term Myc full-length	This study
pRS416	pTco89 C-term FLAG full-length	This study
pRS416	pTco89 C-term FLAG Frag A	This study
pRS416	pTco89 C-term FLAG Frag B	This study
pRS416	pTco89 C-term FLAG Frag C	This study
pRS416	pTco89 C-term FLAG Frag D	This study
pRS416	pTco89 C-term FLAG Frag E	This study
pRS416	pTco89 C-term FLAG Frag F	This study

APPENDIX B. SUPPLEMENTAL FIGURES

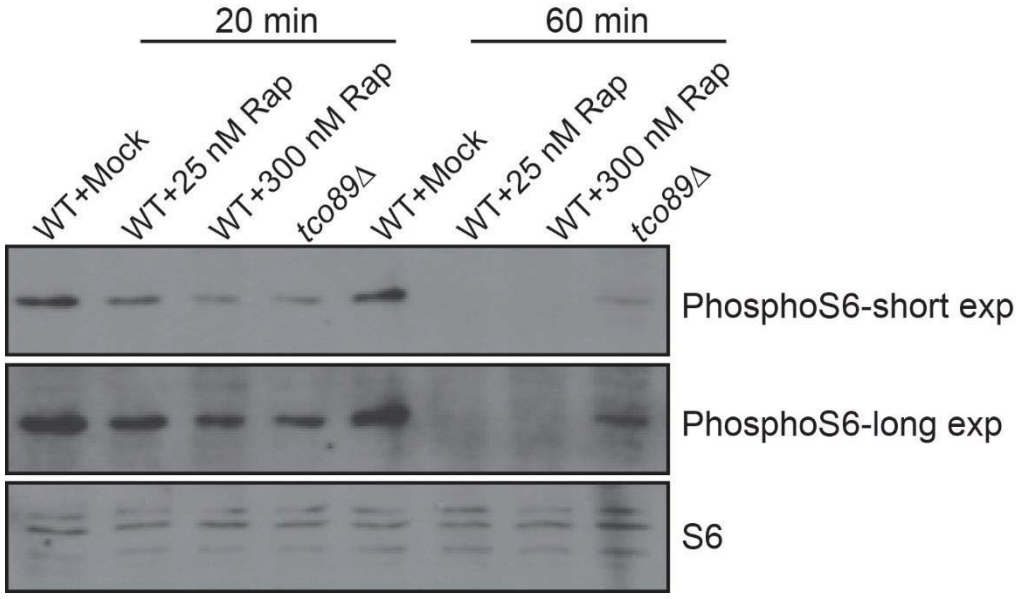

Figure B-1. TORC1 inhibition over a range of rapamycin treatment conditions compared to a *tco89Δ* mutant.
WT and *tco89Δ* were grown to log phase and then mock treated, or treated with 25 nM or 300 nM rapamycin. Treatments shown represent resulting TORC1 activity following 20 and 60 minutes inhibition.

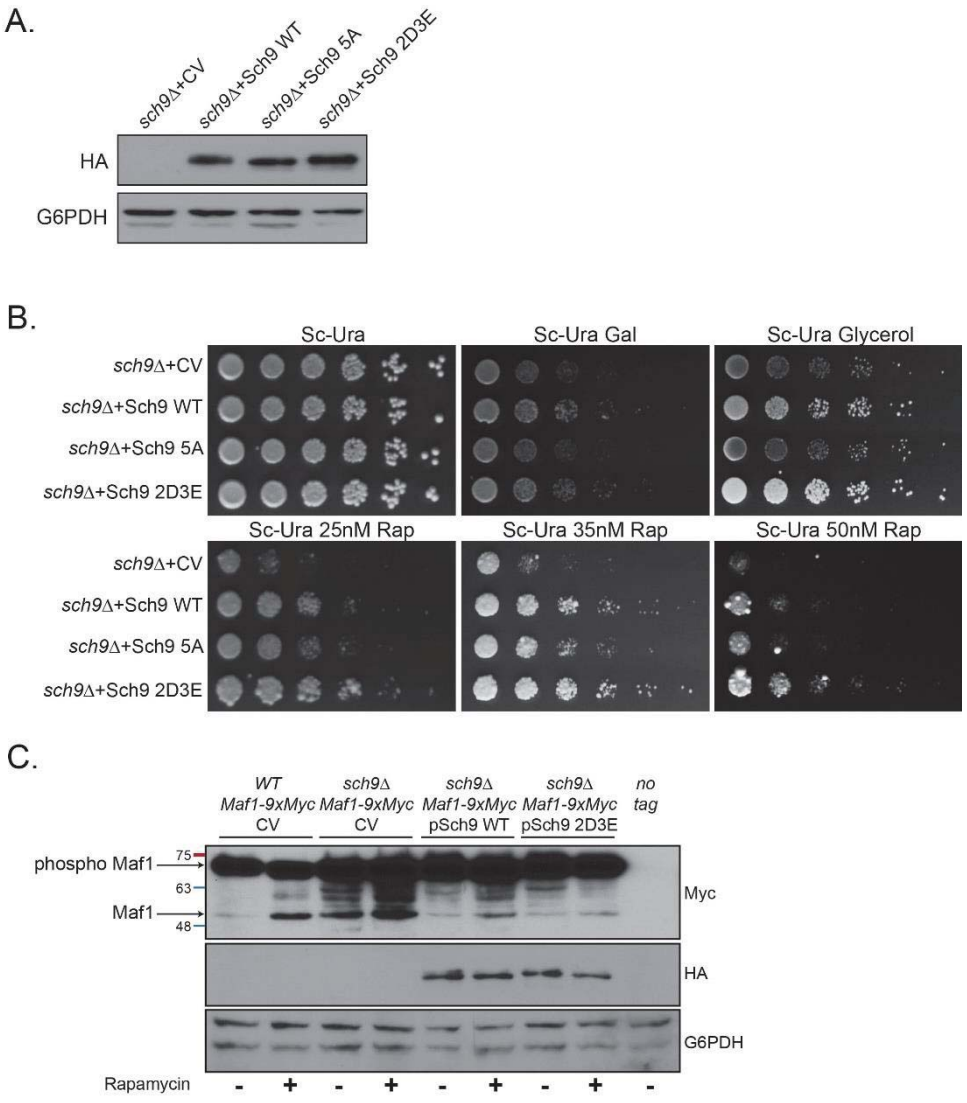

Figure B-2. Control experiments for Sch9^{2D3E} expression vectors.
A. *sch9Δ* cells were transformed with control vector (CV) or expression vectors containing various forms of Sch9 (see text for more details). Strains were grown in selective media to log phase and extracts were prepared and blotted to measure expression of mutant Sch9. G6PDH is included as an additional loading control. **B.** Strains from (A) were grown to stationary phase, five-fold serially diluted, and spotted onto selective media with a wide range of rapamycin concentrations. Plates with galactose and glycerol as the sole carbon sources are included as well. **C.** Wild-type Maf1-9xMyc and *sch9Δ* Maf1-9xMyc cells were transformed with the vectors from (A). Cells were grown to log phase, treated with 300 nM rapamycin for 60 min, and extracts were prepared. Samples were resolved on an 8% PAGE gel and blotted as shown. *Reprinted with permission [304]*. Workman, J.J., H. Chen, and R.N. Laribee, *Saccharomyces cerevisiae TORC1 Controls Histone Acetylation by Signaling Through the Sit4/PP6 Phosphatase To Regulate Sirtuin Deacetylase Nuclear Accumulation.* Genetics, 2016.

Figure B-3. Sirtuin relocalization in response to TORC1 inhibition.
A-E. WT or *tco89Δ* strains, containing 9XMyc epitope tagged sirtuins, were treated as indicated at log phase, fixed, permeabilized, and imaged by indirect immunofluorescence as described in the Chapter 2. Images are representative of at least three independent biological replicates, and are a subset of the quantification shown in **Figure 3-16**. DAPI staining denotes the nucleus and the green channel (FITC-conjugated secondary to α-Myc) tracks the localization of the sirtuins.

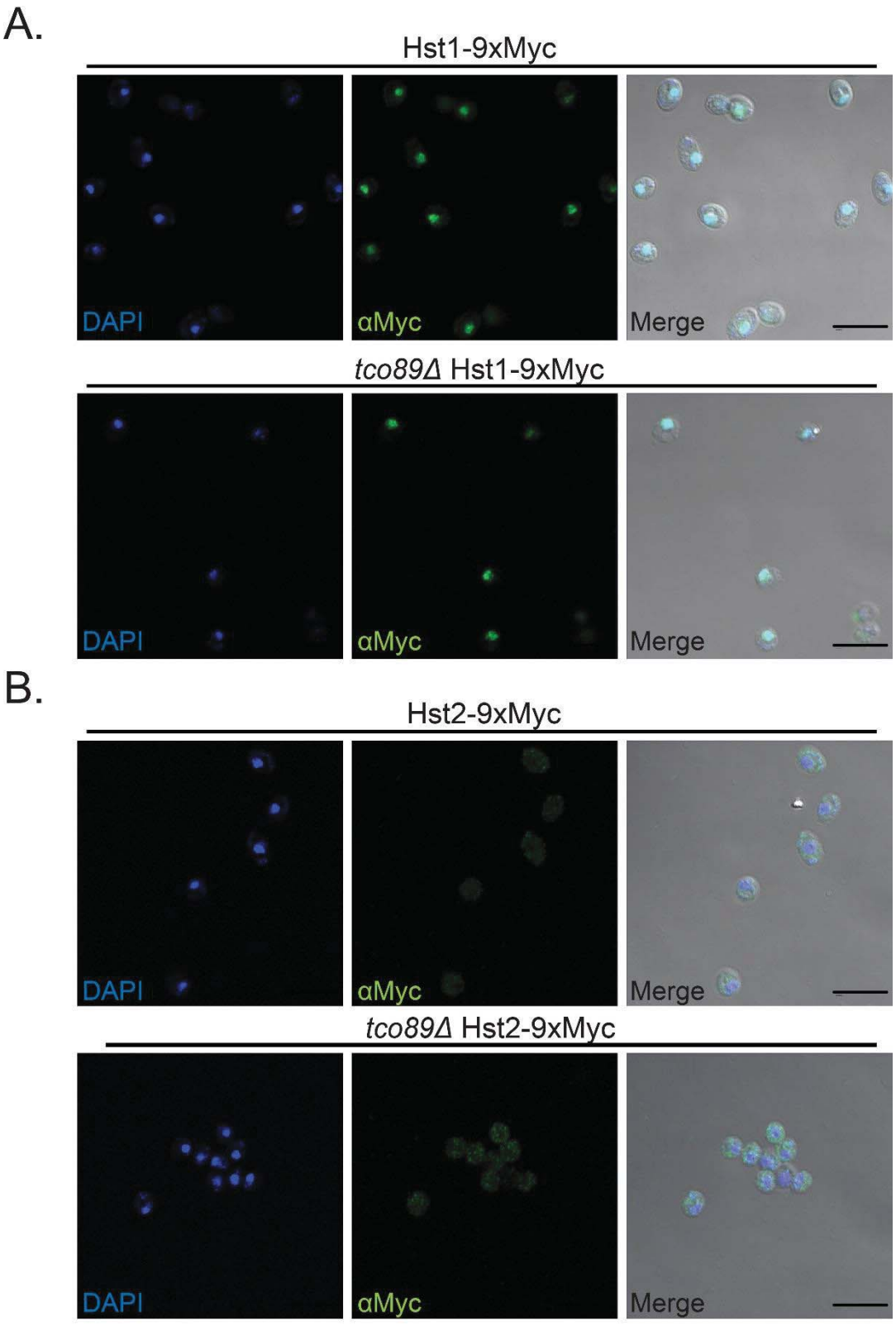
A.
Hst1-9xMyc
DAPI
αMyc
Merge
tco89Δ Hst1-9xMyc
DAPI
αMyc
Merge
B.
Hst2-9xMyc
DAPI
αMyc
Merge
tco89Δ Hst2-9xMyc
DAPI
αMyc
Merge

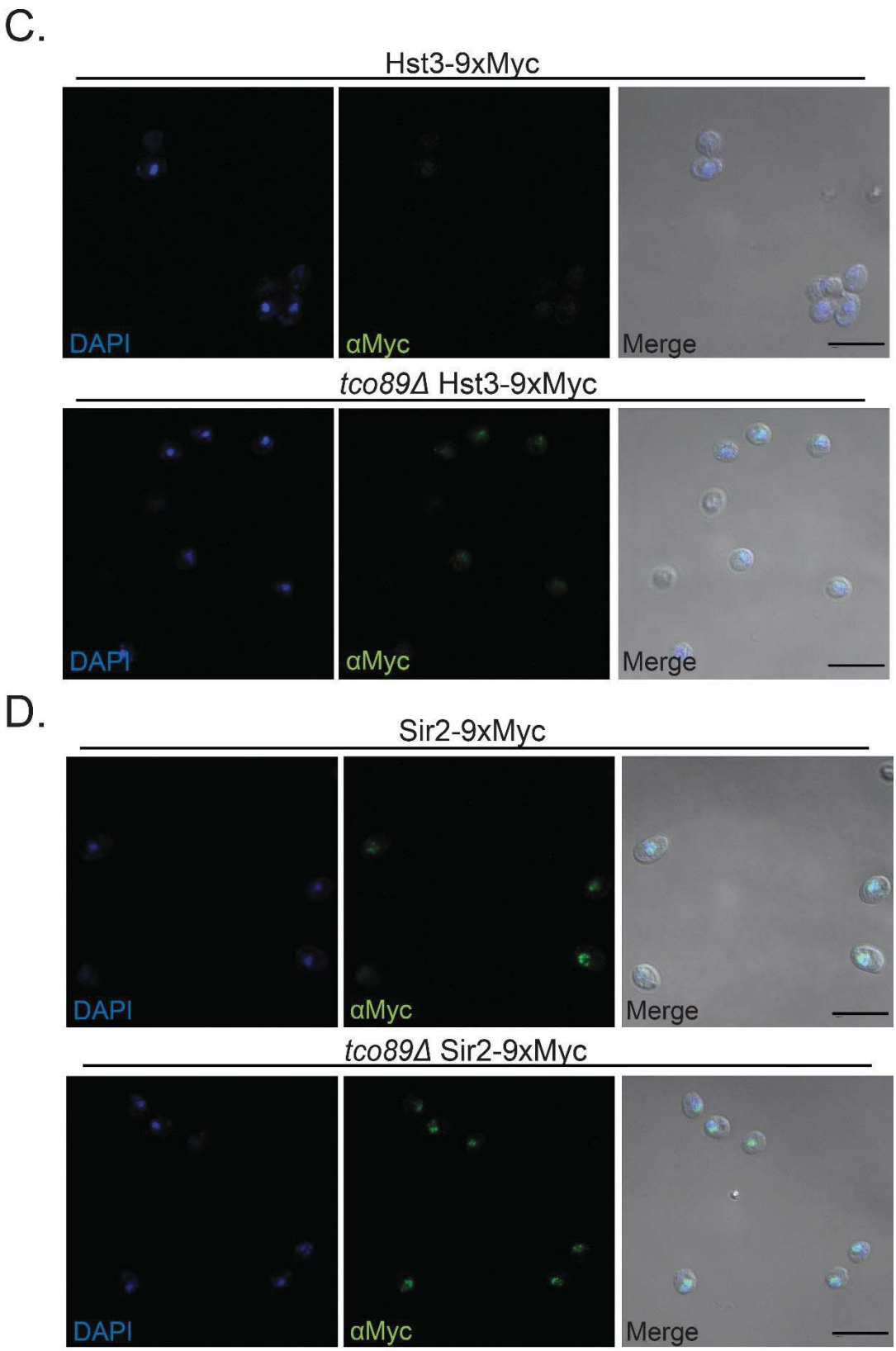

Figure B-3. Continued.

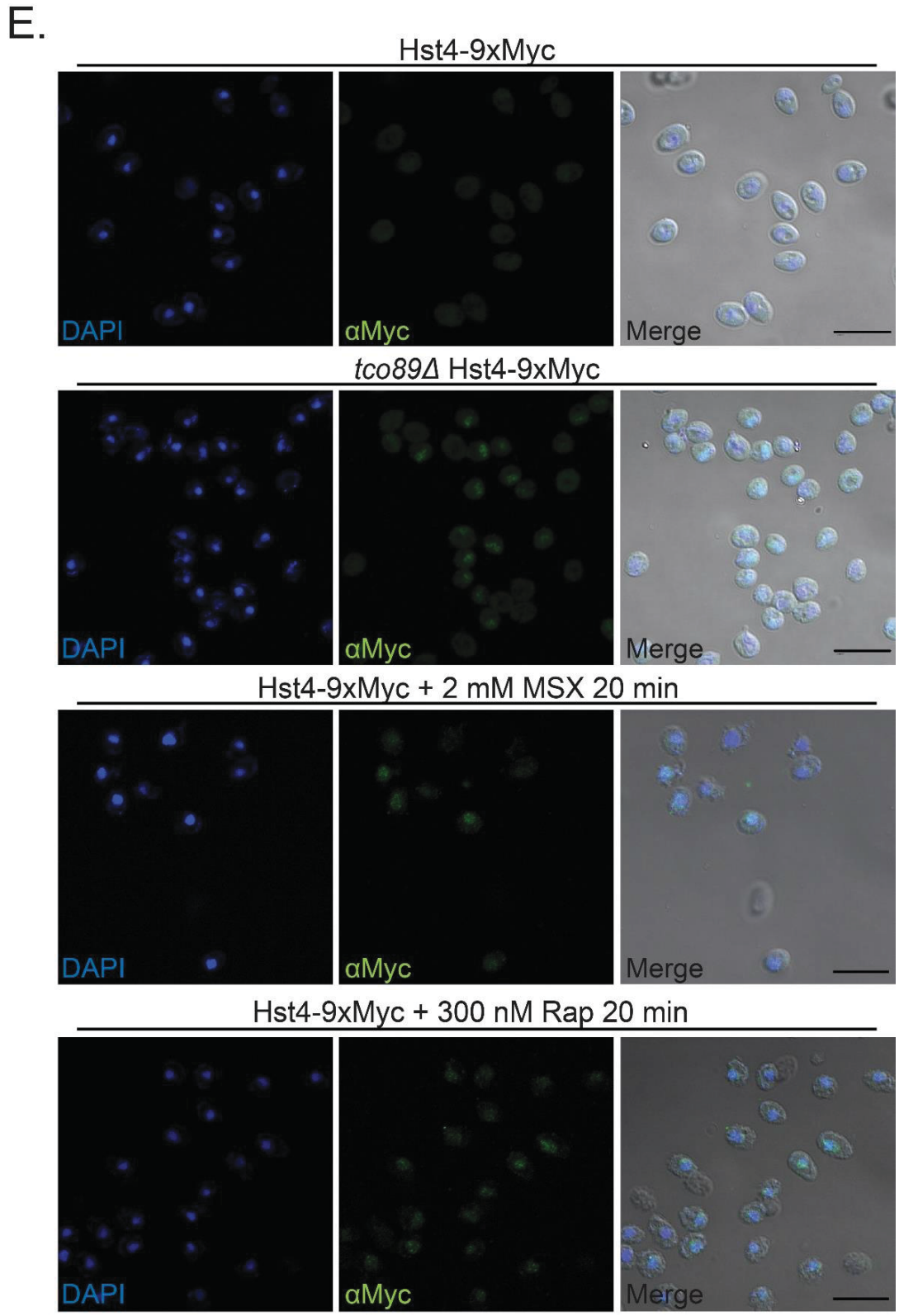

Figure B-3. Continued.

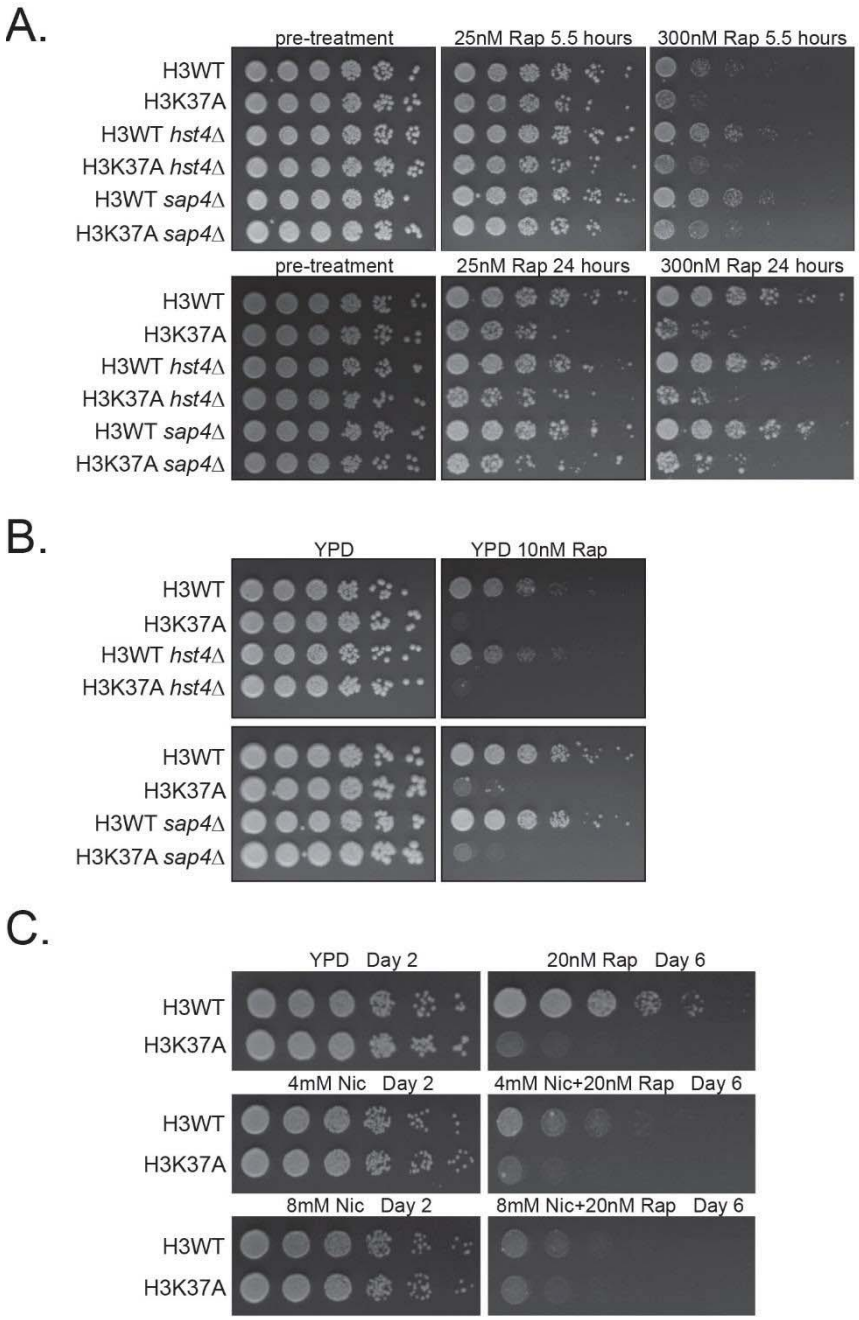

Figure B-4. Disruption of TORC1-responsive histone acetylation has no effect on H3K37A sensitivity to rapamycin.
A. H3WT, H3K37A, H3WT *hst4Δ*, H3K37 *hst4Δ*, H3WT *sap4Δ* and H3K37A *sap4Δ* were grown to log phase. Samples were mock treated or treated with rapamycin (25 nM or 300 nM) for 5.5 hours or 24 hours as indicated. Following treatment, pellets were washed with sterile water and spotted onto YPD plates as described in Chapter 2. **B.** Strains from (A) were grown to stationary phase and spotted onto YPD and YPD 10 nM Rap plates. **C.** H3WT and H3K37A cells were grown and spotted as in (B) to the plate media denoted. Photos are provided for rapidly growing strain/media combinations at 2 days, and at 6 days for the more sensitive pairings.

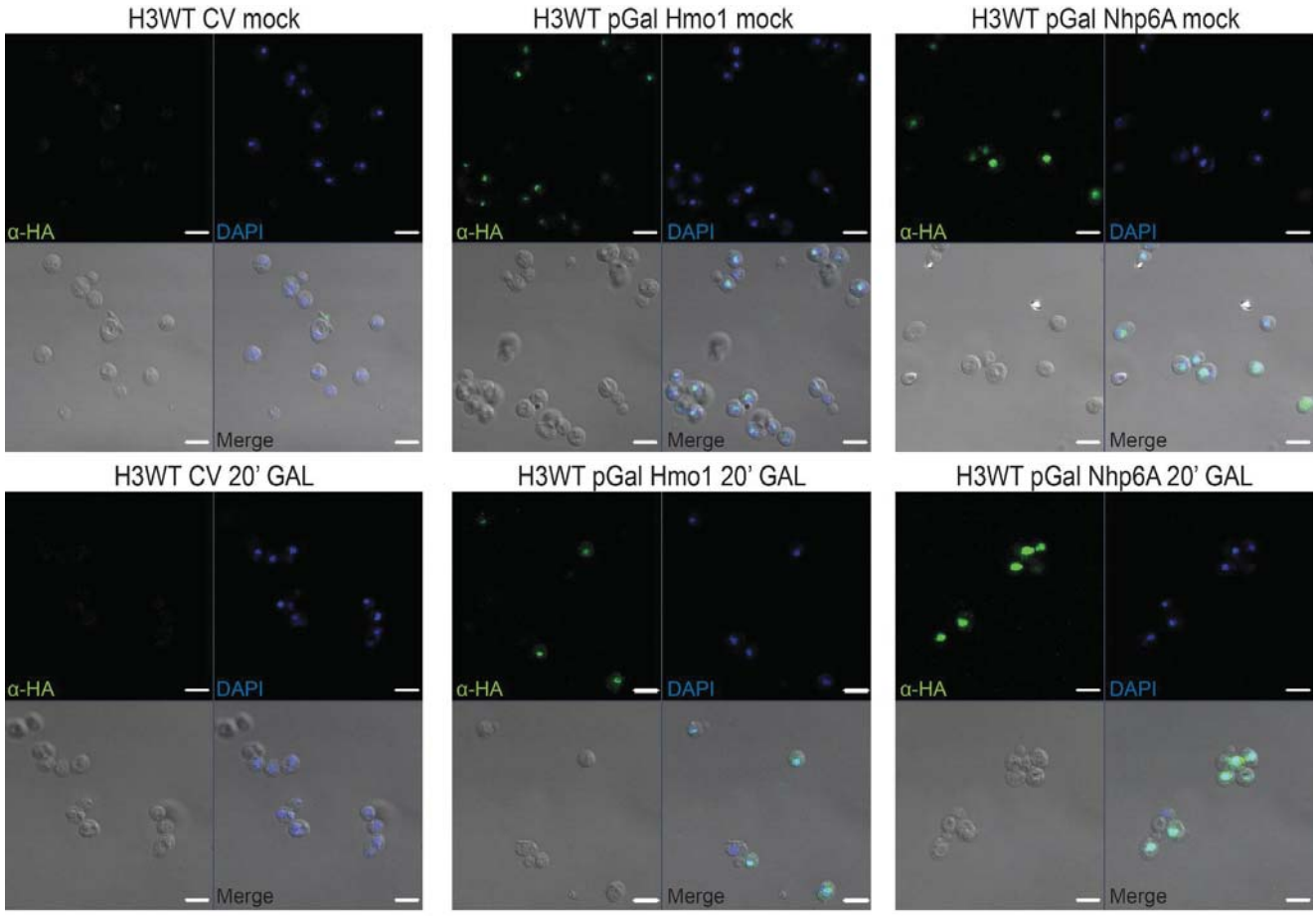

Figure B-5. Galactose-inducible HMGB expression vectors promote aberrant protein levels and distribution of Hmo1 and Nhp6A even prior to addition of galactose.

H3WT cells were transformed with control vector, or galactose inducible expression vectors containing HA-tagged Hmo1 or Nhp6A. Strains were grown to log phase in synthetic complete raffinose media, and then mock treated or induced with 2% galactose for 20 minutes. Cells were fixed, processed by indirect immunofluorescence, and imaged by confocal microscopy, as described in Chapter 2. Images are representative of three independent experiments. DAPI staining denotes the nucleus and the green channel (FITC-conjugated secondary to α-HA) marks the localization of the HMGBs.

VITA

Jason John Workman was born in Grand Rapids, Michigan in 1987. He graduated from Bridgman High School in 2006, before attending Ferris State University in Big Rapids, MI. He received his Bachelor of Science degree in Biotechnology in 2010 and spent the following year working at The Dow Chemical Company in Midland, MI. In 2011, Jason enrolled in the University of Tennessee Health Science Center and spent the next five years in Dr. R Nicholas Laribee's lab studying chromatin and epigenetics. Upon successful defense of the work described in this dissertation, Jason will be awarded a Doctor of Philosophy degree in Cancer and Developmental Biology.

Publications

1. **Workman, J.J.**, H. Chen, and R.N. Laribee, *Saccharomyces cerevisiae TORC1 Controls Histone Acetylation by Signaling Through the Sit4/PP6 Phosphatase To Regulate Sirtuin Deacetylase Nuclear Accumulation.* Genetics, 2016.

2. Laribee RN, Hosni-Ahmed A, **Workman JJ**, Chen H. Ccr4-not regulates RNA polymerase I transcription and couples nutrient signaling to the control of ribosomal RNA biogenesis. PLoS Genet. 2015 Mar 27;11(3):e1005113.

3. **Workman JJ,** Chen H, Laribee RN. Environmental signaling through the mechanistic target of rapamycin complex 1: mTORC1 goes nuclear. Cell Cycle. 2014;13(5):714-25.

4. Chen H, **Workman JJ**, Tenga A, Laribee RN. Target of rapamycin signaling regulates high mobility group protein association to chromatin, which functions to suppress necrotic cell death. Epigenetics Chromatin. 2013 Sep 2;6(1):29.